Oncology and Translational Medicine

Volume 2 • Number 5 • October 2016

Oncology and Translational Medicine Volume 2 • Number 5 • October 2016 pp 195–245

Online First
Immediately Online
otm.tjh.com.cn
Faster publication !

邮发代号：38-121
ISSN 2095-9621

GENERAL INFORMATION
≫otm.tjh.com.cn

ISSN 2095-9621
CN 42-1865/R

Oncology and Translational Medicine

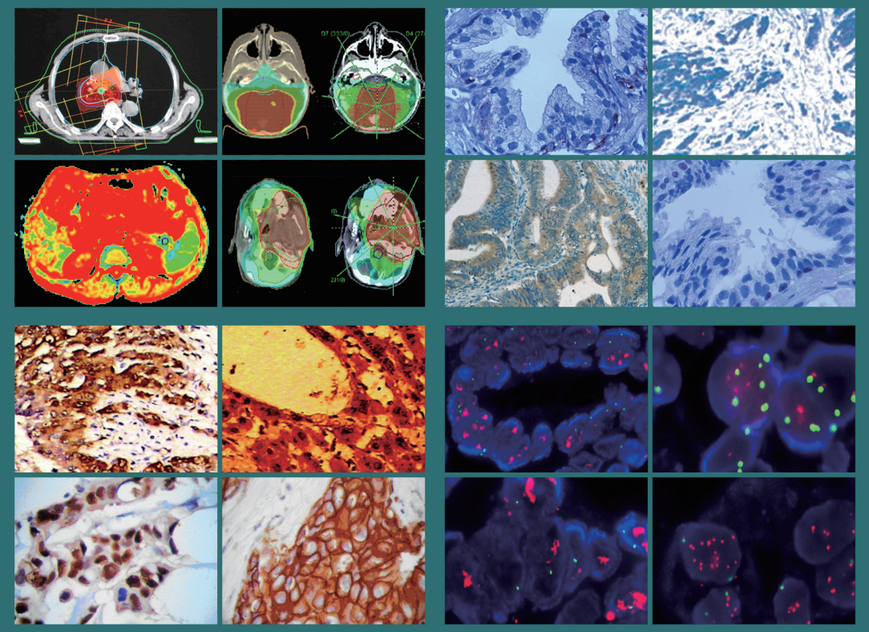

Volume 2
Number 5
October 2016

Oncology and Translational Medicine

Honorary Editors-in-Chief

W.-W. Höpker (Germany)
Mengchao Wu (China)
Yan Sun (China)

Editors-in-Chief

Anmin Chen (China)
Shiying Yu (China)

Associate Editors

Yilong Wu (China)
Shukui Qin (China)
Xiaoping Chen (China)
Ding Ma (China)
Hanxiang An (China)
Yuan Chen (China)

Editorial Board

A. R. Hanauske (Germany)
Adolf Grünert (Germany)
Andrei Iagaru (USA)
Arnulf H. Hölscher (Germany)
Baoming Yu (China)
Bing Wang (USA)
Binghe Xu (China)
Bruce A. Chabner (USA)
Caicun Zhou (China)
Ch. Herfarth (Germany)
Changshu Ke (China)
Charles S. Cleeland (USA)
Chi-Kong Li (China)
Chris Albanese (USA)
Christof von Kalle (Germany)
D Kerr (United Kingdom)
Daoyu Hu (China)
Dean Tian (China)
Di Chen (USA)
Dian Wang (USA)
Dieter Hoelzer (Germany)
Dolores J. Schendel (Germany)
Dongfeng Tan (USA)
Dongmin Wang (China)
Ednin Hamzah (Malaysia)
Ewerbeck Volker (Germany)
Feng Li (China)
Frank Elsner (Germany)
Gang Wu (China)
Gary A. Levy (Canada)
Gen Sheng Wu (USA)
Gerhard Ehninger (Germany)
Guang Peng (USA)
Guangying Zhu (China)
Gunther Bastert (Germany)
Guoan Chen (USA)
Guojun Li (USA)
Guoliang Jiang (China)
Guoping Wang (China)
H. J. Biersack (Germany)
Helmut K. Seitz (Germany)
Hongbing Ma (China)
Hongtao Yu (USA)
Hongyang Wang (China)
Hua Lu (USA)
Huaqing Wang (China)
Hubert E. Blum (Germany)
J. R. Siewert (Germany)
Ji Wang (USA)
Jiafu Ji (China)
Jianfeng Zhou (China)
Jianjie Ma (USA)
Jianping Gong (China)
Jihong Wang (USA)
Jilin Yi (China)
Jin Li (China)
Jingyi Zhang (Canada)
Jingzhi Ma (China)
Jinyi Lang (China)
Joachim W. Dudenhausen (Germany)
Joe Y. Chang (USA)
Jörg-Walter Bartsch (Germany)
Jörg F. Debatin (Germany)
JP Armand (France)
Jun Ma (China)
Karl-Walter Jauch (Germany)
Katherine A Siminovitch (Canada)
Kongming Wu (China)
Lei Li (USA)
Lei Zheng (USA)
Li Zhang (China)
Lichun Lu (USA)
Lili Tang (China)
Lin Shen (China)
Lin Zhang (China)
Lingying Wu (China)
Luhua Wang (China)
Marco Antonio Velasco-Velázqueza (Mexico)
Markus W. Büchler (Germany)
Martin J. Murphy, Jr (USA)
Mathew Casimiro (USA)
Matthias W. Beckmann (Germany)
Meilin Liao (China)
Michael Buchfelder (Germany)
Norbert Arnold (Germany)
Peter Neumeister (Austria)
Qing Zhong (USA)
Qinghua Zhou (China)
Qingyi Wei (USA)
Qun Hu (China)
Reg Gorczynski (Canada)
Renyi Qin (China)
Richard Fielding (China)
Rongcheng Luo (China)
Shenjiang Li (China)
Shenqiu Li (China)
Shimosaka (Japan)
Shixuan Wang (China)
Shun Lu (China)
Sridhar Mani (USA)
Ting Lei (China)
Ulrich Sure (Germany)
Ulrich T. Hopt (Germany)
Ursula E. Seidler (Germany)
Uwe Kraeuter (Germany)
W. Hohenberger (Germany)
Wei Hu (USA)
Wei Liu (China)
Wei Wang (China)
Weijian Feng (China)
Weiping Zou (USA)
Wenzhen Zhu (China)
Xianglin Yuan (China)
Xiaodong Xie (China)
Xiaohua Zhu (China)
Xiaohui Niu (China)
Xiaolong Fu (China)
Xiaoyuan Zhang (USA)
Xiaoyuan (Shawn) Chen (USA)
Xichun Hu (China)
Ximing Xu (China)
Xin Shelley Wang (USA)
Xishan Hao (China)
Xiuyi Zhi (China)
Ying Cheng (China)
Ying Yuan (China)
Yixin Zeng (China)
Yongjian Xu (China)
You Lu (China)
Youbin Deng (China)
Yuankai Shi (China)
Yuguang He (USA)
Yuke Tian (China)
Yunfeng Zhou (China)
Yunyi Liu (China)
Yuquan Wei (China)
Zaide Wu (China)
Zefei Jiang (China)
Zhangqun Ye (China)
Zhishui Chen (China)
Zhongxing Liao (USA)

Oncology and Translational Medicine
October 2016 Volume 2 Number 5

Contents

Oncology and Translational Medicine
DOI 10.1007/s10330-016-0190-4
October 2016, Vol. 2, No. 5, P195–P196

EDITORIAL

Multimodal therapy for brain tumors*

Feng Hu, Ting Lei (✉)

Department of Neurosurgery, Tongji Hospital, Tongji Medical College, Huazhong University of Science and Technology, Wuhan 430030, China

Ting Lei. M.D., Professor of Neurosurgery, Doctoral Supervisor, Director of the Neurosurgery Department, Tongji Hospital, Tongji Medical College of Huazhong University of Science and Technology, China. He obtained his bachelor's and master's degree from Tongji Medical University, China, and became a neurosurgeon afterward. Then, he successfully obtained a German Academic Exchange Service scholarship to undertake his doctorate in medicine at the University of Erlangen-Nuernberg in Germany. Under the supervision of Profs. R. Fahlbusch and M. Buchfelder, he completed his doctoral degree in the same university and returned to Tongji Hospital to become the first postdoctoral fellow in the Department of Neurosurgery. Since 1998, he has been Chief of the Neurosurgical Department.

His scientific interest is basic research and clinical treatment of brain tumors, including pituitary adenoma and glioma. He introduced transsphenoidal surgery in the treatment of pituitary adenoma in Hubei Province, China. Currently, he performs more than 300 transsphenoidal surgeries annually. Over the past years, he also modified this surgical approach to make it less invasive and provide patients with fast postoperative recovery and better quality of life.

He has been an active researcher in the brain tumor research community for over 30 years now. He received several grants from the National Natural Science Foundation and published more than 500 peer-reviewed papers in national and international journals, including the *Journal of Neurosurgery*, *Epilepsy*, *European Journal of Cancer*, and *Cancer Letter*. Meanwhile, he is also an academic editor of several journals. Prof. Lei serves as the chairman of the neurosurgery branch of the Wuhan Medical Association and is a committee member of several academic associations.

Brain tumors are devastating diseases that occur when resident brain cells are transformed. As most other solid tumors, brain tumors are classified as either malignant or benign.

Gliomas are the most common malignant brain tumors in the central nervous system, accounting for around 70% of the newly diagnosed cases in adults. They constitute approximately 30% of all brain tumors, and approximately 60% of gliomas occur in the four lobes of the brain. Overall, brain tumors are relatively rare. The average annual age-adjusted incidence rates of all malignant brain tumors range from 4.95 to 8.97 per 100 000 people, whereas those of nonmalignant brain tumors range from 8.90 to 19.02 per 100 000 people. Males are more frequently affected with gliomas than females [1]. Like that of most malignant cancers, the etiology of gliomas is still unclear. However, occupations, lifestyles, and environmental carcinogens have been reported to be associated with a high risk of gliomas, but the only unequivocal factor identified so far is therapeutic X-irradiation [2].

Multimodal treatments of gliomas include surgery, radiotherapy, chemotherapy, and immunotherapy. However, despite all these possible strategies, most patients with malignant gliomas still have poor prognoses. One of the reasons is drug resistance. Over the last years, several theories have evolved about drug resistance in glioma treatment, such as the glioma stem cell hypothesis and epigenetic changes of the tumor cell genome. In our current issue, Dr. Cai and colleagues summarized the role of histone modifications in brain tumor drug resistance [*Xi GF, Mania-Farnell B, Lei T, et al. Histone modification as a drug resistance driver*

✉ Correspondence to: Ting Lei. Email: tlei@tjh.tjmu.edu.cn
* Supported by a grant from the National Natural Sciences Foundation of China (No. 81270865).
© 2016 Huazhong University of Science and Technology

in brain tumors]. Recent studies showed that posttranslational gene regulation such as histone modification provides a critical regulatory platform for chromosome condensation and segregation, gene transcription, and DNA replication and repair. For brain tumors, several studies reported differences in histone modification in adult and pediatric brain tumors compared with normal tissue, indicating that these changes are also characteristics of brain tumors. Histone modifications, including acetylation, methylation, ubiquitylation, or glycosylation on lysine; methylation on arginine; and phosphorylation on serine or threonine, could indirectly or directly influence the ABC transporter and DNA repair, which are both critical mechanisms of drug resistance. The review also included other possible mechanisms thereby histone modifications contribute to drug resistance in glioma treatments. Understanding and uncovering further mechanisms of histone modification that induce drug resistance by using sophisticated techniques will shed new light on glioma therapies.

Compared with traditional therapies, immunotherapies for gliomas have been subjected to in-depth investigations and have drawn a lot of attention. Dendritic cell (DC) vaccination is an active immunotherapy that trains the immune system of the body to create an antitumoral response. We have been working on basic research and clinical applications of DCs in glioma treatment for several years and have shown in a pilot clinical study that whole tumor extract-pulsed DC injection can significantly prolong the survival of patients with glioblastoma multiforme. However, we could not clearly see any survival benefit in some of the patients. Along with other groups, we realized that whole tumor extract is not really a specific antigen for pulsing DCs. Dr. Wang searched for new antigens for DC vaccination [*Wang Y, Xie RF, Niu HQ, et al. IL-13Ra2- and glioma stem cell-pulsed dendritic cells induce glioma cell death in vitro*]. In this article, she reported that IL-13Ra2 is significantly expressed in gliomas but not in normal brain tissue, and that it does stimulate DC activation. Moreover, she demonstrated that glioma stem cell (GSC) extract significantly triggered DC production, indicating that GSC could also be used as antigen for DC vaccinations. We will continue this work and try to optimize DC immunotherapy to contribute to the improvement of multimodal therapies for glioma in the future.

Malignant brain tumors such gliomas are lethal diseases due to their relapse and drug resistance. Benign tumors could also be fatal because of difficulties in surgeries and complications in the perioperative period. Craniopharyngiomas are epithelial tumors that arise from embryonic epithelial cells of the craniopharyngeal duct, which have a tendency to invade the critical neurovascular structures, particularly the visual pathways and hypothalamus, resulting in high morbidity and mortality. We have been using the transsphenoidal approach to treat infradiaphragmatic craniopharyngioma, and have shared some of our experiences in the current issue. We recommend the transsphenoidal approach because it could preserve pituitary function and avoid damages to the hypothalamic structures and optic nerve. Moreover, for tumors that could not be totally removed at one time, the transsphenoidal approach is an ideal technique for resecting infradiaphragmatic tumors.

Pituitary adenomas are also quite common brain tumors in the central nervous system, different subtypes of pituitary adenoma are identified according to their hormone secretion. Prolactinomas, which has the highest incidence rate in pituitary adenomas, are unique for its treatment with dopamine agonist. A few studies demonstrated that bromocripitne treatment could influence tumor consistency which is a very important factor for surgery. We summarized 238 patients of prolactinoma who underwent transphenoidal surgery in our center (Department of Neurosurgery, Tongji Hospital, Tongji Medical College, Huazhong University of Science and Technology, Wuhan, China), and we found that female patients who took dopamine agonist before surgery have harder tumor consistency, however with male patients we did not see any difference [*Huang YM, Hu F, Wu K, et al. Sex-related changes in tumor consistency in prolactinoma patients after bromocriptine pretreatment*]. This information may give neurosurgeons suggestions before operations.

Brain tumors are complicated cancers because of their location and histology. Understanding their molecular mechanisms of tumorigenesis and drug resistance could help optimize treatments. The last decades have seen great advances in basic and clinical research on brain tumors, and sophisticated techniques such as high throughput sequencing accelerate the development of personalized medicine in brain tumor treatment. This issue presents some of the new findings and summaries of cases of brain tumors in basic and clinical research. Hopefully, this will inspire our colleagues in this field.

References

1. Dolecek TA, Propp JM, Stroup NE, *et al*. CBTRUS statistical report: primary brain and central nervous system tumors diagnosed in the United States in 2005–2009. Neuro Oncol, 2012, 14 Suppl 5: v1–v49.
2. Ohgaki H, Kleihues P. Epidemiology and etiology of gliomas. Acta Neuropathol, 2005, 109: 93–108.

DOI 10.1007/s10330-016-0190-4
Cite this article as: Hu F, Lei T. Multimodal therapy for brain tumors. Oncol Transl Med, 2016, 2: 195–196.

Oncology and Translational Medicine
DOI 10.1007/s10330-016-0170-8
October 2016, Vol. 2, No. 5, P197–P202

ORIGINAL ARTICLE

Transsphenoidal microsurgical treatment of infradiaphragmatic craniopharyngioma*

Ting Lei(✉), Baofeng Wang, Juan Chen, Yu Xu, Kai Shu, Wei Sun, Shaozheng Liu Xiaopeng Li

Department of Neurosurgery, Tongji Hospital, Tongji Medical College, Huazhong University of Science and Technology, Wuhan 430030, China

Abstract

Objective Typically, the transcranial approach has been used for the treatment of craniopharyngiomas with suprasellar extension, whereas the transsphenoidal approach has been used mostly for infradiaphragmatic craniopharyngioma. Total resection of craniopharyngioma can reduce the recurrence rate, especially in young children, but it may lead to severe complications. Therefore, any benefit of the degree of resection must be weighed against the risk of complications by the surgeons. The purpose of this study was to explore the therapeutic outcome after transsphenoidal microsurgical treatment of infradiaphragmatic craniopharyngioma and share our experiences.

Methods Between January 2003 and June 2013, 30 patients with infradiaphragmatic craniopharyngioma underwent transsphenoidal microsurgical resection in our hospital. The neurological, visual, and endocrine functions, and extent of resection were analyzed retrospectively. Recurrence or growth of residual tumor tissue during follow-up was assessed using magnetic resonance imaging (MRI).

Results Total resection was achieved in 25 patients (83.3%), subtotal resection was achieved in 4 patients (13.3%), and partial resection was achieved in 1 patient (3.4%). There were no perioperative deaths. Cerebrospinal fluid (CSF) leakage occurred in 6 patients, and among them, 2 required surgical repair of the sella. New-onset postoperative diabetes insipidus (DI) developed in 8 patients. Vision and visual fields were improved at different levels in 13 out of 16 patients who had sight impediments before treatment. Tumor recurrence and regrowth was observed in 2 patients; 1 patient underwent transsphenoidal reoperation, the condition of the other patient who had undergone several craniotomies grew worse over the 6-month follow-up period.

Conclusion Transsphenoidal surgery is an ideal choice in treating infradiaphragmatic craniopharyngioma. The transsphenoidal approach, which preserves pituitary function and avoids damage to the hypothalamic structures and optic nerve, is associated with fewer complications than the transcranial approach and a low mortality rate.

Received: 8 July 2016
Revised: 15 August 2016
Accepted: 25 September 2016

Key words: craniopharyngioma; transsphenoidal approach; therapeutic effect

Craniopharyngiomas are epithelial tumors that arise from embryonic epithelial cells of the craniopharyngeal duct. They account for 1% of all primary intracranial neoplasms in adults and 1%–3% of intracranial tumors in children [1]. Despite their benign histological nature, craniopharyngiomas have a tendency to invade critical neurovascular structures, particularly the visual pathways and hypothalamus, resulting in high morbidity and mortality.

Craniopharyngiomas are localized to the sella or under the diaphragma sellae, where it is referred to as an infradiaphragmatic craniopharyngioma. The choice of surgical approach for craniopharyngiomas is closely associated with the tumor position, size, and texture. Typically, the transcranial approach has been used for the treatment of craniopharyngiomas with suprasellar extension, whereas the transsphenoidal approach has been used mostly for infradiaphragmatic craniopharyngiomas [2]. Total resection

✉ Correspondence to: Ting Lei. Email: tlei@tjh.tjmu.edu.cn
*Supported by the grants from the National Clinical Key Specialty Construction Project and National Natural Science Foundation of China (No. 81270865).
© 2016 Huazhong University of Science and Technology

Table 1 Clinical characteristics of 30 patients who underwent transsphenoidal surgery for infradiaphragmatic craniopharyngioma

Variable	Children		Adults		Total	
	n	%	*n*	%	*n*	%
Number of patients	8		22		30	
Mean age (years) at surgery	13.4		32.7		27.6	
Female	4	50	13	59.1	17	56.7
Previous surgery	0		2	9.1	2	6.6
Headache	3	37.5	16	72.7	18	63.3
Adrenal function deficit	2	25	8	36.4	10	33.3
Menstrual disorder	1	12.5	7	31.8	8	26.7
Hypogonadism			1	4.5	1	4.5
Growth delay	3	42.9			3	42.9
Hyperprolactinemia	4	50	4	18.2	8	26.7
Polyuria and polydipsia	2	25	2	9.1	4	13.3
Visual deficit	4	50	12	54.5	16	53.3

* Values given as number of patients (%) unless otherwise indicated. Children is defined as <18 years old, adults as ≥ 18 years old

can reduce the recurrence rate, especially in young children, but it may lead to severe complications. Therefore, any benefit of the degree of resection must be weighed against the risk of complications by the surgeons. In this paper, we present our experiences and the therapeutic effects of 30 cases of infradiaphragmatic craniopharyngioma treated with transsphenoidal surgery.

Materials and methods

Patients

From January 2003 to June 2013, 30 patients with infradiaphragmatic craniopharyngioma were treated using transsphenoidal microsurgery in our hospital. Patient consent and approval from the Institutional Review Board of Tongji Hospital were obtained for this study. The patient group consisted of 22 adults (9 men and 13 women) and 8 children (4 boys and 4 girls). The age of the patients ranged from 4 to 50 years (mean 27.6 years). Twenty-seven patients had received no previous treatments. One patient had undergone two craniotomies and one γ-knife treatment elsewhere. One patient presented with recurrence after undergoing a transsphenoidal operation elsewhere. One patient had undergone one γ-knife treatment elsewhere.

Clinical symptoms

The main clinical characteristics of the 30 patients are summarized in Table 1. The preoperative duration of symptoms due to the tumor varied between 1 week and 17 years (mean 2.1 years). Principal complaints and symptoms included decreased vision and/or temporal hemianopsia in 16 cases, headache in 19 cases, hypogonadism in 1 case, growth delay in 3 cases, polyuria and polydipsia in 4 cases, menstrual disorder in 8 cases, and hyperprolactinemia in 4 cases.

Neuroimaging evaluation

Location, size, degree of cystoid variation, calcification, and sellar enlargement of the tumor were evaluated on films of computed tomography (CT) and magnetic resonance imaging (MRI). The masses measured between 5 mm and 35 mm in diameter. The principal mass was located exclusively in the sella in 23 cases, partially in the sella and suprasellar region in 7 cases. Calcifications were found in 16 craniopharyngiomas, and cysts were observed in all cases.

Endocrinological evaluation

During the preoperative period, the prolactin level increased (from 28.07 ng/mL to 76.19 ng/mL) in 8 patients (2 men and 6 women), thyroid function decreased in 6 patients. An adrenal function deficit occurred in 10 patients.

Surgical procedure

The transsphenoidal approach, which has the advantage of offering better exposure of the bottom of the sphenoid sinus, can be used for infradiaphragmatic craniopharyngiomas located in the sella. The sphenoid sinus was opened; using rongeurs and a drill, the sinus opening was widened and its septum removed, especially exposing the window to the slope. Since most of the bony wall of the sphenoid sinus was eroded by the tumor, and the mucus membrane laid directly against the dura mater. It was important to keep the dura intact during mucus membrane and bony dissection. After the dura of the sellar floor was widely opened according to the size of the tumor using micro scissors, a tumor with capsule of variable thickness was often exposed immediately. Subsequently, subcapsule tumor debulking was undertaken gently using aspiration. The capsule of the tumor could be dissected in 3 planes as follows. First, capsular adhesion of the slope was dissected from the dura after coagulation. Capsular

adhesion near the normal pituitary gland was then dissected. Since the normal pituitary gland acted as a barrier, tumor adhesion in this area could be easily detached. Subsequently, the contralateral tumor was dissected. In cases of tight adhesion, it was treated by coagulating the walls of tumor along the cavernous sinuses and then cutting. If the adhesion was difficult to detach, the plane of the diaphragma sellae could be dissected in advance. Finally, dissection of tumor adhesion located in the plane of the diaphragma sellae. The normal pituitary gland was protected cautiously, because it was often seen at the surface. Meanwhile, due to the different levels of collapse, the diaphragma sellae was dissected gently along the capsule, and then the capsule was cut after coagulating the base of capsule. Intraoperative CSF leakage might occur during the dissection, which was controlled either with hemostatic gauze or with a small cotton pad. The resection of the calcified part of the tumor was slow and meticulous. Since the diaphragma sellae was involved with the tumor, it could be deficient to differing extents. Therefore, repair of the diaphragma sellae was crucially important. In our cases, all sellar floor repairs were performed with autogenous fascia and fat.

Follow-up review

Postoperative endocrinological and ophthalmological evaluations were performed 1 week after surgery. MRI and endocrinological evaluation were performed 3 months after surgery. Subsequently, MRI was repeated annually. The duration of follow-up in this study was from 6 months to 116 months. Fig. 1 and 2 present two representative cases.

Results

Extent of resection

The tumors were totally resected in 25 (83.3%; 2 representative cases shown in Fig. 1 and 2), subtotally resected in 4 (13.3%), and partially resection in 1 (3.4%). During the follow-up period, 2 patients demonstrated a recurrence.

Surgical complications

Postoperative CSF leakage occurred in 6 patients. Among them, 2 patients required transsphenoidal sellar repair. In 4 patients, CSF leakage was successfully resolved after continuous lumbar drainage. Other compli-

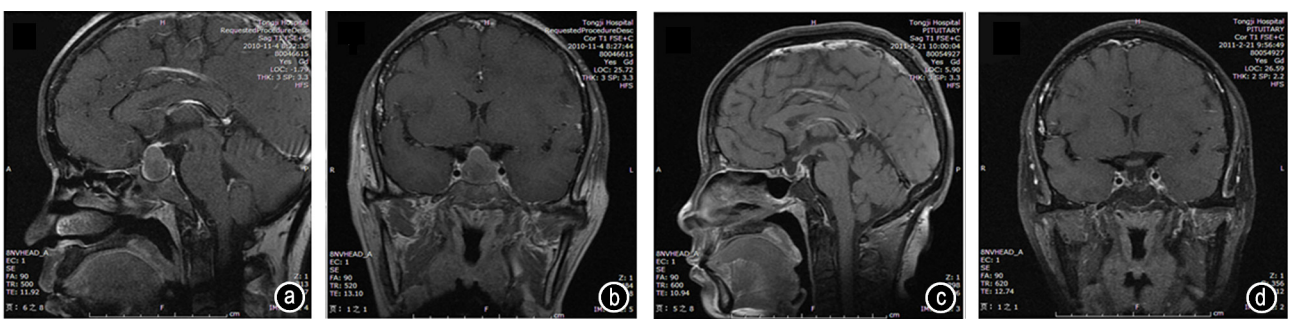

Fig. 1 Preoperative and postoperative enhanced magnetic resonance (MR) images of the treatment of infradiaphragmatic craniopharyngioma. Preoperative sagittal (a) and coronal (b) MR images showing that the sella was enlarged, diaphragma sellae was raised, and tumor was separated from suprasellar structures by the diaphragma sellae. Postoperative sagittal (c) and coronal (d) MR images showing that the diaphragma sellae was collapsed and the pituitary gland together with the pituitary stalk were well preserved

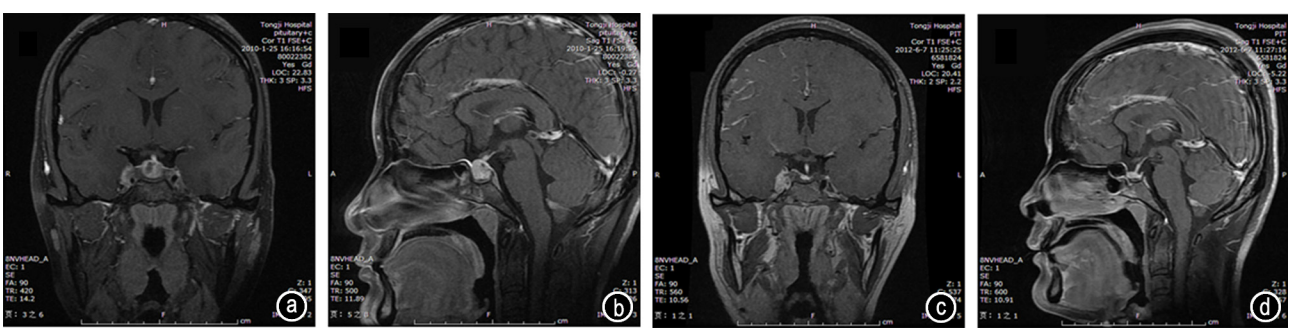

Fig. 2 Preoperative and postoperative enhanced magnetic resonance (MR) images of the treatment of infradiaphragmatic craniopharyngioma. Preoperative coronal (a) and sagittal (b) MR images showing that the tumor was mainly located in the sella and the diaphragma sellae was raised. Postoperative coronal (c) and sagittal (d) MR images showing that the diaphragma sellae was collapsed and the pituitary gland together with the pituitary stalk were well preserved

cations included 7 cases of diabetes insipidus and 2 cases of electrolyte disturbance, which resolved after 3 months. The condition of 1 patient who had undergone several craniotomies grew worse during the follow-up period of half a year.

Visual evaluation

Vision and visual fields improved at different levels in 13 out of 16 patients who had sight impediments before the operation. There were no permanent visual deficits.

Postoperative endocrinological evaluation

A postoperative normalization of excessive prolactin secretion was found in eight patients. Preoperative adrenal function deficit in one patient was back to normal after surgery. Normal thyroid function decreased after surgery in 4 patients. The normal level of cortisol was reduced after surgery in 2 patients. The newly disturbed functions normalized after 3 months.

Discussion

Morbidity characteristic

No significant sex difference was found to exist in terms of the incidence of craniopharyngiomas. However, in an analysis of a large sample of cases, craniopharyngiomas were detected more frequently in male rather than female patients [3]. Seventeen (56.7%) female patients were included in this group. Children aged between 5 and 9 years and adults aged between 40 and 44 years had the highest incidence of this disease. Of the 30 patients, 11 (36.7%) patients were aged between 18 and 30 years; 8 (26.7%) patients aged between 40 and 50 years; 8 (26.7%) patients were younger than 18 years and 2 (6.7%) patients were aged between 30 and 40 years.

Clinical symptoms

Generally, the principal signs and symptoms of craniopharyngiomas included headache, visual impediments, diabetes insipidus, and hypopituitarism. The initial symptoms of young children were different from those of adult patients. Endocrine disorder, progressive loss of vision, and intracranial hypertension mostly occur in children, while impaired vision mostly occurs in adults [4–5]. In our series, 3 (37.5%) children complained of headache and 12 (54.5%) adult patients complained of decreased vision. In our cases, 25% of the patients with visual impediments were diagnosed with bitemporal hemianopsia. Intrasellar craniopharyngiomas can affect the function of the anterior pituitary, resulting in hypopituitarism and developmental delay in patients younger than 18 years of age. In our cases, 2 of 8 juvenile patients demonstrated developmental delay, while those older than 18 years exhibited hypogonadism. Craniopharyngiomas can also increase the occurrence of endocrine symptoms such as amenorrhea-galactorrhea syndrome in female patients and hypogonadism in male patients. In our group, 4 adult patients demonstrated excessive prolactin secretion causing menolipsis together with/ without lactation, other menstrual disorders, and hypogonadism. The tumor can also affect the function of the posterior pituitary, resulting in diabetes insipidus; 6.7% of the patients in our cases developed symptoms of diabetes insipidus.

Neuroimaging evaluation

On imaging studies, most tumors are of lobular shape, while a few are rounded with a clear border. According to their structure, tumors can be separated into 3 types: cystic, solid, and cyst-solid. As to the cyst-solid mass, the cystic region is typically located superiorly and the solid region is located inferiorly. MRI suggests that most regions of cystic change show high signal intensity on T1-weighted images. In tumors with two or more cystic areas, the signal intensity can be the same or different. The reason for the high signal intensity on T1-weighted images in cystic regions is that cystic fluid contains higher protein content, including one or more of the following: cholesterol, triacylglycerol, methemoglobin (with a history of bleeding), calcifications, and epithelial exfoliation. Areas of cystic change generally show high signal intensity on T2-weighted images, but a few regions may show low signal intensity, probably because they contain calcifications or hemosiderin. Solid craniopharyngiomas and the solid part of cystosolid craniopharyngiomas show uniform T1-weighted imaging signal intensity and uniform or high T2-weighted imaging signal intensity. A few lesions with calcifications and keratoprotein or sporadically located in trabecular bone show low signal intensity both on T1-weighted images and T2-weighted images. Both CT and MRI reveal that at times large cysts have an air-fluid level. MR enhancement scans show that the enhanced extent of normal glands is significantly higher than that of tumorous tissues. Normal glands crushed flat by medium-sized tumors appear as a lamellar band with high signal intensity. In general, they are pressed beneath the tumor or are unaffected.

Differential diagnoses

Craniopharyngioma in the sellar region should be distinguished from cystic pituitary adenoma, Rathke cleft cyst, pituitary abscess, and epidermoid cyst. Differential diagnoses are mainly made through imaging tests before surgery; calcification in craniopharyngiomas can be detected on CT imaging, but not in other tumors. MRI demonstrates that the principal differences are as follows:

(1) Cystic pituitary adenomas are always visibly connected with the pituitary gland or the normal pituitary gland is not visible. Due to the different contents of the

cystic fluid, the interface of the two signals frequently appears with an intracapsular air-fluid level. MR enhancement scans show that the capsule wall and solid part of the tumor are significantly enhanced.

(2) Rathke cleft cysts involve the intrasellar region and often extend upward. They usually have the following imaging features: a homogeneous signal intensity within the lesion, lack of internal enhancement, and small variance in the lesion during the follow-up period.

(3) The characteristics of pituitary abscess include a history of fever, lesions involving the whole pituitary gland, disappearance of the normal pituitary gland on imaging, and posterior pituitary symptoms.

(4) The typical signal intensity of epidermoid cysts is equal to that of cerebrospinal fluid. Enhancement scans show that the tumors are not enhanced.

Selection of surgical approach and results

The ideal surgical approach has been controversial since craniopharyngioma was first removed surgically. According to the tumor position, size, texture, and surgeon comfort, there are 3 major types of surgery: transcranial surgery, transsphenoidal surgery, and drainage. Among them, transcranial surgery includes the pterional approach, subfrontal approach, transcallosal approach, and transcortial-transventricular approach [6]. The principal for the selection of different approaches is based on the location and adhesion of the main tumor.

The selections of surgical approach in different treatment groups are related to the preference and experience of the surgeons. The proportional use of the transsphenoidal approach in craniopharyngioma ranges 10%–75% [6]. Transsphenoidal surgery was initially considered to remove intrasellar craniopharyngioma due to the development of tumors from the intrasellar area to the sphenoid sinus. Surgeons could not remove them under visual control by choosing the transcranial approach; therefore, transsphenoidal approach was the absolute operation indication. When a craniopharyngioma in the sellar region was within an enlarged sella turcica, the suprasellar lesion was located under the diaphragma sellae, which acted as an anatomic barrier preventing invasion of or adherence to vital structures. Since a part of suprasellar lesions could be removed by transsphenoidal surgery, the surgical indication was expanded to include infradiaphragmatic craniopharyngioma [7]. Owing to developments in the extended transsphenoidal approach and use of endoscopy, reports of treating craniopharyngiomas located in the suprasellar area, parasellar region, and in the third ventricle using transsphenoidal surgery have increased.

The use of transsphenoidal surgery is convincing. Craniopharyngiomas involving the sella turcica are often cystic or friable [8–9] making intracapsular resection relatively easy. Infradiaphragmatic craniopharyngioma usually does not infiltrate surrounding structures. Therefore, excision of the capsule from the optic chiasm, hypothalamus, and pituitary stalk can be carefully performed [10]. Transsphenoidal surgery involves less severe trauma, better exposure of sellar lesions, and more efficient decompression of the chiasm and optic nerves with reduced risk of vision worsening [11] compared with transcranial approaches. The total resection rate of transsphenoidal microsurgical treatment of infradiaphragmatic craniopharyngioma as reported in the literature ranges from 27.7% to 89.7%; in our study, total resection was achieved in 25 patients (83.3%). The patients who undergo subtotal resection should receive stereotactic or general radiotherapy. During the follow-up period, one patient exhibited recurrence 2 years after surgery, and underwent further transsphenoidal surgery. No recurrence occurred in any other patients. Compared with the 8% reported in a Meta-analysis, the rate of the postoperative recurrence of craniopharyngioma ranges 0–17.6% [6]. In our study, the recurrence rate was 3.6%.

Table 2 Comparison of the results pre-and post operation

Variable	Preoperative cases		Postoperative cases	
	n	%	*n*	%
Diabetes insipidus	4	13.4	12	40
Adrenal function deficit	10	33.3	11	36.7
Thyroid function deficit	2	6.7	6	20
Hyperprolactinemia	8	26.7	0	0
Visual deficit	16	53.3	3	10

The postoperative recovery rate of patients with vision or visual field defects ranges from 70% to 90% in transsphenoidal surgery, a higher recovery rate than transcranial surgery in general [4]. In our study, the recovery rate was 81.3%, similar to results reported in the literature. The patients with preoperative endocrinological diseases did not improve after surgery. Two patients with preoperative diabetes insipidus are receiving long-term pharmacological treatment to control urine volume, and 2 patients with preoperative hypothyroidism also needed to take long-term medication after the operation. Postoperative normalization of excessive prolactin secretion was detected in 8 patients, and the clinical symptoms dissipated. Similar cases were also reported by other groups that preoperative hypopituitarism is rarely cured after surgery, and most patients with high level of prolactin recover after their operation [12]. The results regarding visual deficits and endocrinological function pre-and postoperatively are shown in Table 2.

Complications

Diabetes insipidus is the most frequent endocrinopathy following both transsphenoidal surgery and transcranial surgery for craniopharyngioma [8]. The ratio of patients with postoperative diabetes insipidus reported by

treatment groups differ. One group reported that 60% of patients were diagnosed with diabetes insipidus [8]. The histological type of tumor and frequent disturbance of the pituitary stalk in transcranial surgery are probably the reasons that the ratio of patients with postoperative diabetes insipidus (54.8%) after transcranial surgery is higher than the 31.7% after transsphenoidal surgery. In our group, 8 (26.7%) patients were newly diagnosed with diabetes insipidus after surgery, and they were cured in 3 months. Electrolyte disturbance appeared in 2 patients and resolved after appropriate drug treatment. The most common technical complication of transsphenoidal surgery is CSF leakage. Materials for repairing the sellar floor are varied, including titanium mesh, silicon resin, and nasal bone fragments glued using fibrin glue. Fat, fascia, and fibrin glue were used by Buchfelder M *et al* to reconstruct the sellar floor [1]. As a study in the literature has reported, the incidence of CSF leakage ranges from 2% to 33% [13]. In our cases, all sellar floors were patched with autogenous broad fascia and fat. Postoperative CSF leakage occurred in 6 (20%) patients and was successfully treated through continuous lumbar drainage or repair of the sellar floor. None of the patients with CSF leakage experienced meningitis. Six patients were newly diagnosed with pituitary dysfunction, and the disturbed function normalized after 3 months. Since the 1980s, the perioperative mortality of craniopharyngioma decreased from 9% to 0% with progress in microtechniques and improvement of surgical skills. There were no cases of perioperative death in our group, although in one patient, the condition worsened because of impaired hypothalamus function over the 6-month follow-up period.

Conclusions

Transsphenoidal surgery is an ideal choice in treating infradiaphragmatic craniopharyngioma. The patients whose tumors were not totally resected should receive stereotactic or general radiotherapy to reduce the risks of recurrence. Routine repair of diaphragma sellae is needed during the operation, and postoperative CSF leakage can be mostly cured. The transsphenoidal approach, which preserves pituitary function and avoids damages to the hypothalamic structures and optic nerve, is associated with fewer complications and a lower mortality rate compared with the transcranial approach. For tumors that could not be or were not totally resected in the first operation, total resection would be more difficult or impossible during a secondary operation.

Conflicts of interest

The authors indicated no potential conflicts of interest.

References

1. Prevedello DM, Doglietto F, Jane JA, *et al*. History of endoscopic skull base surgery: its evolution and current reality. J Neurosurg, 2007, 107: 206–213.
2. Honegger J, Tatagiba M. Craniopharyngioma surgery. Pituitary, 2008, 11: 361–373.
3. Nielsen EH, Feldt-Rasmussen U, Poulsgaard L, *et al*. Incidence of craniopharyngioma in Denmark (n = 189) and estimated world incidence of craniopharyngioma in children and adults. J Neurooncol, 2011, 104: 755–763.
4. Komotar RJ, Starke RM, Raper DM, *et al*. Endoscopic endonasal compared with microscopic transsphenoidal and open transcranial resection of craniopharyngiomas. World Neurosurg, 2012, 77: 329–341.
5. Lopez-Serna R, Gomez-Amador JL, Barges-Coll J, *et al*. Treatment of craniopharyngioma in adults: systematic analysis of a 25-year experience. Arch Med Res, 2012, 43: 347–355.
6. Buchfelder M, Schlaffer SM, Lin F, *et al.* Surgery for craniopharyngioma. Pituitary, 2012, 16: 18–25.
7. Laws ER, Jr. Transsphenoidal microsurgery in the management of craniopharyngioma. J Neurosurg, 1980, 52: 661–666.
8. Honegger J, Buchfelder M, Fahlbusch R. Surgical treatment of craniopharyngiomas: endocrinological results. J Neurosurg, 1999, 90: 251–257.
9. Maira G, Anile C, Albanese A, *et al*. The role of transsphenoidal surgery in the treatment of craniopharyngiomas. J Neurosurg, 2004, 100: 445–451.
10. Landolt AM, Zachmann M. Results of transsphenoidal extirpation of craniopharyngiomas and Rathke's cysts. Neurosurgery, 1991, 28: 410–415.
11. Fahlbusch R, Honegger J, Paulus W, *et al*. Surgical treatment of craniopharyngiomas: experience with 168 patients. J Neurosurg, 1999, 90: 237–250.
12. Chakrabarti I, Amar AP, Couldwell W, *et al*. Long-term neurological, visual, and endocrine outcomes following transnasal resection of craniopharyngioma. J Neurosurg, 2005, 102: 650–657.
13. Frank G, Pasquini E, Doglietto F, *et al*. The endoscopic extended transsphenoidal approach for craniopharyngiomas. Neurosurgery, 2006, 59: ONS75–83.

DOI 10.1007/s10330-016-0170-8
Cite this article as: Lei T, Wang BF, Chen J, *et al*. Transsphenoidal microsurgical treatment of infradiaphragmatic craniopharyngioma. Oncol Transl Med, 2016, 2: 197–202.

Oncology and Translational Medicine
DOI 10.1007/s10330-016-0180-6

October 2016, Vol. 2, No. 5, P203–P209

ORIGINAL ARTICLE

Sex-related changes in tumor consistency in prolactinoma patients after bromocriptine pretreatment*

Yimin Huang, Feng Hu, Kang Wu, Juan Chen, Ran Li, Hao Xu, Ting Lei (✉)

Department of Neurosurgery, Tongji Hospital, Tongji Medical College, Huazhong University of Science and Technology, Wuhan 430030, China

Abstract

Objective It has long been reported that prolactinomas treated with bromocriptine increase fibrosis and may affect surgical outcomes. We retrospectively studied 238 consecutive patients with histopathologically confirmed prolactinomas undergoing microsurgery in a single neurosurgery department of Tongji Hospital (Wuhan, China) from 2012 to 2015 in order to evaluate tumor consistency changes after bromocriptine pretreatment and surgical outcomes.

Methods We divided the patients into four groups: males in the dopamine agonist (DA) group, females in the DA group, males in the no DA group, and females in the no DA group, and we compared the surgery process, specimen Masson staining, and clinical outcomes of the four groups. According to a previously published classification, the operative notes from an experienced neurosurgeon were reviewed to classify the consistency of tumors as "fibrous" or "nonfibrous".

Results No differences in tumor consistency were found in male patients with or without DA treatment. However, in female patients with DA treatment, tumors were likely to be harder in texture than the tumors of female patients without DA treatment. Despite tumor consistency differences between sexes, the tumor biological remission rate was similar between groups, as was the rate of tumor resection.

Discussion Our study indicates that preoperative DA therapy impacts tumor consistency in female patients but not male patients. Although the surgical and histopathological outcomes are not influenced, these findings may provide useful information for the choice of operative approach and surgery process for pituitary adenoma.

Received: 4 August 2016
Revised: 4 September 2016
Accepted: 25 September 2016

Key words: prolactinoma; bromocriptine; tumor consistency; surgical outcomes

Pituitary adenoma, a type of benign tumor occurring in the pituitary gland, accounts for 10%–20% of central nervous system tumors [1]. Prolactinoma, which has the highest incidence rate (40%) in pituitary adenoma, is caused by pituitary prolactin hormone secretory cell hyperplasia [2–3]. Prolactinomas are unique, for they are pituitary tumors that can be treated with medical therapy. Dopamine agonists (DA) have been the preferred drug therapy of prolactinoma for many years, with bromocriptine as the treatment of choice [4–6]. Since 1985, bromocriptine has been examined as part of a prospective multicenter trial and has gradually become the first-line medication to treat prolactinomas [7].

However, in many cases, patients of either sex do not experience normalization of prolactin levels or obvious tumor shrinkage as confirmed by MRI, are classified as resistant to the DA therapy, and receive surgical treatment [4, 8–10]. In many clinical centers, neurosurgeons have found that the tumor consistency in some patients tends to be tougher and more tensile or, conversely, softer after long-term treatment with DA agonist. Previous studies have demonstrated that after DA therapy, tumor cells and interstitial tissue undergo tumor cell shrinkage and interstitial tissue and perivascular fibrosis [11–17], which has generated some controversy regarding first-line therapy [18–19]. In our clinical experience, we found that the con-

✉ Correspondence to: Ting Lei. Email: tlei@tjh.tjmu.edu.cn
* Supported by a grant from the National Natural Sciences Foundation of China (No. 81270865).
© 2016 Huazhong University of Science and Technology

Table 1 Demographics of patients in this study

Groups	DA (*n* = 106)		No DA (*n* = 132)	
	Male	Female	Male	Female
Number of patients	11	95	45	87
Age (years)	28.7 ± 10.0	29.1 ± 9.5	31.2 ± 9.6	29.4 ± 9.4
Pre-operative PRL level (ng/mL)	1397.8 ± 544.4	268.4 ± 27.8	1952.2 ± 354.0	344.1 ± 75.0
% Patients presenting with amenorrhea	N/A	74.7%	N/A	67.8%
% Patients presenting with sexual disfunction	81.8%	N/A	75.6%	N/A
% Patients with macroprolactinoma	61%		68%	

sistency of tumors is different between males and females after bromocriptine pretreatment, and the surgical outcomes are not identical.

In this study, our aim was to study sex differences in the relationship between DA pretreatment and tumor consistency. In our clinical center, in order to evaluate the choice of bromocriptine in treating male or female patients with prolactinomas, we assessed prolactinoma tumor consistency after DA therapy and the correlation of DA pretreatment with postoperative remission rates between the two sexes.

Patients and methods

Patient population

In our study, 238 patients were included, all of whom underwent transsphenoidal surgery with histopathologically confirmed prolactinomas from 2012 to 2015 at Tongji Hospital, Wuhan, China. Demographics included: 50 patients (Male, 5; Female, 45) with microprolactinomas and 188 patients (Male, 51; Female, 137) with macroprolactinomas. Of these, 106 patients (Male, 11; Female, 95) previously received DA treatment (> 3 months) and 132 (Male, 45; Female, 87) directly underwent surgery because of tumor local compression, intolerance to bromocriptine, or strong desire for reproduction. Of the 106 patients exposed to bromocriptine, 2 (Male, 0; Female, 2) also received Gamma Knife treatment. The rest of the patients were treated by bromocriptine intake only. The total mean bromocriptine cumulative dose in all patients was 1.2 mg, ranging from 0.25 to 1.5 mg per day, over 90–350 days. Demographic data were shown in Table 1.

Data collection and analysis

All preoperative and postoperative radiographic tests were obtained from our institution, and postoperative MRI scans were collected in the outpatient department when patients were referred to physicians. Initial pre, peri, and postoperative endocrine data were obtained from Tongji Hospital medical records and from records of referring and consulting physicians. Initial prolactin level refers to the earliest known documented level prior to medical therapy. The hormone statics were evaluated within 5 days before surgery, and the postoperative prolactin (PRL) levels were tested 2 days to 3 months after surgery and defined as the immediate postoperative PRL levels. As in a previous classification [20], the patients were separated into two groups: "DA" if they had received preoperative treatment with bromocriptine and "no DA" if surgery was the first-line definitive therapy and there was no known exposure to bromocriptine. The exclusion criteria included missing information of preoperative prolactin levels, patients with a history of prior surgery or radiotherapy, or missing information of prolactin levels after surgical treatment.

Tumor consistency and Masson staining value

According to classification by Menucci [15], tumor consistency was described by the surgeon in the operative notes as "firm", "solid", "difficult to resection", "hard", "close adhesion to peri-tissue", or "difficult to resect tumor by aspirator" indicating fibrous consistency, or "soft", "easily resect tumor by aspirator", or "typical consistency" indicating nonfibrous consistency. We collected prolactinoma tumor tissue from 25 patients to stain using the Masson procedure. In order to concisely conclude the Masson staining result, the fibrous positive was defined as high fibrous expression in a single field.

Radiographic and hormone data analysis

The radiographic tumor volume data were acquired by high resolution MRI and estimated by tracing the tumor using transparent film and measuring mean diameter of each section. The tumor resection rate data were collected by comparing the postoperative and preoperative tumor volume, using an analysis method known as the platform-like volume calculation formula developed by Wang [21]. The surgery efficacy was determined by immediate PRL level and MRI data of the patient more than 6 months after surgery. Patients who necessarily received postoperative bromocriptine treatment were estimated during the postoperative period prior to bromocriptine treatment. Curative conditions were defined as follows: normal PRL levels, menstruation recovery in females, and disappearance of lactation symptoms. Ineffective conditions were defined as follows: PRL level reduction rate < 80% or PRL

level unchanged or higher.

Statistical analysis

The characteristics of tumor consistency, sex, presenting symptoms, preoperative prolactin levels, and rates of tumor resection were compared between groups using the chi-squared test. Bonferroni corrections were performed for subgroup analyses when relevant. $P < 0.05$ was considered statistically significant. All continuous variables were presented as mean ± SE.

Results

Tumor consistency

The tumor consistency of patients preoperatively treated with DA was more likely to be described as "fibrous". About 39.6% of patients in the total DA group had tumors depicted as "fibrous" consistency compared with 12.1% of patients in the no DA group ($P < 0.05$). When the patients were analyzed by sex, male and female patients showed different tendencies of tumor consistency change after DA treatment. In female patients, the "fibrous" consistency description was more likely to be found in the DA group than in the no DA group (40% vs. 16%, $P < 0.05$, Table 2). In male patients, the "fibrous" consistency description was generally less likely to be found in the DA group than in the no DA group, but there was no significant difference between them (43% vs. 47%, $P > 0.05$, Table 2). To adjust for the effect of the significantly higher pre-therapy PRL levels seen in the DA group, we performed two subgroup analyses. In patients with baseline PRL levels lower than 1000 ng/mL, the proportion of "fibrous" tumor consistency was less in the no DA pretreatment group than in the DA group (0% vs. 39.3%, $P < 0.05$). In other words, when male patients' PRL levels preceding surgery were less than 1000 ng/mL, the tumor tissue consistency of those who received DA was more likely to be nonfibrous and easily resected by aspirator. Among female patients, regardless of preoperative PRL level, those treated with bromocriptine prior to transsphenoidal surgery had remarkably more "fibrous" tumor consistency. The representative intraoperative findings of patients were also shown in Fig. 1.

Table 2 Tumor consistency of prolactinoma patients

Gender	DA pretreatment	Number of patients	Number of fibrous tumor	Chi-square test
Male	DA	11	2	$P = 0.680$
	No DA	45	6	($P > 0.05$)
Female	DA	95	38	$P = 0.003$
	No DA	87	14	($P < 0.05$)

Table 3 Masson staining of tumor tissue slices

Gender	DA pretreatment	Number of patients	Number of fibrous positive tumors	Chi-square test
Male	DA	5	1	$P = 0.293$
	No DA	7	4	
Female	DA	8	7	$P = 0.217$
	No DA	5	2	

Masson staining of tumor tissue slices

From male patients in the DA group, 20% (1/5) of specimens were fibrous positive, compared with 57% (4/7) in the male control group. Compared with 40% (2/5) fibrous positive specimens in female patients of the no DA group, specimens from those in the DA group were 87.5% (7/8) fibrous positive (Table 3). Typical samples were shown in Fig. 2.

Biological and radiographic remission rate

The tumor postoperative biological remission rate was not influenced by DA pretreatment among female prolactinoma patients. The number of females in the DA group who had total biological remission was 81.3% (74/91), similar to the 88.0% (73/83) in the no DA group ($P > 0.05$). Nevertheless, 13.2% of female patients in the DA group and 11.0% in the no DA group had partial biological remission (13.2% vs. 11%, $P > 0.05$, Table 4).

According to radiological reports written by several experienced radiologists, the tumor volumes were pre- and postoperatively evaluated to analyze the tumor resection rate. Regardless of preoperative tumor size, male patients in the DA group showed similar tumor resection rates to male patients in the no DA group (0.46 ± 0.69 vs. 0.88 ± 0.13, $P > 0.05$, Table 5). As shown in the MRI in Fig. 3 and 4, the male macroprolactinoma patients who received DA pretreatment had total tumor resection, and the male macroprolactinoma patient in the no DA group

Table 4 Prolactinoma patients' postoperative immediate PRL remission rate

Gender	DA pretreatment	Number of patients	Number of total remission	Number of partial remission	Number of no remission	Chi-square test
Male	DA	11	2	3	5	$P = 0.000$
	No DA	45	16	21	4	($P < 0.01$)
Female	DA	95	78	12	5	$P = 0.254$
	No DA	87	77	9	1	($P > 0.05$)

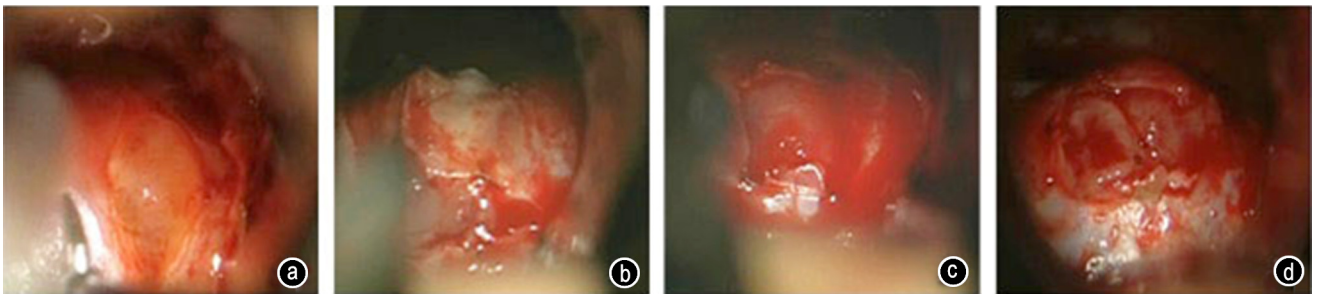

Fig. 1 Typical intraoperative findings in prolactinoma patients. (a and b) Male patients' tumors in both the no DA and DA groups were typically translucent and soft upon incision of the dura mater, which allowed for easy resection by aspirator. (c and d) Tumor of female patient in the DA group was more substantial and solid with fiber separation, and we had to scrape the tumor piecemeal. The texture of the tumor of a female patient in the no DA group was typical and removed by aspirator

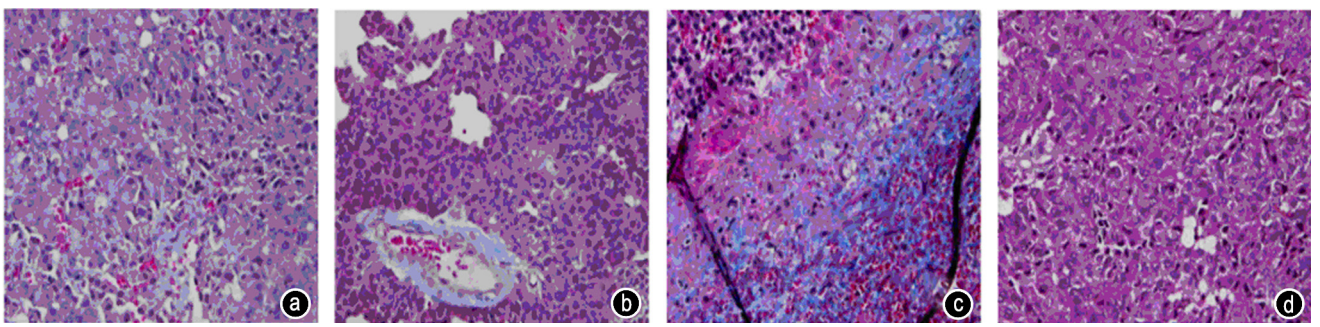

Fig. 2 Masson staining of prolactinoma patients' tumor slices. Tumor tissues of male patients in the DA group (a) showed more tumor cells and vacuole-like cells in single field than those of male patients in the no DA group (b). Interstitial fibrosis (blue staining) was rare in these two slices, and the perivascular fibrosis was not particularly abundant (b). Interstitial fibrosis was much more highly expressed in female patients in the DA group (c) than in females in the no DA group (d)

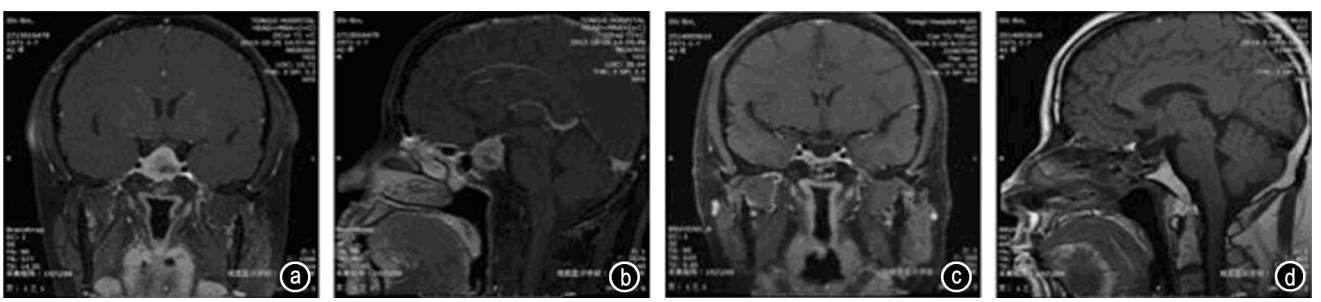

Fig. 3 Representative preoperative (a and b) and postoperative (c and d) MRI of a male prolactinoma patient with DA pretreatment

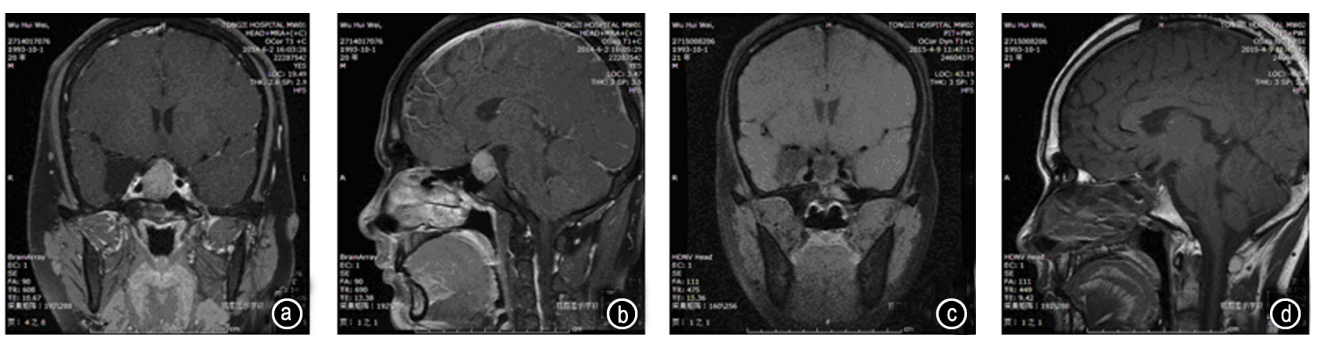

Fig. 4 Representative preoperative (a and b) and postoperative (c and d) MRI of a male prolactinoma patient without DA pretreatment

Table 5 Prolactinoma patients' tumor resection rate

Gender	DA pretreatment	Number of patients	Tumor resection rate	Chi-square test
Male	DA	11	0.46 ± 0.69	$P = 0.319$
	No DA	45	0.88 ± 0.13	($P > 0.05$)
Female	DA	95	0.72 ± 0.54	$P = 0.267$
	No DA	87	0.78 ± 0.23	($P > 0.05$)

also had radiological total tumor removal.

Discussion

Our data suggest that bromocriptine pretreatment increases the tendency of fibrous prolactinoma formation in female patients compared with male patients. We demonstrate that pituitary adenoma texture is sex-related, suggesting that the choice of treatment can be more flexible for male prolactinoma patients. Furthermore, in terms of female prolactinoma patients, contrary to the idea that the increased fibrosis observed in bromocriptine-treated tumors may increase surgery difficulty and the risk of damage to peripheral structures (e.g. normal pituitary), the hormone remission rates and tumor resection rates were identical between the DA and no DA groups. In terms of male prolactinoma patients, DA pretreatment did not influence the surgical outcome or biological remission rate in our clinical center.

Several studies during the last two decades have reported tremendous morphological changes occurring in prolactinomas after treatment with bromocriptine. These changes include: (1) tumor cells often appearing hypercellular because of remarkable cell shrinkage observed by light microscopy; (2) cells exhibiting a significant reduction in cytoplasmic volume, nuclear hyperchromasia, and an increase in the nuclear/cytoplasmic ratio; and (3) long-term treatment causing an increase in extensive interstitial and perivascular fibrosis [11, 13–14, 16]. Our data describe the increased hardness of the tumor from the aspect of surgeon's feeling during the operation process, which in general demonstrates the development of fibrosis in PRL tumors following bromocriptine premedication (Fig. 2c and 2d). Previous studies have not compared male and female patients separately, so the existence of sex differences was unknown. This study suggests that unlike in female patients, the consistency of male patient tumors will not develop a firm texture after pre-surgical bromocriptine treatment. In some cases, particularly those with ordinarily high levels of PRL (under 1000 ng/mL), bromocriptine use pre-surgery may in fact cause soft tumor texture (data not shown).

Prolactinomas are relatively uncommon in men compared to women and are ordinarily large and invasive tumors with high PRL levels at the time of diagnosis. Dopamine agonist therapy can normalize PRL level regardless of tumor size in most men with prolactinomas, although bromocriptine-resistant tumors may be more frequently encountered in men [22–24]. Male patients in the DA group with ordinarily high PRL levels had soft tumors, which may also indicate that prolactinoma consistency is correlated with pre-surgical PRL level. Our Masson staining of tumor specimens suggests that expression of fibrosis in male tumors is not influenced by bromocriptine therapy in comparison with female patients (Fig. 2). We suggest the possible explanation that fibrous formation deficiency occurs in male patients receiving dopamine agonists. Thus, if a tumor is DA-resistant, the structure of the tumor will much more easily collapse, as it is soft because of the lack of interstitial fibrous. In addition, prolactin secreted from the tumor cells is released through the microvasculature to the blood, together with mild prolactin secretion activity due to shrinkage of tumor cells, which eventually presents as ordinarily high, but not extremely high, PRL level.

Compared with female patients, bromocriptine-resistant tumors occur much more frequent in men [22, 25]. Additionally, previous studies showed that male patients' tumors tend to express much more Ki-67 and PCNA, two markers for proliferative activity in tumors [26]. Furthermore, a recent study illustrated that PRL tumors in men are characterized by lower ER-alpha expression, which is related to higher resistance to treatment and worse prognosis [27]. Some researchers discovered a significant down-regulation of the TGF-beta/Smad signaling cascade in DA-resistant prolactinomas, which is the main signaling pathway involved in fibrosis in many organs, including kidney, liver, and lung [28–32]. In summary, we confer that the different changes in tumor consistency between sexes after DA treatment may be caused by different expression of TGF-beta/Smad and ER-alpha between men and women. However, the specific mechanisms of the different results observed in male and female prolactinoma patients remain unclear, requiring further research.

That bromocriptine is related to tumor perivascular/interstitial fibrosis has been reported, but whether fibrosis has a positive or a negative influence on the treatment of prolactinomas is an ongoing debate. In 1982, Landolt first reported that bromocriptine treatment prior to surgery can negatively affect the outcome of microsurgery [33]. The choice of bromocriptine premedication has become a critical question. Surgeons such as Derome and Esiri successively reported the similar discovery that bromocriptine pretreatment may negatively affect operation outcomes [34]. However, the study of DA agonist premedication has shown different results since the 1990s. Turner, Hubbard, and Fahlbusch published their long-term single institutional study reporting that bromocriptine treatment prior to microsurgery had no significant impact on

tumor resection effect and prognosis [13, 35–38]. Conversely, it has been reported that bromocriptine treatment prior to surgery seemed to improve surgical outcome possibly by inducing tumor regression [8, 18, 20, 37].

A possible explanation of these contradictory conclusions is the lack of comparability between the DA group and the no DA group in the former study because the patients were separated only by whether they had received DA pretreatment. The clinical characteristics of patients, such as tumor volume, preoperative PRL level, and sex, were significantly different between groups, which can eventually affect prolactinoma operation outcomes. Further, the entirely contrary results of these reports could be attributed to the small sample number of cases. There have been few multicenter studies using large sample sizes to examine the choice of bromocriptine prior to surgery and related factors. Otherwise, the development of microsurgery techniques, advanced neuronavigation technology, and the application of endoscope-assisted microneurosurgery are important factors that influence the results.

Our results indicate that pretreatment with bromocriptine does not affect surgical outcome as much as previously believed, regardless of patients' sex, and that the biological remission rate does not differ between groups, suggesting that the formation of fibrosis in these patients is irrelevant to their overall outcome.

However, this conclusion is based on an experienced surgeon who performed the microsurgery, along with the tacit cooperation of our surgical team, and we discovered that the presence of fibrosis in the tumor often requires more time and experience to detach the tumor from neighboring tissue. The complexity of hemostasis during the process of separating and resecting tumor was also increased when the tumor fibrous formation was promoted by bromocriptine premedication, according to our and other institutes' surgery reports. These procedures also require more time of the whole surgery, which means the possibility of perioperative events would increase as well. The different morphology of tumor consistency between sexes still can be used as reference for the choice of operative approach. When treating male prolactinoma patients, DA therapy could be more positively chosen by the doctor for the low incidence of tumor consistency changes and negative effects on follow-up operation. In addition, tumors described as fibrous or "hard" may not easily be removed by junior doctors using the transsphenoidal approach; therefore, the level of experience in this study may also provide a reference for choice of surgical approach.

This study is limited by its retrospective nature and small sample size, due to most of the surgery are performed in this year. Thus, long-term follow-up was needed to evaluate the surgical outcome in each group. However, the findings of this study may provide significant reference information for young neurosurgeons, which may offer the most benefit in dealing with nonfibrous tumors. Finally, differences in the outcome of DA pretreatment between male and female patients still require further multicenter study.

Conclusion

Our study indicates that preoperative dopamine agonist therapy impacts tumor consistency in female but not male prolactinoma patients. Although the surgical outcomes and histopathological outcomes were not influenced, our findings may provide some useful information in the choice of pituitary adenoma surgical process. Finally, the mechanisms underlying these differences warrant further exploration.

Conflicts of interest

The authors indicated no potential conflicts of interest.

References

1. Gillam MP, Molitch ME, Lombardi G, *et al*. Advances in the treatment of prolactinomas. Endocr Rev, 2006, 27: 485–534.
2. Colao A. Pituitary tumours: the prolactinoma. Best Pract Res Clin Endocrinol Metab, 2009, 23: 575–596.
3. Kars M, Dekkers OM, Pereira AM, *et al*. Update in prolactinomas. Neth J Med, 2010, 68: 104–112.
4. Klibanski A. Clinical practice. Prolactinomas. N Engl J Med, 2010, 362: 1219–1226.
5. Reichlin S. The prolactinoma problem. N Engl J Med, 1979, 300: 313–315.
6. Vance ML, Evans WS, Thorner MO. Drugs five years later. Bromocriptine. Ann Intern Med, 1984, 100: 78–91.
7. Molitch ME, Elton RL, Blackwell RE, *et al*. Bromocriptine as primary therapy for prolactin-secreting macroadenomas: results of a prospective multicenter study. J Clin Endocrinol Metab, 1985, 60: 698–705.
8. Hamilton DK, Vance ML, Boulos PT, *et al*. Surgical outcomes in hyporesponsive prolactinomas: analysis of patients with resistance or intolerance to dopamine agonists. Pituitary, 2005, 8: 53–60.
9. Losa M, Mortini P, Barzaghi R, *et al*. Surgical treatment of prolactin-secreting pituitary adenomas: early results and long-term outcome. J Clin Endocrinol Metab, 2002, 87: 3180–3186.
10. Smith TR, Hulou MM, Huang KT, *et al*. Current indications for the surgical treatment of prolactinomas. J Clin Neurosci, 2015, 22: 1785–1791.
11. Anniko M, Wersäll J. Morphological changes in bromocriptine-treated pituitary tumours. Acta Otolaryngol, 1983, 96: 337–353.
12. Asa SL, Ezzat S. Medical management of pituitary adenomas: structural and ultrastructural changes. Pituitary, 2002, 5: 133–139.
13. Hubbard JL, Scheithauer BW, Abboud CF, *et al*. Prolactin-secreting adenomas: the preoperative response to bromocriptine treatment and surgical outcome. J Neurosurg, 1987, 67: 816–821.
14. Kontogeorgos G, Horvath E, Kovacs K, *et al*. Morphologic changes of prolactin-producing pituitary adenomas after short treatment with dopamine agonists. Acta Neuropathol, 2006, 111: 46–52.
15. Menucci M, Quiñones-Hinojosa A, Burger P, *et al*. Effect of dopaminergic drug treatment on surgical findings in prolactinomas. Pituitary,

2011, 14: 68–74.
16. Scanarini M. Morphological changes in prolactinoma induced by bromocriptine treatment. Minerva Endocrinol (Italian), 1990, 15: 13–15.
17. Sobrinho LG, Nunes MC, Santos MA, *et al.* Radiological evidence for regression of prolactinoma after treatment with bromocriptine. Lancet, 1978, 2: 257–258.
18. Chakraborty S, Dehdashti AR. Does the medical treatment for prolactinoma remain the standard of care? Acta Neurochir (Wien), 2016, 158: 943–944.
19. Molitch ME, Thorner MO, Wilson C. Management of prolactinomas. J Clin Endocrinol Metab, 1997, 82: 996–1000.
20. Sughrue ME, Chang EF, Tyrell JB, *et al*. Pre-operative dopamine agonist therapy improves post-operative tumor control following prolactinoma resection. Pituitary, 2009, 12: 158–164.
21. Wang S, Lin S, Wei L, *et al*. Analysis of operative efficacy for giant pituitary adenoma. BMC Surg, 2014, 14: 59.
22. Arasho BD, Schaller B, Sandu N, *et al*. Gender-related differences in pituitary adenomas. Exp Clin Endocrinol Diabetes, 2009, 117: 567–572.
23. Nishioka H, Haraoka J, Akada K, *et al*. Gender-related differences in prolactin secretion in pituitary prolactinomas. Neuroradiology, 2002, 44: 407–410.
24. Schaller B. Gender-related differences in prolactinomas. A clinicopathological study. Neuro Endocrinol Lett, 2005, 26: 152–159.
25. Trouillas J, Delgrange E, Jouanneau E, *et al.* Prolactinoma in man: clinical and histological characteristics. Ann Endocrinol (Paris)(French), 2000, 61: 253–257.
26. Delgrange E, Trouillas J, Maiter D, *et al.* Sex-related difference in the growth of prolactinomas: a clinical and proliferation marker study. J Clin Endocrinol Metab, 1997, 82: 2102–2107.
27. Delgrange E, Vasiljevic A, Wierinckx A, *et al*. Expression of estrogen receptor alpha is associated with prolactin pituitary tumor prognosis and supports the sex-related difference in tumor growth. Eur J Endocrinol, 2015, 172: 791–801.
28. Li Z, Liu Q, Li C, *et al*. The role of TGF-beta/Smad signaling in dopamine agonist-resistant prolactinomas. Mol Cell Endocrinol, 2015, 402: 64–71.
29. Meng XM, Tang PM, Li J, *et al*. TGF-beta/Smad signaling in renal fibrosis. Front Physiol, 2015, 6: 82.
30. Recouvreux MV, Lapyckyj L, Camilletti MA, *et al*. Sex differences in the pituitary transforming growth factor-beta1 system: studies in a model of resistant prolactinomas. Endocrinology, 2013, 154: 4192–4205.
31. Saito A, Nagase T. Hippo and TGF-beta interplay in the lung field. Am J Physiol Lung Cell Mol Physiol, 2015, 309: L756–L767.
32. Xu F, Liu C, Zhou D, *et al*. TGF-beta/SMAD pathway and its regulation in hepatic fibrosis. J Histochem Cytochem, 2016, 64: 157–167.
33. Landolt AM, Keller PJ, Froesch ER, *et al.* Bromocriptine: Does it jeopardise the result of later surgery for prolactinomas? Lancet, 1982, 2: 657–658.
34. Esiri MM, Bevan JS, Burke CW, *et al*. Effect of bromocriptine treatment on the fibrous tissue content of prolactin-secreting and non-functioning macroadenomas of the pituitary gland. J Clin Endocrinol Metab, 1986, 63: 383–388.
35. Fahlbusch R, Buchfelder M, Schrell U. Short-term preoperative treatment of macroprolactinomas by dopamine agonists. J Neurosurg, 1987, 67: 807–815.
36. Liu J, Li C, Xiao Q, *et al*. Comparison of pituitary adenomas in elderly and younger adults: Clinical characteristics, surgical outcomes, and prognosis. J Am Geriatr Soc, 2015, 63: 1924–1930.
37. Perrin G, Treluyer C, Trouillas J, *et al*. Surgical outcome and pathological effects of bromocriptine preoperative treatment in prolactinomas. Pathol Res Pract, 1991, 187: 587–592.
38. Turner HE, Adams CB, Wass JA. Trans-sphenoidal surgery for microprolactinoma: an acceptable alternative to dopamine agonists? Eur J Endocrinol, 1999, 140: 43–47.

DOI 10.1007/s10330-016-0180-6
Cite this article as: Huang YM, Hu F, Wu K, *et al*. Sex-related changes in tumor consistency in prolactinoma patients after bromocriptine pretreatment. Oncol Transl Med, 2016, 2: 203–209.

Oncology and Translational Medicine
DOI 10.1007/s10330-016-0172-6

October 2016, Vol. 2, No. 5, P210–P215

ORIGINAL ARTICLE

IL-13Ra2- and glioma stem cell-pulsed dendritic cells induce glioma cell death in vitro

Ying Wang[1], Ruifan Xie[2], Hongquan Niu[2], Ting Lei[2] (✉)

[1] Department of Neurosurgery, Tumor Hospital Affiliated to Zhengzhou University, Zhengzhou 450000, China
[2] Sino-German Neuro-Oncology Molecular Laboratory, Department of Neurosurgery, Tongji Hospital, Tongji Medical College, Huazhong University of Science and Technology, Wuhan 430030, China

Abstract

Objective Gliomas are the most common malignant tumors in the central nervous system. Despite multiple therapies including surgery, chemotherapy, and radiotherapy, the prognosis of patients remains poor. Immunotherapy is an alternative method of treating glioma, and the use of dendritic cell vaccines is one of the promising treatment options. However, there is no specific tumor cell antigen that can trigger dendritic cells (DCs). IL-13Ra2 is a specific antigen expressed in glioma cells; in the current study, we have attempted to explore whether IL-13Ra2 could be the antigen that triggers DCs and to envisage its application as potential therapy for glioma.

Methods The expression of IL-13Ra2 was detected in U251 glioma cell lines and primary glioma tissues using different methods. DCs from human blood were isolated and pulsed with recombinant IL-13Ra2, following which the cytotoxicity of these DCs on glioma cells was detected and analyzed.

Results About 55.9% human glioma tissue cells expressed IL-13Ra2, while normal brain tissue cells did not show any expression. DC vaccines loaded with IL-13Ra2, glioma cell antigen, and brain tumor stem cell (BTSC) antigen could significantly stimulate the proliferation of T lymphocytes and induce cell death in the glioma tissue. Compared to other groups, DC vaccines loaded with BTSC antigen showed the strongest ability to activate cytotoxic T lymphocytes (CTLs), while the glioma cell antigen group showed no significant difference.

Conclusion IL-13Ra2, which is expressed in gliomas and by glioma stem cells, as well as IL-13Ra2 could prove to be potential antigens for DC vaccine-based immunotherapy.

Received: 11 July 2016
Revised: 27 July 2016
Accepted: 5 August 2016

Keywords: dendritic cell; brain tumor stem cell; IL-13Ra2; glioma

Malignant gliomas are the most common and deadly brain tumors and arise from glial cells in the central nervous system (CNS) [1]. Gliomas are classified into four grades according to the histopathological criteria defined by the World Health Organization (WHO). Grade III and grade IV gliomas are the most aggressive types and are characterized by uncontrolled proliferation, necrosis, and infiltration [2]. Glioblastoma multiforme (GBM) is the most malignant type of glioma with a median survival time of 12 months despite an aggressive treatment consisting of surgery, radiotherapy, and chemotherapy. Substantial progress has been made in other malignant cancer therapies over the past decades; however, GBM remains essentially untreatable [3].

Apart from surgery, chemotherapy, and radiotherapy, immunotherapy is believed to be a promising method of treatment for malignant gliomas [4]. Tumor cells are recognized by immunocompetent cells that induce innate and adaptive immune responses. Adaptive immune responses are mostly characterized by tumor-specific T cells in the tumor microenvironment, and it has been demonstrated that these cell numbers are positively correlated with survival [5]. It is accepted that the brain is an immune-privileged organ that lacks dendritic cells (DCs) and T cells; however, recent studies have discovered lymphatic vessels in the brain and showed that tumor-derived antigens are transported to the cervical lymph nodes to stimulate specific T cells [6]. After amplification, these T cells are

✉ Correspondence to: Ting Lei. Email: hufeng268@qq.com
© 2016 Huazhong University of Science and Technology

able to migrate back to the brain and kill tumor cells effectively. These findings indicate that immunotherapy could be a potential method for treatment of gliomas.

Dendritic cells (DCs) are the most powerful antigen presenting cells (APCs) [7]; we showed that immunotherapy using pulsed DCs from whole tumor extracts could significantly prolong the survival of GBM patients in a pilot clinical study [8]. However, by using the whole tumor extract, DCs do not get pulsed in all the patients. Hence, we attempted to find a more specific antigen expressed in gliomas to optimize the treatment.

Interleukin-13 receptor alpha 2 (IL-13Ra2) is a membrane receptor composed of 380 amino acids, belonging to the erythropoietin receptor family [9]. The gene encoding IL-13Ra2 is located on Xq24. Recent studies have demonstrated that IL-13Ra2 exhibits a highly tissue-specific expression in malignant tumors, especially in gliomas [10]. In addition, the expression is positively correlated with tumor malignancy, and no expression of IL-13Ra2 has been found in normal tissue and organs. Other researchers have found that IL-13Ra2 exhibits antigenicity and immunogenicity, which indicates its potential use in cancer immunotherapy [11].

Materials and methods

Human material

All material pertaining to human glioma and normal brain used in this study was obtained from the Department of Neurosurgery and Department of Neuropathology at Tongji Hospital of Tongji Medical College, Huazhong University of Science and Technology, in accordance with the guidelines of the Ethical Committee.

Cell culture

Human glioma cell line U251 was cultured in Dulbecco's modified Eagle's medium (DMEM) supplemented with 200 mM glutamine, 50 units/mL penicillin, 50 mg/mL streptomycin, and 10% FCS, as previously described [12].

Tumor tissue was enzymatically dissociated and cultured as floating neurospheres in serum-free DMEM/F-12 medium containing 20% BIT serum-free supplement (Stemcell Technologies Inc., Vancouver, Canada), EGF and bFGF at 20 ng/mL, respectively. Similarly, glioma U251 stem cells (U251-GSC), derived from the human glioma cell line U251, were cultured as non-adherent neurospheres in a serum-free supplemented medium as previously described. GSCs of more than six passages were used for further experiments. To induce GSC differentiation, we used the conventional serum-containing medium (10% FBS in DMEM) for seven days.

Peripheral blood (50 mL) was drawn from glioma patients; monocytes were isolated and cultured in RPMI-1640 medium supplemented with 10% patients' own serum. On the first, third, fifth and seventh day of culture, GM-CSF and Interleukin-4 were added to the culture medium. DCs were extracted and the samples were analyzed for purity by using flow cytometry, as previously described [8].

Clonal formation assay

Single-cell suspensions were calibrated to reach a concentration of 5,000 cells/mL in serum-free supplemented medium, diluted into gradient cell titers at 1,000, 500, 200, 100, 50, 20, and 10 cells/200, and further transferred into the wells of a 96-well microplate. To confirm the results obtained after the gradient dilution, more stringent clonal assays were performed by plating single cells into the 96-well plate. Clonal spheres (non-adherent, tight and spherical masses >75 μm in diameter) were counted under a microscope (Olympus CKX31, Tokyo, Japan) at the end of two weeks.

CCK-8 assay

Cells were seeded into 96-well plates at a density of 5×10^3 cells per well and maintained in culture medium for the indicated time. Thereafter, 10 μL CCK-8 reagent was added into the medium and incubated with the cells for 4 h. The optical density (OD) was measured at a wavelength of 450 nm using an ELISA plate reader, with subtraction of blank control reading. In addition, the morphological alterations of cells post-incubation were recorded microscopically.

ELISA

IFN-γ secretion was evaluated by detecting IFN-γ in the conditioned culture medium of DCs after indicated treatment for 48 h using a commercial IFN-γ ELISA kit (Uscn Life Science Inc., China) following the manufacturer's instructions.

Flow cytometry

Up to 106 cells were resuspended in the recommended buffer (containing PBS pH 7.2, 0.5% BSA, and 2 mM EDTA) with CD133/1 (AC133) antibody (1:11; Miltenyi Biotec, Bergisch Gladbach, Germany) for 10 min at 4°C. Mouse IgG1 (1:11; Miltenyi Biotec) was used as the isotype control antibody. CD133 detection and analysis were performed on BD FACSAria [12].

Results

IL-13Ra2 was expressed in U251 glioma cells and human glioma tissue, not in normal brain tissue

The expression of IL-13Ra2 in U251 glioma cells and human glioma tissues was analyzed by immunostaining.

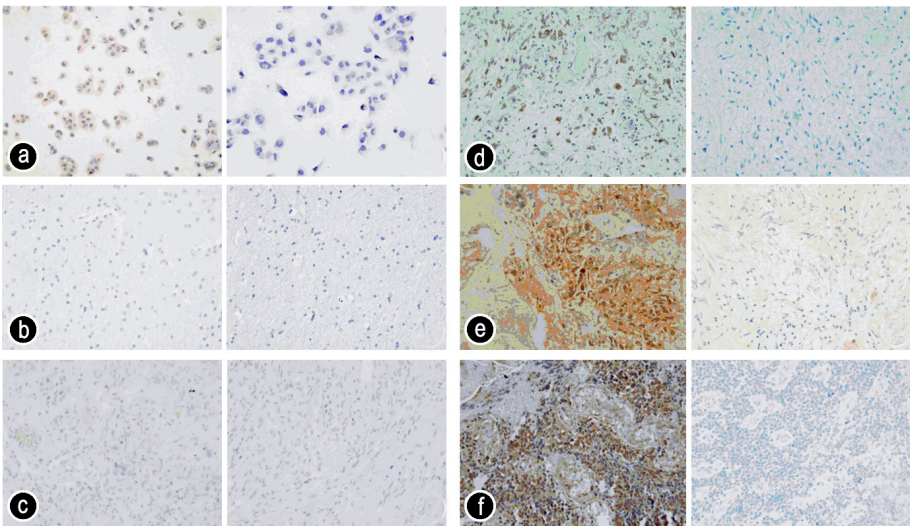

Fig. 1 (a) Expression of IL-13Ra2 in U251 cell line; (b) Expression of IL-13Ra2 in human normal brain tissue; (c) Expression of IL-13Ra2 in grade I gliomas; (d) Expression of IL-13Ra2 in grade II gliomas; (e) Expression of IL-13Ra2 in grade III gliomas; (f) Expression of IL-13Ra2 in glioblastomas

IL-13Ra2 was detected in U251 cells (Fig. 1a). In most of the human glioma tissues, no (or very faint) staining was observed in low-grade gliomas (grade I and grade II) (Fig. 1c, 1d), while in high-grade gliomas (grade III and grade IV), a strong IL-13Ra2 expression was observed (Fig. 1e, 1f). When the expression of IL-13Ra2 was evaluated in normal brain tissues, no signal was detected (Fig. 1b).

Expression of IL-13Ra2 was associated with glioma grades

We analyzed 59 gliomas tissues including 10 grade I gliomas, 17 grade II gliomas, 13 grade III gliomas, and 19 grade IV gliomas (Table 1). Five normal brain tissues were included as controls. The expression rates obtained are listed in Table 1. IL-13Ra2 was found to be significantly expressed in glioma tissues as compared to normal brain tissues ($P = 0.0223$), and high-grade gliomas expressed a level of IL-13Ra2 higher than that of low-grade gliomas ($P = 0.0002$) (Table 2). Although there is no difference in IL-13Ra2 expression between grade I and grade II ($P = 0.1895$), grade II and grade III ($P = 0.1590$), grade III and grade IV ($P = 0.4012$) gliomas, a significant difference was observed between grade I and grade III ($P = 0.0097$), grade I and grade IV ($P = 0.002$) and grade II and grade IV ($P = 0.0140$) gliomas. These data indicate that IL-13Ra2 is negatively correlated with glioma malignancy.

Growth patterns and identification of GSCs

GSCs were initially harvested using the neurosphere assay, with the GSCs growing as suspended spheres enriched with stemness characteristics. U251 glioma cells presented distinctive growth patterns under different culture conditions. The U251 cells showed adherence and had elongated branches (Fig. 2a); trypsinization for passage took ~4–5 min at 37 ℃. The U251 GSCs and human GSCs grew as floating spheres, which proliferated up to 100–200 μm in diameter within 3–4 days. The cells were mechanically filtered and dissociated into single cells without trypsinization, thereby forming secondary spheres for serial passage (Fig. 2b). CD133 was used as a marker and human GSCs showed more than 20% expression of CD133 (Fig. 2c), compared to less than 1% in glioma cells (Fig. 2d).

Table 1 Expression of IL-13Ra2 in gliomas of different grades

Tumor type	Total numbers	Positive	%
Grade I	10	1	10
Grade II	17	7	41.1
Grade III	13	9	69.2
Grade IV	19	16	84.2

Table 2 Expression of IL-13Ra2 in low-grade and high-grade gliomas

Tumor type	Total numbers	Positive	%	*P*
Low grade glioma	27	8	29.6	0.002
High grade glioma	32	5	78.1	

IL-13Ra2- and GSC-pulsed DCs induced T lymphocyte proliferation

Different effector to target cell ratios (E/T 1:5, 1:10, 1:20, and 1:40) were applied to identify the optimal ratio. IL-13Ra2- and GSC-pulsed DCs and T cells were co-cultured for 48 h and the proliferation of T cells was analyzed. In the group of GSC-pulsed DCs, E/T 1:10 induced the highest proliferation of T cells. However, in the group of IL-13Ra2-pulsed DCs, although DCs induced a very high proliferation of T cells, no difference was detected between different E/T subgroups. When DCs were not pulsed by any antigens, a very low rate of T cell proliferation was observed (Table 3). Hence, E/T 1:10 was considered the optimal E/T for T cell proliferation.

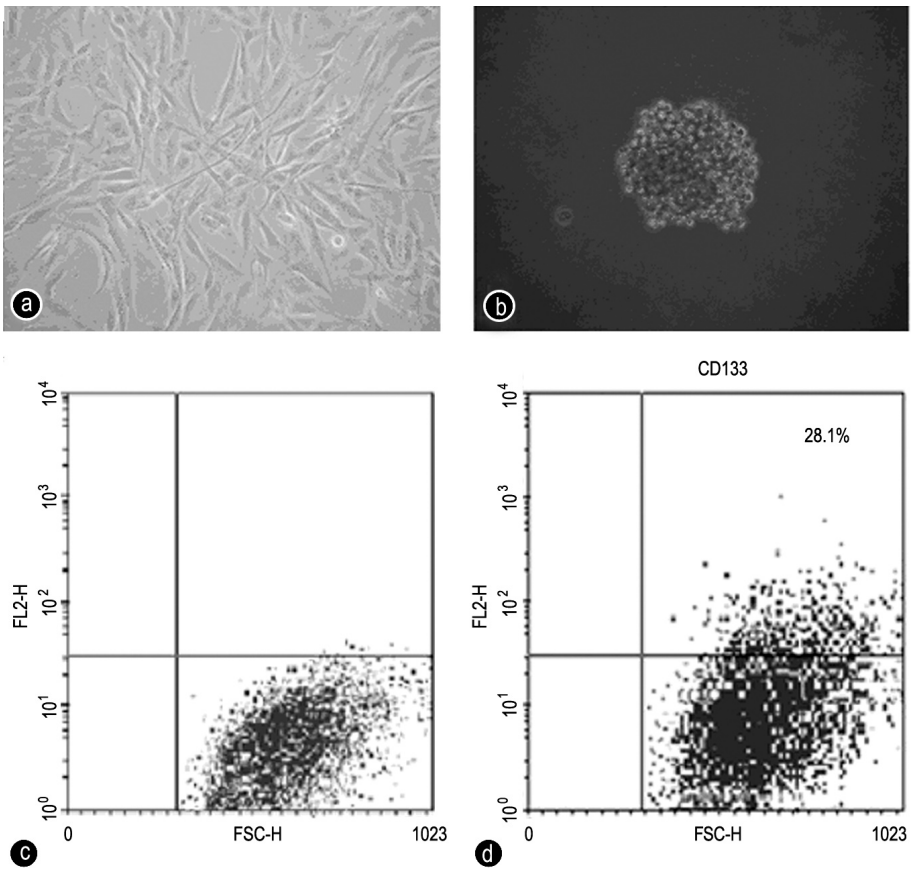

Fig. 2 (a) U251 cells; (b) Clonal formation assay in brain tumor stem cells (BTSCs); (c) Expression of CD133 in fourth generation BTSCs; (d) Expression of CD133 in fourth generation of glioma cells

Table 3 Ability to stimulate T lymphocyte proliferation in dendritic cell (DC) groups pulsed by different antigens

E/T	IL-13Ra2 pulsed DCs	GSCs pulsed DCs	Glioma cells antigen	Pure DCs
1:5	2.69 ± 0.19	3.41 ± 0.39	2.81 ± 0.24	1.11 ± 0.09
1:10	3.67 ± 0.27	4.01 ± 0.66	3.53 ± 0.41	1.44 ± 0.91
1:20	2.94 ± 0.24	3.78 ± 0.41	2.77 ± 0.33	0.91 ± 0.06
1:40	2.67 ± 0.21	3.43 ± 0.29	2.51 ± 0.19	0.69 ± 0.04

Pulsed DCs stimulated cytotoxic T cells to induce glioma cell death in vitro

T cells were stimulated by different groups of pulsed DCs as described. Pulsed DCs were further co-cultured with U251 cells or GSCs and cell death was analyzed. As shown in Table 4, the GSC-pulsed DCs group showed the highest rate of killing glioma cells in the U251 group, and the E/T of 20:1 showed the highest killing rate in both groups. However, in the group of GSCs, IL-13Ra2-pulsed DCs failed to show any effect when compared to the non-pulsed group, indicating that IL-13Ra2 was unable to pulse DCs to kill GSCs (Table 5). In both groups, using GSCs as the antigen showed the highest killing rate.

GSCs induced higher IFN- γ release on DCs

Since GSC-pulsed DCs showed the highest glioma cell killing rate, we attempted to identify the effect factor. IFN- γ was shown to have a capacity to kill glioma cells. IFN- γ concentration was analyzed using ELISA. The GSC group showed a higher concentration of IFN- γ than the IL-13Ra2 group and the non-pulsed group ($P < 0.05$). E/T of 20:1 showed the highest concentration of IFN- γ (Table 6).

Discussion

Previous studies, including ours, have shown that DC vaccines loaded with frozen glioma antigen could be used as a potential therapy for glioma patients. However, its specificity needs to be improved further. In the present study, we have shown that IL-13Ra2 is predominantly expressed in glioma tissue but not in normal brain tissue and its expression is positively correlated with tumor grades. IL-13R is a complex consisting of IL-4Ra, IL-2Rar, IL-13Ra1, and IL-13Ra2, and it has been found that IL-13Ra2 is expressed in several malignant tumors including Kaposi sarcoma and renal carcinoma; however, it is not expressed in normal tissues, thereby indicating its role in tumorigenesis. Kawakami showed that IL-13Ra2 could

Table 4 Killing rate of dendritic cell (DC) groups pulsed with different antigens on glioma cells (%)

E/T	IL-13Ra2 pulsed DCs	GSCs pulsed DCs	Glioma cells antigen	Pure DCs
5:1	16.31 ± 0.92	24.43 ± 0.31	15.6 ± 1.04	5.43 ± 0.51
10:1	32.59 ± 5.43	43.51 ± 5.38	29.21 ± 3.29	7.26 ± 0.41
20:1	42.37 ± 5.18	62.49 ± 6.06	41.28 ± 6.13	8.14 ± 0.46

Table 5 Killing rate of dendritic cell (DC) groups pulsed with different antigens on glioma stem cells (GSCs) (%)

E/T	IL-13Ra2 pulsed DCs	GSCs pulsed DCs	Pure DCs
5:1	6.87 ± 0.71	19.80 ± 2.71	6.42 ± 0.50
10:1	9.21 ± 1.05	25.5 ± 2.24	7.63 ± 0.51
20:1	11.48 ± 0.94	31.46 ± 3.50	10.06 ± 1.21

Table 6 Concentration of IFN- γ in supernatant in dendritic cell (DC) groups pulsed with different antigens, detected by cellular toxicity assay (pg/mL)

E/T	Pure DCs	IL-13Ra2 pulsed DCs	GSCs pulsed DCs
5:1	1012 ± 109	1230 ± 254	1220 ± 137
10:1	1211 ± 225	1444 ± 201	1601 ± 201
20:1	1462 ± 236	1734 ± 337	1856 ± 352

inhibit the JAK-STAT6 signaling pathway by binding to IL-4Ra to promote tumor growth [14]. Joshi reported that about 82% of GBM patients expressed IL-13Ra2; however, this is restricted to the mRNA level [15]. In addition, other groups demonstrated that IL-13Ra2 is mainly expressed in malignant tumors, but not benign ones [16]. These findings, along with our data, indicate that IL-13Ra2 could be a potential specific antigen for DC vaccine therapy for gliomas.

Immunotherapy is one of the promising methods in the treatment of malignant tumors. However, most of the immunotherapies for gliomas are still under clinical trials. Some of the patients showed a good response to immunotherapy involving DC vaccines; however, no benefit was observed in other patients. There are a few probable explanations for this difference: (1) CNS is a relative immune-surveillance organ that lacks immune cells. (2) Glioma presents an immunosuppressive environment, wherein immune cells including DCs and T cells are inactivated by glioma-released factors such as IL-10 and TGF-β [17]. (3) So far, there is no specific antigen that could be used for DC vaccines [18]. DCs are the most powerful antigen presenting cells; however, very few DCs could be found in the peripheral blood and in the brain. GM-CSF and IL-4 have been used to stimulate monocytes to differentiate into DCs, which are capable of producing cytokines. In the current study, we found that IL-13Ra2-pulsed DCs could significantly induce glioma cell death. However, this effect is not valid in case of GSCs. This result may explain why the DC vaccine failed with some patients, who showed a high percentage of GSCs.

The GSC hypothesis indicates that a subpopulation of cells within gliomas has true clonogenic and tumorigenic potential [19]. These cells are not only responsible for tumor recurrence but also resistant to chemotherapy and radiotherapy. GSCs could also influence the tumor microenvironment to impact immunotherapy [20]. Our data showed that IL-13Ra2-pulsed DCs could induce normal glioma cell death but not GSC death, demonstrating that GSCs are resistant to immunotherapy. Interestingly, GSCs can also be treated as the antigen for stimulating DCs. The data obtained in this study showed that GSC-pulsed DCs have a stronger effect on inducing glioma cell death than IL-13Ra2-pulsed DCs and normal glioma cells pulsed-DCs. However, the mechanism underlying this observation is not very clear.

We further analyzed the IFN-γ concentration in DCs after different stimulations, since IFN-γ is believed to be the key factor that induces glioma cell death [21]. It was found that GSC-pulsed DCs released the highest level of IFN-γ. Collectively, we found that both GSCs and IL-13Ra2 could induce glioma cells death probably by releasing IFN-γ, indicating that IL-13Ra2 could be used as a potential antigen for DC vaccines.

Conflicts of interest

The authors indicated no potential conflicts of interest.

References

1. Van Meir EG, Hadjipanayis CG, Norden AD, *et al.* Exciting new advances in neuro-oncology: the avenue to a cure for malignant glioma. CA Cancer J Clin, 2010, 60: 166–193.
2. Louis DN, Ohgaki H, Wiestler OD, *et al*. The 2007 WHO classification of tumours of the central nervous system. Acta Neuropathol, 2007, 114: 97–109.
3. Wen PY, Kesari S. Malignant gliomas in adults. New Engl J Med, 2008, 359: 492–507.
4. Rosenberg SA, Yang JC, Restifo NP. Cancer immunotherapy: moving beyond current vaccines. Nat Med, 2004,10: 909–915.
5. Han S, Zhang C, Li Q, *et al.* Tumour-infiltrating CD4(+) and CD8(+) lymphocytes as predictors of clinical outcome in glioma. Br J Cancer, 2014, 110: 2560–2568.
6. Louveau A, Smirnov I, Keyes TJ, *et al*. Structural and functional features of central nervous system lymphatic vessels. Nature, 2015, 523: 337–341.
7. Nouri-Shirazi M, Banchereau J, Fay J. Dendritic-cell-based therapeutic cancer vaccines. Immunity, 2013, 39: 38–48.
8. Niu HQ, Dong Z, Dong FY, *et al.* Experimental and clinical research of dendritic cell and syngeneic immunotherapy of brain glioma. Chinese-German J Clin Oncol, 2004, 3: 147–150.
9. Ranasinghe C, Trivedi S, Wijesundara DK, *et al.* IL-4 and IL-13 receptors: Roles in immunity and powerful vaccine adjuvants. Cytokine Growth Factor Rev, 2014, 25: 437–442.
10. Liu H, Jacobs BS, Liu J, *et al*. Interleukin-13 sensitivity and receptor phenotypes of human glial cell lines: non-neoplastic glia and low-

grade astrocytoma differ from malignant glioma. Cancer Immunol Immunother, 2000, 49: 319–324.
11. Thaci B, Brown CE, Binello E, *et al*. Significance of interleukin-13 receptor alpha 2-targeted glioblastoma therapy. Neuro Oncology, 2014, 16: 1304–1312.
12. Zhang S, Xie R, Wan F, *et al*. Identification of U251 glioma stem cells and their heterogeneous stem-like phenotypes. Oncol Lett, 2013, 6: 1649–1655.
13. Zeppernick F, Ahmadi R, Campos B, *et al*. Stem cell marker CD133 affects clinical outcome in glioma patients. Clin Cancer Res, 2008, 14: 123–129.
14. Niu Y, Murata T, Watanabe K, *et al*. MIP-T3 associates with IL-13Ralpha1 and suppresses STAT6 activation in response to IL-13 stimulation. FEBS Lett, 2003, 550: 139–143.
15. Gonzalez-Moreno O, Calvo A, Joshi BH, *et al*. Gene expression profiling identifies IL-13 receptor alpha 2 chain as a therapeutic target in prostate tumor cells overexpressing adrenomedullin. Int J Cancer, 2005, 114: 870–878.
16. Debinski W, Dickinson P, Rossmeisl JH, *et al.* New agents for targeting of IL-13RA2 expressed in primary human and canine brain tumors. PloS One, 2013, 8: e77719.
17. Han J, Chen X, Chu J, *et al*. TGFβ treatment enhances glioblastoma virotherapy by inhibiting the innate immune response. Cancer Res, 2015, 75: 5273–5282.
18. Kalinski P, Edington H, Zeh HJ, *et al*. Dendritic cells in cancer immunotherapy: vaccines or autologous transplants? Immunol Res, 2011, 50: 235–247.
19. Vescovi AL, Galli R, Reynolds BA. Brain tumour stem cells. Nat Rev Cancer, 2006, 6: 425–436.
20. Heddleston JM, Hitomi M, Venere M, *et al.* Glioma stem cell maintenance: the role of the microenvironment. Curr Pharm Des, 2011, 17: 2386–2401.
21. Fuertes MB, Woo SR, Burnett B, *et al.* Type I interferon response and innate immune sensing of cancer. Trends Immunol, 2013, 34: 67–73.

DOI 10.1007/s10330-016-0172-6
Cite this article as: Wang Y, Xie RF, Niu HQ, *et al*. IL-13Ra2- and glioma stem cell-pulsed dendritic cells induce glioma cell death *in vitro*. Oncol Transl Med, 2016, 2: 210–215.

Oncology and Translational Medicine
DOI 10.1007/s10330-016-0165-5

October 2016, Vol. 2, No. 5, P216–P226

REVIEW ARTICLE

Histone modification as a drug resistance driver in brain tumors*

Guifa Xi[1, 2, 3] (✉), Barbara Mania-Farnell[4], Ting Lei[5], Tadanori Tomita[1, 3]

[1] Falk Brain Tumor Center, Division of Pediatric Neurosurgery, Ann & Robert H. Lurie Children's Hospital of Chicago, Northwestern University Feinberg School of Medicine, Chicago, USA
[2] Development Biology Program, Stanley Manne Children's Research Institute, Ann & Robert H. Lurie Children's Hospital of Chicago, Northwestern University Feinberg School of Medicine, Chicago, USA
[3] Department of Neurological Surgery, Northwestern University Feinberg School of Medicine, Chicago, USA
[4] Department of Biological Sciences, Purdue University Calumet, Hammond, USA
[5] Department of Neurosurgery, Tongji Hospital, Tongji Medical College, Huazhong University of Science and Technology, Wuhan 430030, China

Abstract

Patients with brain tumors, specifically, malignant forms such as glioblastoma, medulloblastoma and ependymoma, exhibit dismal survival rates despite advances in treatment strategies. Chemotherapeutics, the primary adjuvant treatment for human brain tumors following surgery, commonly lack efficacy due to either intrinsic or acquired drug resistance. New treatments targeting epigenetic factors are being explored. Post-translational histone modification provides a critical regulatory platform for processes such as chromosome condensation and segregation, apoptosis, gene transcription, and DNA replication and repair. This work reviews how aberrant histone modifications and alterations in histone-modifying enzymes can drive the acquisition of drug resistance in brain tumors. Elucidating these mechanisms should lead to new treatments for overcoming drug resistance.

Received: 16 June 2016
Revised: 15 July 2016
Accepted: 25 August 2016

Key words: histone modification; drug resistance; brain tumor

Brain tumors are among the most formidable and devastating cancers in children and adults. Over 30,000 new malignant or benign brain tumors are diagnosed annually, accounting for 1.4% of all tumors and 2.3% of cancer-related deaths [1–2]. The overall 5-year survival following diagnosis and treatment of a primary malignant brain tumor is approximately 30% [2].

Tumor treatment generally consists of surgical resection in conjunction with radiotherapy and/or treatment with one or more chemotherapeutic agents. Irrespective of the chemotherapeutic agent employed, acquisition of multidrug resistance (MDR) is a major challenge [3]. Mechanisms of MDR acquisition differ in response to reagents and genetic factors, and these mechanisms have been comprehensively studied in recent decades. However, understanding the role epigenetics plays in MDR acquisition is limited and continues to be an active area of research.

Higher order chromatin structure is an important regulator of gene expression [4–5]. Chromatin is the condensed combination of DNA and histones within the nucleus of a cell. The structural and functional unit of chromatin is the nucleosome, which consists of a disc-shaped octamer composed of two copies of each histone protein (H2A, H2B, H3, and H4) wrapped twice by ~147 base-pairs of DNA [6]. Nucleosomal arrays are visualized with electron microscopy as a series of 'beads on a string'; the 'beads' are the individual nucleosomes and the 'string' is the linker DNA. Linker histones, such as histone H1, and other non-histone proteins interact with the nucleosomal arrays to

✉ Correspondence to: Guifa Xi. Email: guifa.xi@northwestern.edu
*Supported by the Rory David Deutsch Foundation, the Surgical Neuro-oncology Research Fund of Ann & Robert H Lurie Children's Hospital (A&RLCH) of Chicago, and the Dr. Ralph and Marian C. Falk Medical Research Trust.
© 2016 Huazhong University of Science and Technology

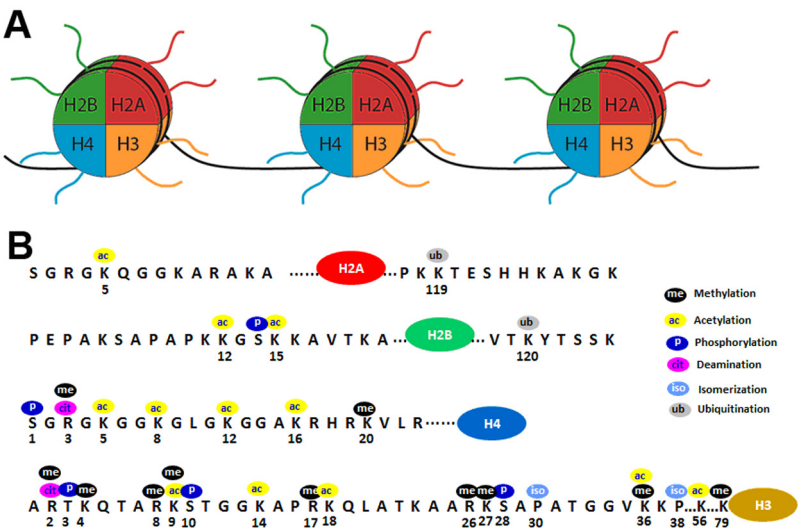

Fig. 1 Nucleosome structure. (a) The core protein of the nucleosome: disc-shaped octamer composed of two copies each of histones H2A, H2B, H3, and H4 wrapped twice by DNA; (b) Amino-terminal tails of core histones showing potential modifications

further package the nucleosomes into higher-order chromatin structures (Fig. 1a).

Histones, the key protein components of chromatin, are regulators of chromatin dynamics. These proteins are subject to a wide variety of post-translational modifications including acetylation, methylation, ubiquitylation, or glycosylation on lysine; methylation on arginine; phosphorylation on serine or threonine (Fig. 1b); and diphosphate ribosylation or carbonylation on adenosine. All of these modifications are catalyzed by histone-modifying enzyme complexes in a dynamic manner [7]. Modifications occur primarily within histone amino-terminal tails protruding from the surface of the nucleosome, but may also be present on the globular core region [8]. Recent studies have observed differential histone modification in adult and pediatric brain tumors compared to normal tissue as summarized in Table 1.

Histone modification in brain tumors

Histone modification has significant roles in brain tumorigenesis, proliferation, invasiveness, therapeutic response, and clinical outcome. Global histone modification patterns are prognostic markers in glioma patients [20]. Increased histone H3 acetylation is observed more frequently in glioblastomas than in low-grade astrocytomas and normal brain tissue [21]. Increased trimethylation of lysine 4 on H3 (H3K4me3) alters the transcriptional landscape and leads to oncogenic protein overexpression in glioblastomas [9]. Genes associated with H3K4me3 and H3K27me3 are potential therapeutic targets for inducing differentiation in glioblastomas [22]. Decreased H3K27me3 has been found in glioblastomas expressing the K27M mutation in the *H3F3A* gene, which codes for the replacement histone H3.3 [13]. H3K4me3 and H3K27me3 [11], as well as monomethylation of lysine 9 on H3 (H3K9me) [17] also play critical roles in the pathogenesis of medulloblastomas (MBs). H3K27 methylation is a therapeutic target for CpG island methylator-positive hindbrain ependymomas [14]. H3K9Ac inversely correlates with ependymoma prognosis [23]. Enhanced H3 acetylation and diminished H3 methylation control the balance between FGF7/FGFR2-IIIb signals in pituitary neoplasia [19, 24–25].

As expected, enzymes targeting histones are also altered in brain tumors. Class II and IV histone deacetylases (HDACs) are downregulated in glioblastomas [21]. HDACs 1, 2, 3, and 9, histone demethylases (JMJD1A and JMJD1B), and histone methyltransferases (SET7, SETD7, MLL3, and MLL4) also have altered expression patterns in gliomas [25–26], and have been linked to tumor recurrence and progression [26]. Inhibition of the lysine demethylase, KDM1, is associated with increased H3K4me2 and H3K9Ac and decreased H3K9me2, leading to apoptosis of glioma xenograft tumors [16]. The gene encoding BMI-1, a member of the polycomb group complex that regulates histone H3K27 methylation, is frequently subjected to copy number alterations in gliomas, and BMI-1 deletions are associated with poor prognosis in these tumors [21]. In MB, restoration of genes controlling H3K9 methylation diminishes proliferation *in vitro* [17]. HDAC2 is upregulated in primary MB subgroups with poor prognosis (Sonic hedgehog, Groups 3 and 4) compared to normal brain and MB of the WNT subgroup, and inhibition of HDAC2 is a valid target in patients with myelocytomatosis gene-amplified MBs [27].

Finally, mutations in genes coding for histones or histone-modifying enzymes can bring about gene dysregulation in brain tumors. For example, mutations in H3F3A are observed in pediatric and young adult gliomas, and the presence of these mutations is associated with alternative lengthening of telomeres and specific gene expression profiles [28]. Mutations for genes coding for MLL2,

Table 1 Histone modification, histone modifying enzymes and target genes deregulated in brain tumors

Histone modification	Enzymes	Genes affected	Gene function	Brain tumor	References
H3K4me3	Unknown	hTERT	Limitless replication potential	Glioblastoma	Nagarajan RP, *et al* [9]
		GLI3	Cell growth, cell specialization, and patterning of structures		
		TP73	Cell cycle arrest, apoptosis		
	MLL2	MLL2 mutation	Histone lysine methyltransferase	MB	Parsons DW, *et al* [10]
	MLL3	MLL3 mutation			
	ZMYM3	KDM1A			Robinson G, *et al* [11]
H3K27me3	N/A	H3F3A$^{G34/RV}$ mutation	Coding histone H3.3	Glioblastoma	Costa BM, *et al* [12]
	EZH2	HOXA9	Apoptosis		Venneti S, *et al* [13]
	EZH2	PRC2	Polycomb group	Ependymoma	Mack SC, *et al* [14]
	KDM6A	KDM6A mutation	Histone methyltransferase	MB	Dubuc AM, *et al* [15]
	KDM6B	KDM6B mutation			Parsons DW, *et al* [10]
H3K4me2, H3K9Ac	KDM1	P21, PUMA	Proliferation, apoptosis	Glioblastoma	Sareddy GR, *et al* [16]
H3K9me2	EHMT1	EHMT1 amplification	Histone lysine methyltransferase	MB	Northcott PA, *et al* [17]
	SMYD4	SMYD4 amplification			
	L3MBTL2	L3MBTL2 deletion	Polycomb group		
	L3MBTL3	L3MBTL3 deletion			
	SCML2	SCML2 deletion			
	JMJD2B	JMJD2B amplification	Histone lysine demethyltransferase		
	JMJD2C	JMJD2C amplification			
	MYST3	MYST3 amplification	Histone lysine acetyltransferase		
	KDM1	P21, PUMA	Proliferation, apoptosis	Glioblastoma	Sareddy GR, *et al* [16]
H4K20me, H3K36me	NSD1	MEIS1	Homeobox gene, normal development	NB, glioma	Berdasco M, *et al* [18]
H3Ac, H3me	N/A	MAGE-A3	Enhanced ubiquitin ligase activity	Pituitary tumor	Zhu X, *et al* [19]

Abbreviations: me, methylation; Ac, acetylation; MB, medulloblastoma; NB, neuroblastoma

MLL3, KDM6A, and ZMYM3, enzymes for H3K27 and H3K4 trimethylation, are defined novel targets for subgroup 3 and 4 MBs [11, 15, 29–30].

As illustrated, histone modifications are key regulators of gene expression in brain tumors. Increasing evidence indicates cell-specific and spatiotemporal histone marks related to brain tumor chemo- and radio-sensitivity. MDR is a major clinical challenge that hampers the success of brain tumor pharmacotherapy. This review summarizes major MDR mechanisms in brain tumors, and presents an overview of the current findings on the role of histone modifications in MDR in pediatric and adult brain tumors. Future directions to further elucidate how epigenetic changes impact these mechanisms will also be discussed.

Classic MDR mechanisms in brain tumors

Mechanisms of MDR include increased drug efflux by ATP-binding cassette (ABC) transporters, perturbed DNA damage repair, inactivation of pro-apoptotic genes, activation of parallel or downstream signal transduction pathways and secondary mutations in drug targets, as summarized in Table 2. This section will review MDR mechanisms, with the following section outlining current knowledge of epigenetic modifications associated with these mechanisms.

ABC transporters

ATP-dependent efflux pumps impair chemotherapeutic efficacy by lowering intracellular drug concentrations. These pumps belong to a family of ABC transporters that share sequence and structural homology. Presently, 48 human ABC genes have been identified and divided into seven distinct subfamilies (ABCA-ABCG) [31] [refer to Gottesman PA, *et al* (2002) for a complete review on the role of these molecules in cancer [32]].

P-glycoprotein (P-gp), also known as multi-drug resistance protein 1 (MDR1), mediates drug resistance and is the most extensively characterized brain tumor MDR mechanism. P-gp is an ATP-driven transmembrane drug transporter that decreases intracellular drug accumulation bidirectionally by both decreasing drug uptake and increasing drug efflux. High expression of P-gp, encoded by the ABCB1 or MDR1 gene is associated with chemoresistance and poor outcome in brain tumors including MBs [33–34], gliomas [35] and ependymomas [36–38].

Regulatory mechanisms that induce the overexpression of P-gp in brain tumors remain largely undefined, however there is growing evidence that protein kinase C, the RAS oncogene, the TP53 tumor-suppressor gene, and the murine double minute 2 (MDM2) gene are involved

Table 2 Chemotherapy drugs are currently in use for brain tumors and their potential relevant mechanisms of resistance

Mode of action	Drugs	Mechanism of resistance	Brain tumor
DNA crosslink	Nimustine (ACNU)	MGMT, PKC, DNA repair	Glioblastoma, anaplastic astrocytoma
	Carmustine (BCNU)	MGMT, GST/GSH, PKC, DNA repair	Glioblastoma, anaplastic astrocytoma
	Lomustine (CCNU)	MGMT, PKC, DNA repair	Glioblastoma, anaplastic astrocytoma, anaplastic oligodendroglioma, PNET, MBs
	Fotemustine	MGMT, DNA repair	Glioblastoma, anaplastic astrocytoma
	Cisplatin, carboplatin	Metallothioneins, GST/GSH, MRP, PKC, cell cycle arrest	PNET, MBs, anaplastic ependymoma
	Ifosfamide	DNA alkylation by attachment at the N-7 guanine	PNET, MBs, anaplastic ependymoma
	Cyclophosphamide	DNA alkylation	PNET, MBs, anaplastic ependymoma
Topoisomerase II interference	Teniposide	Topoisomerase Iiα, P-gp *, MRP, PKC	Glioblastoma, anaplastic astrocytoma
	Etoposide (VP-16)	Topoisomerase Iiα, P-gp, MRP, PKC	PNET, MBs, anaplastic ependymoma
MGMT	Temozolomide	MGMT, DNA repair	Recurrent of progressive high grade glioma
	Procarbazine	MGMT, DNA repair	Glioblastoma, anaplastic astrocytoma, anaplastic oligodendroglioma, PNET, MBs
	Dacarbazine	MGMT, DNA repair	PNET, MBs
Inhibition of microtubule formation	Vincristine	P-gp, MRP, PKC	Anaplastic oligodendroglioma, progressive high grade glioma, PNET, MBs
Folate pathway interference	Methotrexate	DHFR	PNET, MBs, anaplastic ependymoma

Abbreviations: MGMT, O6-methylguanine-DNA methyltransferase; PKC, protein kinase C; GSH, reduced glutathione; GST, glutathione-s-transferase; MRP, multidrug resistant-associated protein; DHFR, dihydrofolate reductase; MB, medulloblastoma; PNET, primitive neuroectodermal tumors. * ABCG2 may work with P-gp in this process

in modulating MDR1 expression and P-gp phosphorylation [39]. Our laboratory has demonstrated that ABCB1 is overexpressed in glioblastoma cells following prolonged chemotherapy, and this process is regulated by CD133 and DNA dependent protein kinase (DNA-PK) via the PI3K- or Akt-NF-κB signaling pathway [40].

In addition to P-gp, multidrug-resistance-related proteins (MRPs), which belong to ABC transporter subfamily C, may also be a factor in the formation of intrinsic or acquired MDR in brain tumors [41–44]. MRP-mediated drug transport is influenced by intracellular glutathione levels [45]; the details of this interaction are still being elucidated. The mechanism of MRP induction in brain tumors remains unclear, however post-transcriptional regulation is likely the primary mode of MRP upregulation [45]. A link between MRP overexpression and decreased patient survival has been shown for neuroblastomas [46].

A number of additional drug transporters, ABCG2 (breast cancer resistance protein, BCRP) [47–49], ABCA1 [50-51], and ABCB6 [52], are overexpressed in brain tumors and are involved in the formation of either intrinsic or acquired MDR. For instance, ABCG2 is a dominant drug transporter in brain tumors [53], and its expression and activity are upregulated in neuroepithelial tumors such as ependymomas and in glioma tumor stem-like cells [54]. However, ABCG2 protein expression and transport activity are downregulated in primary CNS lymphoma [55]. ABCG2 is highly expressed in the plasma membrane of human neural stem cells and tumor stem cells [56–57]. At a functional level, ABCG2 significantly overlaps with P-gp [58–59]. Anticancer drugs transported by ABCG2 include tyrosine kinase inhibitors [60–65], topotecan, irinotecan, epirubicin, doxorubicin, daunorubicin, and mitoxantrone [66–67]. ABCG2 restricts brain tumor penetration by these chemotherapeutics.

Overall, enhanced ABC transporter activity is a primary mechanism for drug resistance and a significant impediment to successful brain tumor treatment.

DNA repair

DNA repair is another crucial mechanism associated with chemotherapeutic resistance in human brain tumors. The majority of chemotherapeutic agents used to treat brain tumors, including chloroethylnitrosourea (CENU), carmustine (BCNU), cisplatin, carboplatin, and temozolomide (TMZ), target rapidly dividing cancer cells directly or indirectly, which in turn induces DNA damage. Upon recognizing DNA damage, cells initiate a complex variety of signaling pathways collectively referred to as the DNA damage response. Some repair mechanisms target specific lesions, such as mismatch repair, excision repair, double-strand break repair, and the addition of

poly-ADP ribose, while other more general mechanisms can act on a wide range of lesions. Enhanced DNA repair capability has been implicated as a cause of increased chemoresistance in brain tumors including gliomas [40, 68–70], ependymomas [71], MBs [36, 71–72], primitive neuroectodermal tumors (PNET) [71], and pituitary carcinoma [73].

Alkylating agent-based chemotherapy increases response rates and survival times for glioma patients. The most frequently used alkylating agent, TMZ, crosses the blood-brain barrier, and exhibits schedule-dependent antitumor activity. The efficacy of TMZ for glioblastoma treatment is influenced by the expression of the ubiquitous DNA repair enzyme O^6-methylguanine-DNA-methyl-transferase (MGMT). MGMT is overexpressed in gliomas and is the primary mechanism for TMZ resistance. TMZ induces cytotoxic O^6-guanine methyl adducts that are removed by functional MGMT. MGMT promoter methylation lowers MGMT protein expression, improves clinical outcomes in adults and children with high grade gliomas, and is thus a predictor for TMZ response [74]. Deficiencies in DNA mismatch repair (MMR) are also linked with resistance to alkylating agents like TMZ [74], as are elevated levels of Ape1/Ref-1, a major component of the base excision repair (BER) system [75]. Attempts to enhance TMZ-induced cytotoxicity by disrupting BER via poly-(ADP-ribose)-polymerase inhibition has been proposed as a treatment for malignant gliomas, particularly in tumors deficient in DNA mismatch repair [76].

Other DNA damage repair factors also contribute to drug resistance in brain tumors. For example, functional alterations of the MMR system, such as overexpression of the MMR gene *hMSH2*, are associated with drug resistance in gliomas [77]. The double strand break (DSB) DNA repair enzyme DNA-dependent protein kinase catalytic subunit (DNA-PKcs), a critical enzyme for DSB repair via non-homogeneous end joining, is overexpressed and regulates drug resistance in glioblastoma cells [40]. PARP1, which is essential in single strand break DNA repair through BER, is overexpressed in malignant pediatric brain tumors including ependymomas, atypical teratoid/rhabdoid tumors, MBs, choroid plexus papillomas, and PNET [78]. Rad51-mediated homologous recombination directed DNA repair contributes to cisplatin resistance in MB cells [79] and oligodendrogliomas [80]. ARTD-5, a poly ADP-ribose enzyme (PARP) involved in non-homologous end-joining the major pathway for DSB repair, enhances DNA damage repair through DNA-PKcs activation in MB cells [81].

Additional mechanisms of drug resistance in brain tumors

In addition to efflux pumps and DNA repair mechanisms, apoptosis, cell cycle, and cell transduction pathways are also factors in drug resistance. For instance, anti-apoptotic BCL2 proteins such as BCL2, BCL-XL, MCL1, and BCL2A1 are overexpressed and appear to be involved in MDR of various cancer types, including glioma [82–83] and MB [84–86]. The tumor suppressor p53, which can limit cell proliferation through several mechanisms, is also associated with drug resistance. Artificial expression of wild-type p53 curtails MGMT transcription in human tumor cells and enhances their sensitivity to alkylating agents [87]. Mutant TP53 enhances glioblastoma cell resistance to TMZ by upregulating MGMT [88], while abrogation of wild-type p53 function strongly attenuates TMZ cytotoxicity [70]. The oncogenes RB [89], c-Myc, c-Jun [90] and Ras [91], the cell cycle regulators p21 and p27 [92], the MDM2 gene [93], signal transduction elements such as protein kinase C [94–95] and NF-κB [40], and tyrosine kinase receptors such as EGFR [96–97] and c-Met [98–99] also demonstrate critical roles in the genesis of drug resistance in brain tumors.

Histone modifications and drug resistance in brain tumors

Drug resistance mechanisms were initially associated with genetic alterations, however, recent studies indicate that histone modifications also play a role in drug efflux, perturbed DNA repair, and silencing of apoptotic genes. Post-translational histone modification provides an important regulatory platform for biological processes such as chromosome condensation and segregation, gene expression, proliferation, apoptosis, and DNA replication and repair. Recent studies demonstrated that histone modifications also contribute to brain tumorigenesis [11, 14, 25, 28–30, 100–104]. These studies established a critical role for epigenetics as a driving force in tumorigenesis and provide a rationale for epigenetic changes and non-genetic heterogeneity observed in brain tumors. The establishment of tumor epigenomes further allows for the determination of additional epigenetic changes that regulate biological processes, including MDR.

Histone modification of ABC transporters

Histone modification has not yet been shown to directly affect ABCB1 expression in brain tumors, however, histone modification and changes in activity of key chromatin remodeling complexes do alter ABCB1 promoter methylation, and thus ABCB1 expression. Chemotherapeutic drugs can actively induce H3 and H4 acetylation, H3K4 methylation [105], and H3K9 acetylation [106] within discrete regions of the ABCB1 locus. Acetylated histone H3, H3K4me3, H3S10 phosphorylation, and H3K9me3 are associated with the ABCG2 promoter following selection for drug resistance [107]. Overall, it is highly likely that histone modification regulates ABC transporter expression in brain tumors.

In addition to global aberrations at the histone level, enzymes for histone modification and their effects on drug tolerance have been studied. Trimethylation of H3K4 at the ABCB1 promoter is dependent on the methyltransferase MLL1. MLL1 knockdown decreases constitutive ABCB1 expression and sensitizes cancer cells to chemotherapeutic agents [108]. HDAC inhibition enhances global histone acetylation, and results in upregulation of several members of the ABC transporter family, MDR1, ABCG2, and MRP8 [45, 107, 109–112]. MeCP2, a methyl-CpG-binding protein [113], binds to hypermethylated DNA at the ABCB1 promoter [114] and provides a docking platform for nucleosome modifiers and remodelers, such as SWI/SNF, HDAC1, HDAC2, and mSIN3, thereby altering the chromatin state of gene promoters and subsequent transcription [115–117]. Although a direct interaction of these corepressors with ABCB1 promoter-bound MeCP2 has not been described, ABCB1 expression is induced upon inhibition of HDAC activity or by overexpression of the p300/CREB lysine acetyltransferase, KAT3B [105, 118–119]. The MeCP2/HDAC complex represses ABCB1 expression [114], however, removal of HDAC inhibition dramatically reduces ABCB1 protein levels, suggesting that other factors may also regulate ABCB1 expression [120]. Overall, the data indicate that ABC transporter expression is regulated by promoter histone modification, and these changes can contribute to acquisition of drug resistance in response to chemotherapy.

Histone modification and DNA repair in brain tumors

Eukaryotic cells encounter numerous endogenous and exogenous genotoxic stresses that trigger DNA damage, including DNA DSBs. To overcome these threats, cells have evolved mechanisms of DNA damage repair to maintain genomic stability and prevent oncogenic transformation or disease. Compacted chromatin is a major obstacle in the orchestration of DNA repair. For efficient DNA repair, chromatin must first be relaxed to give repair proteins access to the break sites, thus chromatin remodeling is an early event in the DNA repair process [121].

Histone modifications, such as acetylation, methylation, phosphorylation, and ubiquitylation, as well as histone dynamics promoted by histone chaperones and remodeling factors, play critical regulatory roles in response to DNA damage. H4K16Ac and an intact acidic pocket at H2AX are required for recruitment of the DNA repair complex adapter protein Mdc1 to DNA damage sites [122]. H3K56Ac and H3K9Ac are downregulated by DNA damage [123], while H3K56Ac accumulates in response to DNA damage [124–125]. H3K36me3 is involved in MMR [126] and H4K20me1/2 is recognized by the checkpoint mediator 53BP1, which targets it to DNA damage sites [127]. H2AX phosphorylation is required for the recruitment of HATs to DNA break sites; this recruitment is mediated by Arp4 and leads to acetylation of the chromatin surrounding the breaks, thereby relaxing the chromatin and facilitating access for repair proteins [128]. Mono-ubiquitylation of H2A at lysine 119 (H2AK119Ub) mediated by BMI-1 occurs at DNA double-strand breaks [129]. Histone loss, enhanced histone mobility/turnover, histone chaperones and enrichment of histone variants are also associated with DNA repair, as recently reviewed by Adam S *et al* [130] and House NC *et al* [131]. Finally, crosstalk between histone modifications during the DNA damage response is also crucial for DNA repair [132].

Histone modification is involved in the DNA damage response in brain tumors. Phosphorylation of H2AX at serine 139 (Ser139), termed γH2AX, accumulates at DNA damage sites in glioblastoma cells [133]. Acetylated H3, along with the γH2AX/53BP1 complex increase following DNA damage induced by radiation in glioblastoma cells [134]. Inhibition of LSD1 (also known as KDM1A), a demethyltransferase of H3K4me2, sensitizes glioblastoma cells to DNA damage induced by HDAC inhibitors [135]. Overexpression of γH2AX following valproic acid and pyrimethamine treatment sensitizes meningioma cells to radiotherapy [136] and pituitary adenomas cells to TMZ [137], respectively. Accumulation of γH2AX occurs in MBs following DNA damage induced by irradiation and SPARC, a putative radioresistance-reversal gene, increases γH2AX levels [138]. These studies indicate that chromatin remodeling, including histone modification, is involved in DNA repair induced by irradiation or DNA-damaging pharmacotherapy in brain tumors.

Histone modification and other drug resistance mechanisms in brain tumors

Epigenetic perturbations, including histone modification, may result in defective apoptotic response, cell cycle arrest, and/or cell signal transduction, which may in turn produce drug-resistant tumor cells.

The tumor suppressor gene TP53 promotes cell-cycle arrest or apoptosis in response to chemotherapy. TP53 loss or inhibition can induce drug resistance [70]. Inhibition of LSD1 increases H3K4me2 and H3K9Ac, reduces H3K9me2, and promotes p53 target genes p21 and PUMA, leading to apoptosis of glioma xenograft tumors [16]. Treatment of glioma cells with the HDAC inhibitor vorinostat enhances H3 and H4 acetylation, increases p21 levels in a p53-independent manner, and decreases cyclin B1, resulting in G2 phase cell cycle arrest followed by apoptosis [139]. HDAC4 suppresses the expression of the cell cycle regulator $p21^{WAF1/CIP1}$ in tumor cells by reducing H3 acetylation at the proximal promoter of the CDKN1A gene (cyclin dependent kinase inhibitor 1A). Silencing HDAC4 induces $p21^{WAF1/CIP1}$ expression and decreases tumor growth of glioblastoma cells independently of p53 [140].

Histone modifications regulate a number of other apoptotic genes. For example, CHI3L1 (chitinase-3-like protein 1, also known as YKL-40) is overexpressed in glioma cells, where it affects chemo- and radio-sensitivity [141]. TNF-α (tumor necrosis factor-alpha)-mediated recruitment of NF-κB subunits p65 and p50 to the YKL-40 promoter suppresses its expression. Recruitment of HDAC1 and HDAC2 deacetylates H3 at the YKL-40 promoter region, preventing NF-κB binding [142]. RASL10A (RAS-like family 10, member A, also named RRP22), a novel neural tumor suppressor that induces caspase-independent cell death [143], is downregulated in astrocytomas [144]. RASL10A is repressed by H3K9me3 and reduced pan-Ac-H3 in its promoter region [145]. Apoptosis has been observed in response to HDAC inhibition in PNET [146], atypical teratoid/rhabdoid tumors [147], and MBs [148]. Histone modification regulates the expression of NEURL1, thereby downregulating Notch target genes [149], which are potentially associated with drug resistance [150]. The oncogenic PI3K–AKT pathway, frequently altered in malignant gliomas, upregulates expression of the transcription factor HOXA9 (homeobox A9) through histone modification. Pro-proliferative, anti-apoptotic properties of HOXA9 are associated with poor glioma prognosis. These modifications could possibly be initiated by AKT-induced EZH2 histone methyltransferase activity [12].

Histone modification: therapeutic targets for treating brain tumors

Four epigenome-targeted anticancer drugs have been approved by the U.S. Food and Drug Administration: two DNA methyltransferase inhibitors, azacitidine and decitabine, and two HDAC inhibitors: vorinostat and romidepsin. Only HDAC inhibitors are being tested in glioblastomas, as reviewed by Spyropoulou A *et al* [151]. HDACs cooperate with LSD1 to regulate key cell death pathways in glioblastoma cell lines but not in normal cells, therefore a combination of LSD1 and HDAC inhibitors is being investigated as a therapeutic approach for glioblastoma [135].

A major challenge for cancer treatment via epigenetic therapy is target specificity. For instance, genes that are normally inactive due to histone deacetylation may become activated in response to HDAC inhibitors. Moreover, HDACs not only catalyze deacetylation of lysine residues in core histones but also in non-histone proteins, and as a result, they exhibit complex, unpredictable effects. In addition, interactions between histone modification, DNA methylation, and DNA binding proteins are crucial in DNA repair and cellular signaling and function [132, 152]. These interactions have yet to be fully elucidated. Overall, molecular mechanisms that bring about histone modifications and their outcomes should be further studied to get an overall understanding of their role in these biological processes.

Conclusion

Histone modifications described in this review and their roles in development of drug resistance are only the tip of the iceberg. With advances in high throughput studies, including methylated DNA immuno-precipitation and sequencing, RNA-seq, and chromatin immunoprecipitation and sequencing (ChIP-seq), new patterns of histone modifications as well as their interactions with DNA methylation and non-coding RNAs are likely to be uncovered in brain tumors and other tissues. Gaining insight into the causes and consequences of aberrant histone modifications will extend our understanding of brain tumor carcinogenesis, adaption, and survival in response to environmental factors such as drug treatment. This knowledge will accelerate the development of "epigenetic drugs" for prevention or treatment of drug-resistant cells.

Conflict of interest

The authors declare no conflict of interest.

Acknowledgement

We are grateful to Dr. Ben Yang for his assistance in the preparation of figure for this review. We apologize to authors whose primary references could not be cited due to space limitation.

Conflicts of interest

The authors indicated no potential conflicts of interest.

References

1. Jemal A, Siegel R, Ward E, *et al*. Cancer statistics, 2006. CA Cancer J Clin, 2006, 56: 106–130.
2. Ostrom QT, Gittleman H, Liao P, *et al*. CBTRUS statistical report: primary brain and central nervous system tumors diagnosed in the United States in 2007-2011. Neuro Oncol, 2014, 16: 1–63.
3. Bredel M, Zentner J. Brain-tumour drug resistance: the bare essentials. Lancet Oncol, 2002, 3: 397–406.
4. Dixon JR, Jung I, Selvaraj S, *et al*. Chromatin architecture reorganization during stem cell differentiation. Nature, 2015, 518: 331–336.
5. Phillips-Cremins JE, Sauria ME, Sanyal A, *et al*. Architectural protein subclasses shape 3D organization of genomes during lineage commitment. Cell, 2013, 153: 1281–1295.
6. Kornberg RD, Lorch Y. Twenty-five years of the nucleosome, fundamental particle of the eukaryote chromosome. Cell, 1999, 98: 285–294.
7. Khorasanizadeh S. The nucleosome: from genomic organization to genomic regulation. Cell, 2004, 116: 259–272.
8. Cosgrove MS, Boeke JD, Wolberger C. Regulated nucleosome mobility and the histone code. Nat Struct Mol Biol, 2004, 11: 1037–1043.
9. Nagarajan RP, Zhang B, Bell RJ, *et al*. Recurrent epimutations activate gene body promoters in primary glioblastoma. Genome Res,

2014, 24: 761–774.
10. Parsons DW, Jones S, Zhang X, *et al*. An integrated genomic analysis of human glioblastoma multiforme. Science, 2008, 321: 1807–1812.
11. Robinson G, Parker M, Kranenburg TA, *et al.* Novel mutations target distinct subgroups of medulloblastoma. Nature, 2012, 488: 43-48.
12. Costa BM, Smith JS, Chen Y, *et al*. Reversing HOXA9 oncogene activation by PI3K inhibition: epigenetic mechanism and prognostic significance in human glioblastoma. Cancer Res, 2010, 70: 453–462.
13. Venneti S, Garimella MT, Sullivan LM, *et al*. Evaluation of histone 3 lysine 27 trimethylation (H3K27me3) and enhancer of Zest 2 (EZH2) in pediatric glial and glioneuronal tumors shows decreased H3K27me3 in H3F3A K27M mutant glioblastomas. Brain Pathol, 2013, 23: 558–564.
14. Mack SC, Witt H, Piro RM, *et al.* Epigenomic alterations define lethal CIMP-positive ependymomas of infancy. Nature, 2014, 506: 445–450.
15. Dubuc AM, Remke M, Korshunov A, *et al*. Aberrant patterns of H3K4 and H3K27 histone lysine methylation occur across subgroups in medulloblastoma. Acta Neuropathol, 2013, 125: 373–384.
16. Sareddy GR, Nair BC, Krishnan SK, *et al*. KDM1 is a novel therapeutic target for the treatment of gliomas. Oncotarget, 2013, 4: 18–28.
17. Northcott PA, Nakahara Y, Wu X, *et al.* Multiple recurrent genetic events converge on control of histone lysine methylation in medulloblastoma. Nat Genet, 2009, 41: 465–472.
18. Berdasco M, Ropero S, Setien F, *et al.* Epigenetic inactivation of the Sotos overgrowth syndrome gene histone methyltransferase NSD1 in human neuroblastoma and glioma. Proc Natl Acad Sci USA, 2009, 106: 21830–21835.
19. Zhu X, Asa SL, Ezzat S. Fibroblast growth factor 2 and estrogen control the balance of histone 3 modifications targeting MAGE-A3 in pituitary neoplasia. Clin Cancer Res, 2008, 14: 1984–1996.
20. Liu BL, Cheng JX, Zhang X, *et al.* Global histone modification patterns as prognostic markers to classify glioma patients. Cancer Epidemiol Biomarkers Prev, 2010, 19: 2888–2896.
21. Lucio-Eterovic AK, Cortez MA, Valera ET, *et al.* Differential expression of 12 histone deacetylase (HDAC) genes in astrocytomas and normal brain tissue: class II and IV are hypoexpressed in glioblastomas. BMC cancer, 2008, 8: 243.
22. Lin B, Lee H, Yoon JG, *et al*. Global analysis of H3K4me3 and H3K27me3 profiles in glioblastoma stem cells and identification of SLC17A7 as a bivalent tumor suppressor gene. Oncotarget, 2015, 6: 5369–5381.
23. Ebrahimi A, Schittenhelm J, Honegger J, *et al.* Prognostic relevance of global histone 3 lysine 9 acetylation in ependymal tumors. J. Neurosurg, 2013, 119: 1424–1431.
24. Pease M, Ling C, Mack WJ, *et al.* The role of epigenetic modification in tumorigenesis and progression of pituitary adenomas: a systematic review of the literature. PloS one, 2013, 8: 82619.
25. Yacqub-Usman K, Richardson A, Duong CV, *et al*. The pituitary tumour epigenome: aberrations and prospects for targeted therapy. Nat Rev Endocrinol, 2012, 8: 486–494.
26. Campos B, Bermejo JL, Han L, *et al*. Expression of nuclear receptor corepressors and class I histone deacetylases in astrocytic gliomas. Cancer Sci, 2011, 102: 387–392.
27. Ecker J, Oehme I, Mazitschek R, *et al*. Targeting class I histone deacetylase 2 in MYC amplified group 3 medulloblastoma. Acta Neuropathol Commun, 2015, 3: 22.
28. Schwartzentruber J, Korshunov A, Liu XY, *et al*. Driver mutations in histone H3.3 and chromatin remodelling genes in paediatric glioblastoma. Nature, 2012, 482: 226–231.
29. Pugh TJ, Weeraratne SD, Archer TC, *et al*. Medulloblastoma exome sequencing uncovers subtype-specific somatic mutations. Nature, 2012, 488: 106–110.
30. Northcott PA, Shih DJ, Peacock J, *et al*. Subgroup-specific structural variation across 1,000 medulloblastoma genomes. Nature, 2012, 488: 49–56.
31. Northcott PA, Korshunov A, Pfister SM, *et al.* The clinical implications of medulloblastoma subgroups. Nature reviews. Neurology, 2012, 8: 340–351.
32. Gottesman MM, Fojo T, Bates SE. Multidrug resistance in cancer: role of ATP-dependent transporters. Nat Rev Cancer, 2002, 2: 48–58.
33. Ang C, Guiot MC, Ramanakumar AV, *et al*. Clinical significance of molecular biomarkers in glioblastoma. Can J Neurol Sci, 2010, 37: 625–630.
34. Ramaswamy V, Remke M, Adamski J, *et al*. Medulloblastoma subgroup-specific outcomes in irradiated children: who are the true high-risk patients? Neuro Oncol, 2016, 18: 291–297.
35. Zhukova N, Ramaswamy V, Remke M, *et al.* WNT activation by lithium abrogates TP53 mutation associated radiation resistance in medulloblastoma. Acta neuropathologica communications, 2014, 2: 174.
36. Othman RT, Kimishi I, Bradshaw TD, *et al*. Overcoming multiple drug resistance mechanisms in medulloblastoma. Acta Neuropathol Commun, 2014, 2: 57.
37. Gottardo NG, Hansford JR, McGlade JP, *et al*. Medulloblastoma Down Under 2013: a report from the third annual meeting of the International Medulloblastoma Working Group. Acta Neuropathol, 2014, 127: 189–201.
38. Ellison DW. Childhood medulloblastoma: novel approaches to the classification of a heterogeneous disease. Acta Neuropathol, 2010, 120: 305–316.
39. Bredel M. Anticancer drug resistance in primary human brain tumors. Brain Res Brain Res Rev, 2001, 35: 161–204.
40. Xi G, Hayes E, Lewis R, *et al*. CD133 and DNA-PK regulate MDR1 via the PI3K- or Akt-NF-kappaB pathway in multidrug-resistant glioblastoma cells in vitro. Oncogene, 2016, 35: 241–250.
41. Alexiou GA, Goussia A, Voulgaris S, *et al*. Prognostic significance of MRP5 immunohistochemical expression in glioblastoma. Cancer Chemother Pharmacol, 2012, 69: 1387–1391.
42. Kuan CT, Wakiya K, Herndon JE 2nd, *et al*. MRP3: a molecular target for human glioblastoma multiforme immunotherapy. BMC Cancer, 2010, 10: 468.
43. Burkhart CA, Watt F, Murray J, *et al*. Small-molecule multidrug resistance-associated protein 1 inhibitor reversan increases the therapeutic index of chemotherapy in mouse models of neuroblastoma. Cancer Res, 2009, 69: 6573–6580.
44. Dallas S, Miller DS, Bendayan R. Multidrug resistance-associated proteins: expression and function in the central nervous system. Pharmacol Rev, 2006, 58: 140–161.
45. Gomi A, Masuzawa T, Ishikawa T, *et al*. Posttranscriptional regulation of MRP/GS-X pump and gamma-glutamylcysteine synthetase expression by 1-(4-amino-2-methyl-5-pyrimidinyl) methyl-3-(2-chloroethyl)-3-nitrosourea and by cycloheximide in human glioma cells. Biochem Biophys Res Commun, 1997, 239: 51–56.
46. Norris MD, Bordow SB, Marshall GM, *et al*. Expression of the gene for multidrug-resistance-associated protein and outcome in patients with neuroblastoma. N Engl J Med, 1996, 334: 231–238.
47. Lin F, de Gooijer MC, Roig EM, *et al.* ABCB1, ABCG2, and PTEN determine the response of glioblastoma to temozolomide and ABT-888 therapy. Clin Cancer Res, 2014, 20: 2703–2713.
48. de Vries NA, Zhao J, Kroon E, *et al.* P-glycoprotein and breast can-

cer resistance protein: two dominant transporters working together in limiting the brain penetration of topotecan. Clin Cancer Res, 2007, 13: 6440–6449.
49. Veringa SJ, Biesmans D, van Vuurden DG, *et al*. In vitro drug response and efflux transporters associated with drug resistance in pediatric high grade glioma and diffuse intrinsic pontine glioma. PloS One, 2013, 8: 61512.
50. Ingram WJ, Crowther LM, Little EB, *et al*. ABC transporter activity linked to radiation resistance and molecular subtype in pediatric medulloblastoma. Exp Hematol Oncol, 2013, 2: 26.
51. Rama AR, Alvarez PJ, Madeddu R, Aranega A. ABC transporters as differentiation markers in glioblastoma cells. Mol. Biol. Rep, 2014, 41: 4847–4851.
52. Zhao SG, Chen XF, Wang LG, *et al*. Increased expression of ABCB6 enhances protoporphyrin IX accumulation and photodynamic effect in human glioma. Ann Surg Oncol, 2013, 20: 4379–4388.
53. Agarwal S, Hartz AM, Elmquist WF, *et al*. Breast cancer resistance protein and P-glycoprotein in brain cancer: two gatekeepers team up. Curr Pharm Des, 2011, 17: 2793–2802.
54. Bleau AM, Hambardzumyan D, Ozawa T, *et al*. PTEN/PI3K/Akt pathway regulates the side population phenotype and ABCG2 activity in glioma tumor stem-like cells. Cell Stem Cell, 2009, 4: 226–235.
55. Sakata S, Fujiwara M, Ohtsuka K, *et al*. ATP-binding cassette transporters in primary central nervous system lymphoma: decreased expression of MDR1 P-glycoprotein and breast cancer resistance protein in tumor capillary endothelial cells. Oncol Rep, 2011, 25: 333–339.
56. Islam MO, Kanemura Y, Tajria J, *et al*. Functional expression of ABCG2 transporter in human neural stem/progenitor cells. Neurosci. Res, 2005, 52: 75–82.
57. Zhou S, Schuetz JD, Bunting KD, *et al*. The ABC transporter Bcrp1/ABCG2 is expressed in a wide variety of stem cells and is a molecular determinant of the side-population phenotype. Nat Med, 2001, 7: 1028–1034.
58. Allen JD, Brinkhuis RF, Wijnholds J, *et al.* The mouse Bcrp1/Mxr/Abcp gene: amplification and overexpression in cell lines selected for resistance to topotecan, mitoxantrone, or doxorubicin. Cancer Res, 1999, 59: 4237–4241.
59. Sarkadi B, Ozvegy-Laczka C, Nemet K, *et al*. ABCG2 -- a transporter for all seasons. FEBS Lett, 2004, 567: 116–120.
60. Mi YJ, Liang YJ, Huang HB, *et al*. Apatinib (YN968D1) reverses multidrug resistance by inhibiting the efflux function of multiple ATP-binding cassette transporters. Cancer Res, 2010, 70: 7981–7991.
61. Perry J, Ghazaly E, Kitromilidou C, *et al*. A synergistic interaction between lapatinib and chemotherapy agents in a panel of cell lines is due to the inhibition of the efflux pump BCRP. Mol Cancer Ther, 2010, 9: 3322–3329.
62. Shukla S, Sauna ZE, Ambudkar SV. Evidence for the interaction of imatinib at the transport-substrate site(s) of the multidrug-resistance-linked ABC drug transporters ABCB1 (P-glycoprotein) and ABCG2. Leukemia, 2008; 22:445–447.
63. Yang JJ, Milton MN, Yu S, *et al.* P-glycoprotein and breast cancer resistance protein affect disposition of tandutinib, a tyrosine kinase inhibitor. Drug Metab Letters, 2010, 4: 201–212.
64. Agarwal S, Sane R, Gallardo JL, *et al*. Distribution of gefitinib to the brain is limited by P-glycoprotein (ABCB1) and breast cancer resistance protein (ABCG2)-mediated active efflux. J Pharmacol Exp Ther, 2010, 334: 147–155.
65. Agarwal S, Sane R, Ohlfest JR, *et al*. The role of the breast cancer resistance protein (ABCG2) in the distribution of sorafenib to the brain. J Pharmacol Exp Ther, 2011, 336: 223–233.
66. Han B, Zhang JT. Multidrug resistance in cancer chemotherapy and xenobiotic protection mediated by the half ATP-binding cassette transporter ABCG2. Current Med Chem Anti Cancer Agents, 2004, 4: 31–42.
67. Schellens JH, Maliepaard M, Scheper RJ, *et al*. Transport of topoisomerase I inhibitors by the breast cancer resistance protein. Potential clinical implications. Ann NY Acad Sci, 2000, 922: 188–194.
68. Balvers RK, Lamfers ML, Kloezeman JJ, *et al*. ABT-888 enhances cytotoxic effects of temozolomide independent of MGMT status in serum free cultured glioma cells. Journal of translational medicine, 2015, 13: 74.
69. Annovazzi L, Caldera V, Mellai M, *et al*. The DNA damage/repair cascade in glioblastoma cell lines after chemotherapeutic agent treatment. Int J Oncol, 2015, 46: 2299–2308.
70. Frosina G. DNA repair and resistance of gliomas to chemotherapy and radiotherapy. Mol Cancer Res, 2009, 7: 989–999.
71. Hussein D, Punjaruk W, Storer LC, *et al.* Pediatric brain tumor cancer stem cells: cell cycle dynamics, DNA repair, and etoposide extrusion. Neuro Oncol, 2011, 13: 70–83.
72. Lee Y, Miller HL, Jensen P, *et al.* A molecular fingerprint for medulloblastoma. Cancer Res, 2003, 63: 5428–5437.
73. Murakami M, Mizutani A, Asano S, *et al.* A mechanism of acquiring temozolomide resistance during transformation of atypical prolactinoma into prolactin-producing pituitary carcinoma: case report. Neurosurgery, 2011, 68: 1761–1767.
74. Middlemas DS, Stewart CF, Kirstein MN, *et al*. Biochemical correlates of temozolomide sensitivity in pediatric solid tumor xenograft models. Clin. Cancer Res, 2000, 6: 998–1007.
75. Silber JR, Bobola MS, Blank A, *et al.* The apurinic/apyrimidinic endonuclease activity of Ape1/Ref-1 contributes to human glioma cell resistance to alkylating agents and is elevated by oxidative stress. Clin. Cancer Res, 2002, 8: 3008–3018.
76. Cheng CL, Johnson SP, Keir ST, *et al.* Poly(ADP-ribose) polymerase-1 inhibition reverses temozolomide resistance in a DNA mismatch repair-deficient malignant glioma xenograft. Mol Cancer ther, 2005, 4: 1364–1368.
77. Rellecke P, Kuchelmeister K, Schachenmayr W, *et al.* Mismatch repair protein hMSH2 in primary drug resistance in in vitro human malignant gliomas. J Neurosurg, 2004, 101: 653–658.
78. Barton VN, Donson AM, Kleinschmidt-DeMasters BK, *et al*. PARP1 expression in pediatric central nervous system tumors. Pediatr Blood Cancer, 2009, 53:1227–1230.
79. Wilk A, Waligorska A, Waligorski P, *et al*. Inhibition of ERbeta induces resistance to cisplatin by enhancing Rad51-mediated DNA repair in human medulloblastoma cell lines. PloS one, 2012, 7: 33867.
80. See WL, Miller JP, Squatrito M, *et al.* Defective DNA double-strand break repair underlies enhanced tumorigenesis and chromosomal instability in p27-deficient mice with growth factor-induced oligodendrogliomas. Oncogene, 2010, 29: 1720–1731.
81. Renna C, Salaroli R, Cocchi C, *et al.* XAV939-Mediated ARTD Activity Inhibition in Human MB Cell Lines. PloS One, 2015, 10: 0124149.
82. Harrison JF, Rinne ML, Kelley MR, *et al*. Altering DNA base excision repair: use of nuclear and mitochondrial-targeted N-methylpurine DNA glycosylase to sensitize astroglia to chemotherapeutic agents. Glia, 2007, 55: 1416–1425.
83. Lu C, Shervington A. Chemoresistance in gliomas. Mol Cell Biochem, 2008, 312: 71–80.
84. Huang S, Sinicrope FA. BH3 mimetic ABT-737 potentiates TRAIL-mediated apoptotic signaling by unsequestering Bim and Bak in hu-

man pancreatic cancer cells. Cancer Res, 2008, 68: 2944–2951.
85. Cragg MS, Harris C, Strasser A, *et al*. Unleashing the power of inhibitors of oncogenic kinases through BH3 mimetics. Nat Rev Cancer, 2009, 9: 321–326.
86. Vogler M, Dinsdale D, Dyer MJ, *et al*. Bcl-2 inhibitors: small molecules with a big impact on cancer therapy. Cell Death Differ, 2009, 16: 360–367.
87. Srivenugopal KS, Shou J, Mullapudi SR, *et al.* Enforced expression of wild-type p53 curtails the transcription of the O(6)-methylguanine-DNA methyltransferase gene in human tumor cells and enhances their sensitivity to alkylating agents. Clin Cancer Res, 2001, 7: 1398–1409.
88. Wang X, Chen JX, Liu YH, *et al*. Mutant TP53 enhances the resistance of glioblastoma cells to temozolomide by up-regulating O(6)-methylguanine DNA-methyltransferase. Neurol Sci, 2013, 34: 1421–1428.
89. Nakamura M, Konishi N, Tsunoda S, *et al*. Retinoblastoma protein expression and MIB-1 correlate with survival of patients with malignant astrocytoma. Cancer, 1997, 80: 242–249.
90. Pourquier P, Montaudon D, Huet S, *et al*. Doxorubicin-induced alterations of c-myc and c-jun gene expression in rat glioblastoma cells: role of c-jun in drug resistance and cell death. Biochem Pharmacol, 1998, 55: 1963–1971.
91. Bredel M, Pollack IF. The p21-Ras signal transduction pathway and growth regulation in human high-grade gliomas. Brain Res Brain Res, Rev, 1999, 29: 232–249.
92. Ruan S, Okcu MF, Ren JP, *et al.* Overexpressed WAF1/Cip1 renders glioblastoma cells resistant to chemotherapy agents 1,3-bis(2-chloroethyl)-1-nitrosourea and cisplatin. Cancer Res, 1998, 58: 1538–1543.
93. Kondo S, Barnett GH, Hara H, *et al*. MDM2 protein confers the resistance of a human glioblastoma cell line to cisplatin-induced apoptosis. Oncogene, 1995, 10: 2001–2006.
94. Bredel M, Pollack IF. The role of protein kinase C (PKC) in the evolution and proliferation of malignant gliomas, and the application of PKC inhibition as a novel approach to anti-glioma therapy. Acta Neurochir (Wien), 1997, 139: 1000–1013.
95. Kusne Y, Carrera-Silva EA, Perry AS, *et al.* Targeting aPKC disables oncogenic signaling by both the EGFR and the proinflammatory cytokine TNFalpha in glioblastoma. Sci Signal, 2014, 7: 75.
96. Wykosky J, Hu J, Gomez GG, *et al*. A urokinase receptor-Bim signaling axis emerges during EGFR inhibitor resistance in mutant EGFR glioblastoma. Cancer Res, 2015, 75: 394–404.
97. Nakada M, Kita D, Watanabe T, *et al*. Mechanism of chemoresistance against tyrosine kinase inhibitors in malignant glioma. Brain Tumor Pathol, 2014, 31: 198–207.
98. Zhang Y, Farenholtz KE, Yang Y, *et al*. Hepatocyte growth factor sensitizes brain tumors to c-MET kinase inhibition. Clin Cancer Res, 2013, 19: 1433–1444.
99. Joo KM, Jin J, Kim E, *et al*. MET signaling regulates glioblastoma stem cells. Cancer Res, 2012, 72: 3828–3838.
100. Sepsa A, Levidou G, Gargalionis A, *et al*. Emerging role of linker histone variant H1x as a biomarker with prognostic value in astrocytic gliomas. A multivariate analysis including trimethylation of H3K9 and H4K20. PloS One, 2015, 10: 0115101.
101. Suzuki H, Aoki K, Chiba K, *et al*. Mutational landscape and clonal architecture in grade II and III gliomas. Nat Genet, 2015, 47: 458–468.
102. Zhang L, Chen LH, Wan H, *et al*. Exome sequencing identifies somatic gain-of-function PPM1D mutations in brainstem gliomas. Nat Genet, 2014, 46: 726–730.
103. Jones C, Baker SJ. Unique genetic and epigenetic mechanisms driving paediatric diffuse high-grade glioma. Nat Rev Cancer, 2014, 14. doi: 10.1038/nrc3811.
104. Hovestadt V, Jones DT, Picelli S, *et al*. Decoding the regulatory landscape of medulloblastoma using DNA methylation sequencing. Nature, 2014, 510: 537–541.
105. Baker EK, Johnstone RW, Zalcberg JR, *et al*. Epigenetic changes to the MDR1 locus in response to chemotherapeutic drugs. Oncogene, 2005, 24: 8061–8075.
106. Toth M, Boros IM, Balint E. Elevated level of lysine 9-acetylated histone H3 at the MDR1 promoter in multidrug-resistant cells. Cancer Sci, 2012, 103: 659–669.
107. To KK, Polgar O, Huff LM, *et al*. Histone modifications at the ABCG2 promoter following treatment with histone deacetylase inhibitor mirror those in multidrug-resistant cells. Mol Cancer Res, 2008, 6: 151–164.
108. Huo H, Magro PG, Pietsch EC, *et al*. Histone methyltransferase MLL1 regulates MDR1 transcription and chemoresistance. Cancer Res, 2010, 70: 8726–8735.
109. Hauswald S, Duque-Afonso J, Wagner MM, *et al.* Histone deacetylase inhibitors induce a very broad, pleiotropic anticancer drug resistance phenotype in acute myeloid leukemia cells by modulation of multiple ABC transporter genes. Clin Cancer Res, 2009, 15: 3705–3715.
110. Wu CP, Hsiao SH, Su CY, *et al*. Human ATP-Binding Cassette transporters ABCB1 and ABCG2 confer resistance to CUDC-101, a multi-acting inhibitor of histone deacetylase, epidermal growth factor receptor and human epidermal growth factor receptor 2. Biochem Pharmacol, 2014, 92: 567–576.
111. Chikamatsu K, Ishii H, Murata T, *et al*. Alteration of cancer stem cell-like phenotype by histone deacetylase inhibitors in squamous cell carcinoma of the head and neck. Cancer Sc, 2013, 104: 1468–1475.
112. Basseville A, Tamaki A, Ierano C, *et al*. Histone deacetylase inhibitors influence chemotherapy transport by modulating expression and trafficking of a common polymorphic variant of the ABCG2 efflux transporter. Cancer Res, 2012, 72: 3642–3651.
113. Nan X, Campoy FJ, Bird A. MeCP2 is a transcriptional repressor with abundant binding sites in genomic chromatin. Cell, 1997, 88: 471–481.
114. El-Osta A, Kantharidis P, Zalcberg JR, *et al.* Precipitous release of methyl-CpG binding protein 2 and histone deacetylase 1 from the methylated human multidrug resistance gene (MDR1) on activation. Mol Cell Biol, 2002, 22: 1844–1857.
115. Nan X, Ng HH, Johnson CA, *et al*. Transcriptional repression by the methyl-CpG-binding protein MeCP2 involves a histone deacetylase complex. Nature, 1998, 393: 386–389.
116. Harikrishnan KN, Chow MZ, Baker EK, *et al*. Brahma links the SWI/SNF chromatin-remodeling complex with MeCP2-dependent transcriptional silencing. Nat Genet, 2005, 37: 254–264.
117. Jones PL, Veenstra GJ, Wade PA, *et al*. Methylated DNA and MeCP2 recruit histone deacetylase to repress transcription. Nat. Genet, 1998, 19: 187–191.
118. Jin S, Scotto KW. Transcriptional regulation of the MDR1 gene by histone acetyltransferase and deacetylase is mediated by NF-Y. Mol Cell Biol, 1998, 18: 4377–4384.
119. Tabe Y, Konopleva M, Contractor R, *et al*. Up-regulation of MDR1 and induction of doxorubicin resistance by histone deacetylase inhibitor depsipeptide (FK228) and ATRA in acute promyelocytic leukemia cells. Blood, 2006, 107: 1546–1554.
120. Xiao JJ, Huang Y, Dai Z, *et al*. Chemoresistance to depsipeptide FK228 [(E)-(1S,4S,10S,21R)-7-[(Z)-ethylidene]-4,21-diisopropyl-2-oxa-12,13-dithia-5,8,20,23-tetraazabicyclo[8,7,6]-tricos-16-ene-

3,6,9,22-pentanone] is mediated by reversible MDR1 induction in human cancer cell lines. J Pharmacol Exp Ther, 2005, 314: 467–475.
121.Price BD, D'Andrea AD. Chromatin remodeling at DNA double-strand breaks. Cell, 2013, 152: 1344–1354.
122.Li X, Corsa CA, Pan PW, *et al*. MOF and H4 K16 acetylation play important roles in DNA damage repair by modulating recruitment of DNA damage repair protein Mdc1. Mol Cell Biol, 2010, 30: 5335–5347.
123.Tjeertes JV, Miller KM, Jackson SP. Screen for DNA-damage-responsive histone modifications identifies H3K9Ac and H3K56Ac in human cells. EMBO J, 2009, 28: 1878–1889.
124.Das C, Lucia MS, Hansen KC, *et al.* CBP/p300-mediated acetylation of histone H3 on lysine 56. Nature, 2009, 459: 113–117.
125.Yuan J, Pu M, Zhang Z, *et al*. Histone H3-K56 acetylation is important for genomic stability in mammals. Cell Cycle, 2009, 8: 1747–1753.
126.Li GM. Decoding the histone code: Role of H3K36me3 in mismatch repair and implications for cancer susceptibility and therapy. Cancer Res, 2013, 73: 6379–6383.
127.Jorgensen S, Elvers I, Trelle MB, *et al*. The histone methyltransferase SET8 is required for S-phase progression. J Cell Biol, 2007, 179: 1337–1345.
128.Downs JA, Allard S, Jobin-Robitaille O, *et al*. Binding of chromatin-modifying activities to phosphorylated histone H2A at DNA damage sites. Mol Cell, 2004, 16: 979–990.
129.Gieni RS, Ismail IH, Campbell S, *et al*. Polycomb group proteins in the DNA damage response: a link between radiation resistance and "stemness". Cell cycle, 2011, 10: 883–894.
130.Adam S, Dabin J, Polo SE. Chromatin plasticity in response to DNA damage: The shape of things to come. DNA Repair, 2015, 32: 120–126.
131.House NC, Koch MR, Freudenreich CH. Chromatin modifications and DNA repair: beyond double-strand breaks. Frontiers Genetics, 2014, 5: 296.
132.van Attikum H, Gasser SM. Crosstalk between histone modifications during the DNA damage response. Trends Cell Biol, 2009, 19: 207–217.
133.Facchino S, Abdouh M, Chatoo W, *et al*. BMI1 confers radioresistance to normal and cancerous neural stem cells through recruitment of the DNA damage response machinery. J Neurosci, 2010, 30: 10096–10111.
134.Pont LM, Naipal K, Kloezeman JJ, *et al.* DNA damage response and anti-apoptotic proteins predict radiosensitization efficacy of HDAC inhibitors SAHA and LBH589 in patient-derived glioblastoma cells. Cancer Lett, 2015, 356: 525–535.
135.Singh MM, Manton CA, Bhat KP, *et al*. Inhibition of LSD1 sensitizes glioblastoma cells to histone deacetylase inhibitors. Neuro Oncol, 2011, 13: 894–903.
136.Chiou HY, Lai WK, Huang LC, *et al*. Valproic acid promotes radiosensitization in meningioma stem-like cells. Oncotarget, 2015, 6: 9959–9969.
137.Dai C, Zhang B, Liu X, *et al*. Pyrimethamine sensitizes pituitary adenomas cells to temozolomide through cathepsin B-dependent and caspase-dependent apoptotic pathways. Int J Cancer, 2013, 133: 1982–1993.
138.Chetty C, Dontula R, Gujrati M, *et al*. Blockade of SOX4 mediated DNA repair by SPARC enhances radioresponse in medulloblastoma. Cancer Lett, 2012, 323:188–198.
139.Xu J, Sampath D, Lang FF, *et al*. Vorinostat modulates cell cycle regulatory proteins in glioma cells and human glioma slice cultures. J Neurooncol, 2011, 105: 241–251.
140.Mottet D, Pirotte S, Lamour V, *et al*. HDAC4 represses p21(WAF1/Cip1) expression in human cancer cells through a Sp1-dependent, p53-independent mechanism. Oncogene, 2009, 28: 243–256.
141.Francescone RA, Scully S, Faibish M, *et al*. Role of YKL-40 in the angiogenesis, radioresistance, and progression of glioblastoma. J Biol. Chem, 2011, 286: 15332–15343.
142.Bhat KP, Pelloski CE, Zhang Y, *et al*. Selective repression of YKL-40 by NF-kappaB in glioma cell lines involves recruitment of histone deacetylase-1 and -2. FEBS Lett, 2008, 582: 3193–3200.
143.Elam C, Hesson L, Vos MD, *et al.* RRP22 is a farnesylated, nucleolar, Ras-related protein with tumor suppressor potential. Cancer Res, 2005, 65: 3117–3125.
144.Chen R, Yang L, Fang J, *et al*. RRP22: a novel neural tumor suppressor for astrocytoma. Med Oncol, 2012, 29: 332–339.
145.Schmidt N, Windmann S, Reifenberger G, *et al*. DNA hypermethylation and histone modifications downregulate the candidate tumor suppressor gene RRP22 on 22q12 in human gliomas. Brain Pathol, 2012, 22: 17–25.
146.Kumar KS, Sonnemann J, Beck JF. Histone deacetylase inhibitors induce cell death in supratentorial primitive neuroectodermal tumor cells. Oncol Rep, 2006, 16: 1047–1052.
147.Furchert SE, Lanvers-Kaminsky C, Juurgens H, *et al*. Inhibitors of histone deacetylases as potential therapeutic tools for high-risk embryonal tumors of the nervous system of childhood. Int J Cancer, 2007, 120: 1787–1794.
148.Aguilera DG, Das CM, Sinnappah-Kang ND, *et al*. Reactivation of death receptor 4 (DR4) expression sensitizes medulloblastoma cell lines to TRAIL. J Neurooncol, 2009, 93: 303–318.
149.Teider N, Scott DK, Neiss A, *et al.* Neuralized1 causes apoptosis and downregulates Notch target genes in medulloblastoma. Neuro Oncol, 2010, 12: 1244–1256.
150.Schreck KC, Taylor P, Marchionni L, *et al*. The Notch target Hes1 directly modulates Gli1 expression and Hedgehog signaling: a potential mechanism of therapeutic resistance. Clin Cancer Res, 2010, 16: 6060–6070.
151.Spyropoulou A, Piperi C, Adamopoulos C, *et al.* Deregulated chromatin remodeling in the pathobiology of brain tumors. Neuromolecular Med, 2013, 15: 1–24.
152.Biggar KK, Li SS. Non-histone protein methylation as a regulator of cellular signalling and function. Nat Rev Mol Cell Biol, 2015, 16: 5–17.

DOI 10.1007/s10330-016-0165-5
Cite this article as: Xi GF, Barbara Mania-Farnell, Lei T, *et al*. Histone modification as a mechanism drives drug resistance driver in brain tumors. Oncol Transl Med, 2016, 2: 216–226.

Oncology and Translational Medicine
DOI 10.1007/s10330-016-0153-9

October 2016, Vol. 2, No. 5, P227–P233

ORIGINAL ARTICLE

Analysis of long-term outcomes and application of the tumor regression grading system in the therapeutic assessment of resectable limited-disease small cell lung cancer

Shuonan Xu[1, 2, 3*], Jianfei Zhu[1, 3*], Yawei Dou[1, 3*], Wei Tian[1, 3], Yun Dai[1, 3], Xianghui Luo[1, 3], Hongtao Wang[1, 3] (✉)

[1] Department of Thoracic Surgery, Shaanxi Provincial People's Hospital, Xi'an 710000, China
[2] Medical College of Yan'an University, Yan'an 716000, China
[3] The Third Affiliated Hospital of the School of Medicine Xi'an JiaoTong University, Xi'an 710000, China

Abstract

Objective The present study attempted to evaluate the value of neoadjuvant chemotherapy in limited-disease small cell lung cancer (LD-SCLC), and to identify the predictive value of the tumor regression grading (TRG) system in LD-SCLC treatment-response and prognosis.

Methods The records of patients with LD-SCLC (p-Stage I–IIIa) who underwent definitive radical resection at Shaanxi Provincial People's Hospital between March 1, 2000 and March 31, 2014 were retrospectively analyzed. We compared the disease-free survival (DFS) and overall survival (OS) rates between Group A patients (patients who underwent surgery combined with pre- and post-operative chemotherapy) and Group B patients (patients who underwent surgery combined with adjuvant chemotherapy only) using the Kaplan-Meier method and the Mantel-Cox test. The specimens of patients who received neoadjuvant chemotherapy were reassessed according to the TRG system.

Results The median DFS for 27 patients was 16.267 months and the median OS was 81.167 months (1-year OS, 74.07%; 3-year OS, 22.22%; 5-year OS, 14.81%). Thirteen patients received neoadjuvant chemotherapy, and their specimens were reassessed by TRG (pathological complete remission, 3/13, 23.08%). Patients in group A had a longer OS than those in group B (mean, 93.782 months versus 42.322 months, $P = 0.025$), although there was no significant difference in DFS between the two groups (median 20.100 months versus 14.667 months, $P = 0.551$). Statistical analysis revealed that TRG Grade (G) 0 (mean, 61.222 months) was associated with better OS than G1-2 (mean, 31.213 months) ($P = 0.311$).

Conclusion Our study indicated that neoadjuvant chemotherapy combined with surgical resection may represent a feasible treatment method for patients with LD-SCLC. The TRG system may be a valuable prediction tool to assess neoadjuvant chemotherapeutic efficacy, especially in patients with G0 disease as determined by TRG; these patients may attain an improved survival benefit with neoadjuvant chemotherapy.

Key words: small cell lung cancer; tumor regression grading; neoadjuvant chemotherapy

Received: 24 March 2016
Revised: 24 April 2016
Accepted: 25 May 2016

Radical surgical resection is the recommended treatment for patients with early-stage (limited-stage, lymphadenopathy-negative) small cell lung cancer (SCLC), according to the latest National Comprehensive Cancer Network (NCCN) guidelines [1]. SCLC is characterized by a number of malignant biological features, such as rapid proliferation, early metastases, and frequent relapse; as a result, the majority of SCLC patients have dismal long-term survival outcomes [2]. Patients suitable for resection represent < 5% of all SCLC patients [3]. It has been determined that multimodality treatment methods, combining surgery with chemoradiotherapy, provide patients with

✉ Correspondence to: Hongtao Wang. Email: whtsyy139@qq.com
* These authors contibuted equally to this work.
© 2016 Huazhong University of Science and Technology

more survival benefits. In a study of 41 patients with limited-disease (LD)-SCLC, Chen *et al* [4] reported that for patients with p-Stage IIIa (N2-positive), the 5-year overall survival (OS) rate in patients who underwent both pre- and post-operative chemotherapy was significantly better than that in patients who received only postoperative chemotherapy (34% versus 12%, $P = 0.020$). A multicenter clinical trial (JCOG9101) [5] showed that 61 patients with stage I–IIIa SCLC who received adjuvant chemotherapy, consisting of four cycles of cisplatin and etoposide, followed by surgical resection yielded a 3-year OS rate of 61%. However, an essential role for preoperative adjuvant chemotherapy in LD-SCLC treatment has not yet been established.

The Response Evaluation Criteria In Solid Tumor (RECIST) guidelines are routinely used to evaluate the efficacy of chemotherapy in lung cancer [6–7]. Given that surgical resection is infrequently performed in patients with LD-SCLC, there is a strong demand for tools that will inform the choice of therapy. The tumor regression grading (TRG) system has been used to evaluate the efficacy of treatment in digestive tract tumors [8–10], but to our knowledge, it has been rarely used to assess response to neoadjuvant chemotherapy in patients with SCLC. In this study, we analyzed the clinical outcomes of patients with SCLC and evaluated the prognostic ability of the TRG system in these patients. Furthermore, we evaluated the association between response to preoperative chemotherapy and postoperative survival.

Patients and methods

Criteria

We retrospectively evaluated the cases of 37 patients with SCLC who underwent radical surgical resections in Shaanxi Provincial People's Hospital between March 1, 2000 and March 31, 2014. The selection criteria were as follows:

(1) Patients were diagnosed with LD-SCLC on routine workup. Tumor location was limited to one hemithorax; local involvement of the supraclavicular, hilar, or mediastinal lymph nodes was acceptable (ipsilateral and/or contralateral). Diagnosis and location was confirmed through evaluation of bronchoscopic biopsies and surgical specimens; clinical stage did not progress beyond IIIa.

(2) Complete preoperative evaluations were performed; this included brain magnetic resonance imaging (MRI)/computed tomography (CT), chest CT, upper abdominal ultrasonography/CT, bronchoscopy, and whole-body bone scintigraphy. These evaluations confirmed that there was no distant metastasis. Of note, one male patient did not undergo the above-mentioned workup. However, he underwent positron emission tomography, and was therefore included.

(3) All patients received adjuvant therapy.

(4) All surgical resections were R0 resections.

(5) Patients were not diagnosed with second primary tumors or serious cardiac or pulmonary disease.

(6) Patients did not die during the perioperative period (survived for > 3 months).

Pathological diagnosis, preoperative clinical stage, and postoperative pathological stage were defined based on the WHO classification of tumors and the Tumor, Node, Metastasis (TNM) staging system (7th edition) [11]. Ten patients were excluded because their postoperative follow-up was too short (< 3 weeks after surgery) or their treatment involved resection only. Finally, 27 patients were enrolled in our study group.

Neoadjuvant chemotherapy

In accordance with SCLC management guidelines and the Eastern Cooperative Oncology Group guidelines [12–13], neoadjuvant chemotherapy was administered to patients with a performance status (PS) < 2 (0 or 1), following an accurate pathological diagnosis of SCLC. Neoadjuvant treatment included a platinum-based regimen (100 mg/m^2 cisplatin or 400 mg/m^2 carboplatin on Day 1 for at least two cycles at 3-weeks intervals). After neoadjuvant therapy, resection was performed.

TRG

In accordance with the histological TRG criteria and NCCN guidelines for gastroesophageal carcinoma [8–10], the extent of any residual cancer was evaluated under the microscope. To ensure accuracy, two pathologists were invited to double-check the results. No residual cancer was defined as TRG Grade (G) 0, < 50% residual cancer was defined as G1, and > 50% residual cancer was defined as G2 [9].

Postoperative treatments

During the postoperative period, all patients underwent adjuvant chemotherapy. Neoadjuvant and adjuvant chemotherapy were administered to 13 patients. Adjuvant chemotherapy alone was administered to 14 patients. Prophylactic cranial irradiation (PCI) and irradiation of the region of recurrence was performed in five and eight patients, respectively. Adjuvant platinum-based therapy was continued unless serious hematologic toxicity or death occurred; however, some patients refused to accept further treatment. Similar to the neoadjuvant treatment format, the adjuvant chemotherapy was administered to patients with PS < 2 and consisted of 80 mg/m^2 etoposide on Days 1–3 plus cisplatin/carboplatin, for two to six cycles at 3-week intervals. The radiotherapy dosage was 1.5–2.0 Gy per fraction, to a total dose of 24–40 Gy.

Follow-up

Follow-up information included outpatient clinic visits and phone and mail correspondence. Brain CT/MRI, chest CT, upper abdominal ultrasonography, and whole-body bone scintigraphy were assessed. The tracking intervals were every 6 months for first 2 postoperative years, followed by once a year thereafter. The follow-up end-point was defined as the date of recurrence or death, or the date of last follow-up. All records were updated before May 31, 2014.

Statistical analysis

Pearson's *chi-square* test was used to compare the differences across categorical variables. Kaplan-Meier curves and the Mantel-Cox test were used to calculate and evaluate disease-free survival (DFS) and OS, respectively. Tests were two-sided. A P value < 0.05 was considered statistically significant. All statistical analyses were performed using SPSS version 16.0.

Results

General information

Our study cohort consisted of 22 males (81.48%) and 5 females (18.52%) patients with SCLC who underwent radical surgical resections. The mean patient age was 56.59 years (range, 37.00–77.00 years). Based on the postoperative pathological examinations, solid tumors were confirmed in all 27 cases: 21 cases of single small-cell carcinoma and 3 cases of mixed carcinoma (small-cell carcinoma and squamous carcinoma); in 3 cases, cancer cells were not found in the remainder of the removed lung tissues. The specific characteristics are listed in Table 1. Group A represented patients who received neoadjuvant chemotherapy, and Group B represented patients who did not receive neoadjuvant chemotherapy.

Survival analysis

The median postoperative follow-up time for the 27 patients in our study was 20.50 months. Fig. 1 show that the median DFS was 16.267 months, and the median OS was 81.167 months, with overall 1-, 3- and 5-year survival rates of 74.07%, 22.22%, and 14.81%, respectively. Subgroup evaluation was performed using univariate analysis. Comparing group A with group B, the former had better postoperative survival outcomes: mean DFS, 20.100 months versus 14.667 months, P = 0.551; mean OS, 93.782 months versus 42.322 months, P = 0.025 (Fig. 2–3). Moreover, we confirmed that the pathological lymph node stage influenced DFS in our study. Patients diagnosed with pN0-1 disease attained more survival benefit than those diagnosed with pN2, especially in terms of DFS (P = 0.036) (Table 2).

Table 1 Patient characteristics (n = 27)

Variate	Group A		Group B		P value
	n	%	*n*	%	
Numbers of cases	13		14		
Age (years)	52.7		60.4		0.017
≥ 65	0	0	5	35.7	
< 65	13	100	9	64.3	
Gender					0.557
Male	10	76.9	12	85.7	
Female	3	23.1	2	14.3	
Smoking index					0.085
≥ 400	5	38.5	10	71.4	
< 400	8	61.5	4	28.6	
Histopathology					0.155
Pure SCLC	9	69.2	12	85.7	
Mixed SCLC	1	7.7	2	14.3	
None	3	23.1	0	0	
cT-stage					0.037
T1	0	0	4	28.6	
T2–T4	13	100	10	71.4	
cTNM					0.315
I	1	7.7	3	21.4	
II–IIIa	12	92.3	11	78.6	
pT-stage					0.010
T0	3	23.1	0	0	
T1	7	53.8	3	21.4	
T2–T4	3	23.1	14	78.6	
pN-stage					0.148
N0–1	10	76.9	7	50.0	
N2	3	23.1	7	50.0	
Surgery method					0.557
Segmentectomy	0	0	1	7.1	
Lobectomy	8	61.5	8	57.1	
Bilolobectomy	0	0	1	7.1	
Pneumonectomy	5	38.5	4	28.6	
Radiotherapy				7.1	0.050
Yes	5	38.5	1		
No	8	61.5	13	92.9	
PCI					0.017
Yes	0	0	5	35.7	
No	13	100	9	64.3	

group A: neoadjuvant chemtherapy; group B: adjuvant chemotherapy; SCLC: small lung cell cancer; mixed SCLC: squamous cell carcinoma and small cell carcinoma

Efficacy assessment

In our cohort, 13 patient received neoadjuvant chemotherapy. Pathological evaluation revealed nine cases of single SCLC and one case of mixed SCLC; in three cases, no cancerous cells were found. The pathological complete remission (PCR) rate reached 23.08%. In view of the small-scale nature of our study, TRG was categorized into three grades; three patients were confirmed as having G0 disease. Statistical analysis results showed that the DFS of G0 patients was similar to that of than G1-2 patients (median 16.267 versus 20.100 months, P = 0.956).

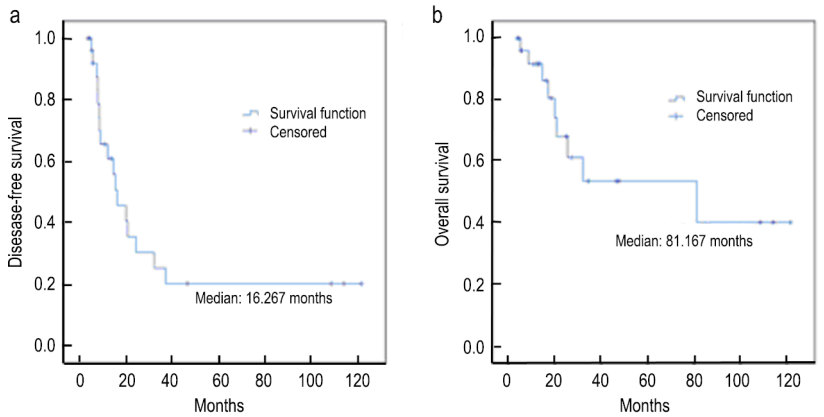

Fig. 1 Kaplan-Meier survival curves for 27 patients with limited-disease small cell lung cancer after surgical resection. (a) Disease-free survival; (b) Overall survival

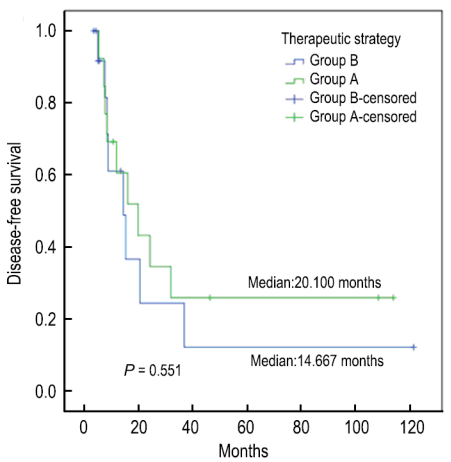

Fig. 2 Comparison of disease-free survival in patients with limited-disease small cell lung cancer between group A and group B

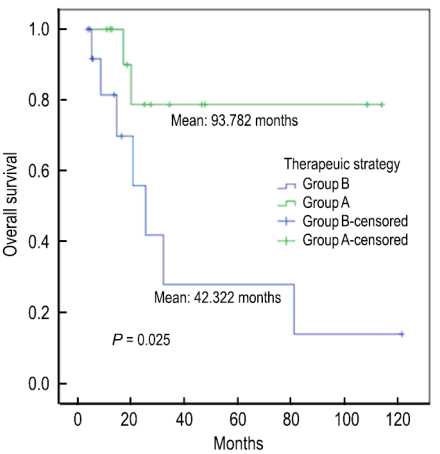

Fig. 3 Comparison of overall survival in patients with limited-disease small cell lung cancer between group A and group B

However, G0 patients were associated with better, albeit not statistically significant, OS than G1-2 patients (mean, 61.222 versus 31.213 months, $P = 0.311$).

Discussion

Although chemotherapy represents the mainstay treatment option for LD-SCLC [14–15], surgical treatment still plays a crucial role. More attention is being paid to multimodal therapies for SCLC, and many studies have shown that resection therapy in the multimodal treatment setting is associated with less local relapse and increased survival benefits [16–18]. A meta-analysis of 13 randomized control trials of non-small cell lung cancer (NSCLC) patients, revealed than neoadjuvant chemotherapy combined with surgery could significantly prove the OS of patients with operable NSCLC [17]. However, surgical resection combined with neoadjuvant therapy is not feasible for all patients with LD-SCLC.

Hara *et al* [19] reported that, in patients with LD-SCLC, preoperative chemotherapy combined with subsequent surgery resulted in a better survival outcome than an initial surgery followed by adjuvant chemotherapy (5-year rate, 42% versus 33%). In addition, surgical resection after neoadjuvant chemotherapy may represent the optimal treatment choice for resectable stage III SCLC (particularly for patients with N2-positive disease). It is encouraging that neoadjuvant treatment extends the life of LD-SCLC patients undergoing surgical resection. Preoperative chemotherapy shrinks solid tumors, reduces the rate of recurrence, and prevents potential metastasis. As a result, the down-staging and subsequent tumor-removal rates are improved. We believe that pre- and post-operative chemotherapy in combination with surgery result in improved outcome due to the effects of the preoperative chemotherapy.

The TRG system is frequently used to evaluate the efficacy of neoadjuvant chemotherapy in esophageal carcinoma and gastroesophageal junction tumors [8–10, 20–21]; it is also a valuable survival prediction tool for patients with rectal cancer [22–23]. There is currently much debate regarding the standards in the TRG system. Some

Table 2 Univariate survival analyses on enrolled 27 patients

Variate	*n*	DFS		OS	
		95% CI (median)	*P* value	95% CI (mean)	*P* value
Age (years)			0.207		0.002
≥ 65	5	8.351–9.782 (9.067)		8.310–25.103 (16.707)	
< 65	22	9.156–23.377 (16.267)		57.301–109.323 (83.312)	
Gender			0.594		0.970
Male	22	8.435–22.631 (15.533)		42.355–96.784 (69.570)	
Female	5	7.631–33.969 (33.964)		20.395–35.191 (27.793)	
Smoking index			0.670		0.676
≥ 400	15	2.912–28.155 (15.533)		32.344–92.434 (62.389)	
< 400	12	8.701–23.833 (16.267)		46.138–111.163 (78.650)	
Histopathology			0.923		0.196
Pure SCLC	21	10.683–29.517 (20.100)		None	
Mixed SCLC	3	7.206–17.128 (12.167)		None	
None	3	0.000–33.124 (16.267)		None	
cT-stage			0.532		0.506
T1	4	None		0.000–111.143 (50.983)	
T2–T4	23	5.931–23.402 (14.667)		47.976–101.240 (74.593)	
cTNM			0.354		0.875
I	4	0.000–84.787 (37.133)		31.795–117.255 (74.525)	
II–IIIa	23	10.091–20.976 (15.533)		42.362–97.711 (70.037)	
pT-stage			0.812		0.288
T0	3	0.000–33.124 (16.267)		None	
T1	10	14.578–27.022 (20.800)		None	
T2–T4	14	7.016–17.317 (12.167)		None	
pN-stage			0.036		0.094
N0–1	17	6.037–42.897 (24.467)		58.011–110.213 (84.112)	
N2	10	1.976–16.155 (9.067)		17.518–30.629 (23.876)	
PCI			0.886		0.189
Yes	5	0.000–27.621 (9.067)		0.000–84.525 (42.196)	
No	22	9.009–23.525 (16.267)		51.140–105.358 (78.249)	
Therapeutic strategy			0.551		0.025
Group A	13	7.254–32.945 (20.100)		68.768–118.797 (93.782)	
Group B	14	6.140–23.193 (14.667)		14.890–69.754 (42.322)	
TRG			0.956		0.311
G0	3	0.000–33.124 (16.267)		No CI (61.222)	
G1–2	10	2.972–37.228 (20.100)		No CI (31.213)	

CI: confidence interval; DFS: disease-free survival; OS: overall survival

experts recommend categorizing TRG into three grades [9], while others recommend four (G0, 0%; G1, 1%–10%; G2, 11%–50%; G3, > 50%) [10], or even five grades [24]. In this study, we prudently took the characteristics of our samples into consideration and chose to use three, rather than four or five, grades. Patients in the G0 group demonstrated a significantly greater survival benefit than patients in the other groups. While our survival evaluation did not show a significant difference in survival between patients in the G0 and G1-2 subgroups, there was a trend towards improved OS in the G0 subgroup. This may be explained by the high PCR rate in the patients who received preoperative chemotherapy. In studies of NSCLC, PCR has been shown to be a powerful prognostic factor for survival; it is also associated with better clinical outcome following neoadjuvant chemotherapy or chemoradiotherapy. Neoadjuvant therapy has been proven to prolong long-term local control rates and reduce progression in patients with locally advanced NSCLC (N2-positive) [25–26]. Considering that SCLC is generally sensitive to chemoradiotherapy, we believe that similar results may be achieved with neoadjuvant treatment of SCLC. Additionally, it has been shown that 60–90% of patients with LD-SCLC and 40-70% of patients with extensive disease respond to first-line chemotherapy [27]. All of the patients who achieved PCR received the etoposide and cisplatin (EP) regimen. Effective preoperative chemotherapy could diminish the pathological stage; an earlier stage is associated with a better prognosis. However, patients who received chemotherapy as a second-line treatment only and patients with mixed tumors did not achieve PCR.

In LD-SCLC, PCI has been proven improve survival

outcomes in patients who achieve complete response [28–29]. However in this study, there was no significant difference in DFS between patients who underwent PCI and those who did not (P = 0.886). On the contrary, patients who did not undergo PCI appeared to have a slightly better OS than patients who underwent PCI (P = 0.189). Some studies [28, 30] have reported that PCI resulted in long-lasting neurotoxicity and potentially deleterious effects that negatively affected survival. Lee *et al* [30] showed that in cases of severe neurotoxicity, no PCI was superior to PCI. In addition, in a recent meta-analysis, PCI had a detrimental effect on the OS of patients with extensive-disease SCLC [30], including NSCLC [31]. Therefore, PCI should be used with caution.

Our study has some clear limitations. The retrospective nature and the small cohort size reduced the statistical power, and may have introduced confounding factors and biases. In spite of these limitations, our evaluation is authentic. In an upcoming prospective controlled study, we will focus on more factors, including PCI and adjuvant thoracic radiation therapy.

Conclusion

Neoadjuvant chemotherapy combined with surgical resection results in a significant survival benefit (OS) and is a feasible treatment for patients with LD-SCLC. Our results, based on the TRG system, indicate that patients who receive neoadjuvant chemotherapy and who have no residual cancer after surgery will attain the best survival outcome.

Conflicts of interest

The authors indicated no potential conflicts of interest.

References

1. Kalemkerian GP. Running in Place: The 20th Anniversary of the NCCN Small Cell Lung Cancer Guidelines Panel. J Natl Compr Canc Netw, 2015, 13: 704–706.
2. Amini A, Byers LA, Welsh JW, *et al.* Progress in the management of limited-stage small cell lung cancer. Cancer, 2014, 120: 790–708.
3. Veronesi G, Bottoni E, Finocchiaro G, *et al*. When is surgery indicated for small-cell lung cancer? Lung Cancer, 2015, 90: 582–589.
4. Xu YJ, Zheng H, Gao W, *et al*. Is neoadjuvant chemotherapy mandatory for limited-disease small-cell lung cancer? Interact Cardiovasc Thorac Surg, 2014, 19: 887–893.
5. Tsuchiya R, Suzuki K, Ichinose Y, *et al.* Phase II trial of postoperative adjuvant cisplatin and etoposide in patients with completely resected stage I-IIIa small cell lung cancer: the Japan Clinical Oncology Lung Cancer Study Group Trial (JCOG9101). J Thorac Cardiovasc Surg, 2005, 129: 977–983.
6. Therasse P, Arbuck SG, Eisenhauer EA, *et al*. New guidelines to evaluate the response to treatment in solid tumors. European Organization for Research and Treatment of Cancer, National Cancer Institute of the United States, National Cancer Institute of Canada. J Natl Cancer Inst, 2000, 92: 205–216.
7. Eisenhauer EA, Therasse P, Bogaerts J, *et al*. New response evaluation criteria in solid tumours: revised RECIST guideline (version 1.1). Eur J Cancer, 2009, 45: 228–247.
8. Ajani JA, Barthel JS, Bentrem DJ, *et al*. Esophageal and esophagogastric junction cancers. J Natl Compr Canc Netw, 2011, 9: 830–887.
9. Wu TT, Chirieac LR, Abraham SC, *et al*. Excellent interobserver agreement on grading the extent of residual carcinoma after preoperative chemoradiation in esophageal and esophagogastric junction carcinoma: a reliable predictor for patient outcome. Am J Surg Pathol, 2007, 31: 58–64.
10. Chirieac LR, Swisher SG, Ajani JA, *et al.* Posttherapy pathologic stage predicts survival in patients with esophageal carcinoma receiving preoperative chemoradiation. Cancer, 2005, 103: 1347–1355.
11. van Meerbeeck JP, Janssens A. The seventh tumour-node-metastasis staging system for lung cancer: Sequel or prequel? EJC Suppl, 2013,11: 150–158.
12. Sandler A, Gray R, Perry MC, *et al*. Paclitaxel-carboplatin alone or with bevacizumab for non-small-cell lung cancer. N Engl J Med, 2006, 355: 2542–2550.
13. Schiller JH, Harrington D, Belani CP, *et al*. Comparison of four chemotherapy regimens for advanced non-small-cell lung cancer. N Engl J Med, 2002, 346: 92–98.
14. Lim E, Belcher E, Yap YK, *et al*. The role of surgery in the treatment of limited disease small cell lung cancer: time to reevaluate. J Thorac Oncol, 2008, 3: 1267–1271.
15. Liu JJ, Zhang S, Ma LX, *et al*. Efficacy analysis and multi-factor retrospective study of third-line chemotherapy in 82 Chinese patients with small cell lung cancer. Oncol Transl Med, 2015, 1: 26–31.
16. Song WA, Zhou NK, Wang W, *et al*. Survival benefit of neoadjuvant chemotherapy in non-small cell lung cancer: an updated meta-analysis of 13 randomized control trials. J Thorac Oncol, 2010, 5: 510–516.
17. Elliott JA, Osterlind K, Hirsch FR, *et al.* Metastatic patterns in small-cell lung cancer: correlation of autopsy findings with clinical parameters in 537 patients. J Clin Oncol, 1987, 5: 246–254.
18. Shepherd FA, Ginsberg RJ, Evans WK, *et al*. Reduction in local recurrence and improved survival in surgically treated patients with small cell lung cancer. J Thorac Cardiovasc Surg, 1983, 86: 498–506.
19. Hara N, Ohta M, Ichinose Y, *et al.* Influence of surgical resection before and after chemotherapy on survival in small cell lung cancer. J Surg Oncol, 1991, 47: 53–61.
20. Chao YK, Chang CB, Chuang WY, *et al*. Correlation between tumor regression grade and clinicopathological parameters in patients with squamous cell carcinoma of the esophagus who received neoadjuvant chemoradiotherapy. Medicine (Baltimore), 2015, 94: e1407.
21. Guo K, Cai L, Zhang Y, *et al.* The predictive value of histological tumor regression grading (TRG) for therapeutic evaluation in locally advanced esophageal carcinoma treated with neoadjuvant chemotherapy. Chin J Cancer, 2012, 31: 399–408.
22. Li J, Liu H, Hu J, *et al*. New tumor regression grade for rectal cancer after neoadjuvant therapy and radical surgery. Oncotarget, 2015, 6: 42222–42231.
23. Kim SH, Chang HJ, Kim DY, *et al*. What is the ideal tumor regression grading system in rectal cancer patients after preoperative chemoradiotherapy? Cancer Res Treat, 2016, 48: 998–1009.
24. Mandard AM, Dalibard F, Mandard JC, *et al*. Pathologic assessment of tumor regression after preoperative chemoradiotherapy of esophageal carcinoma. Clinicopathologic correlations. Cancer, 1994, 73: 2680–2686.

25. Lococo F, Cesario A, Margaritora S, *et al*. Long-term results in patients with pathological complete response after induction radiochemotherapy followed by surgery for locally advanced non-small-cell lung cancer. Eur J Cardiothorac Surg, 2013, 43: e71–81.
26. Pottgen C, Stuschke M, Graupner B, *et al*. Prognostic model for long-term survival of locally advanced non-small-cell lung cancer patients after neoadjuvant radiochemotherapy and resection integrating clinical and histopathologic factors. BMC Cancer, 2015,15: 363.
27. Hagmann R, Hess V, Zippelius A, *et al*. Second-line therapy of small-cell lung cancer: topotecan compared to a combination treatment with Adriamycin, Cyclophosphamide and Vincristine (ACO) - a single center experience. J Cancer, 2015, 6: 1148–1154.
28. Kong FM, Lally BE, Chang JY, *et al*. ACR Appropriateness Criteria(R) radiation therapy for small-cell lung cancer. Am J Clin Oncol, 2013, 36: 206–213.
29. Auperin A, Arriagada R, Pignon JP, *et al*. Prophylactic cranial irradiation for patients with small-cell lung cancer in complete remission. Prophylactic Cranial Irradiation Overview Collaborative Group. N Engl J Med, 1999, 341: 476–484.
30. Lee JJ, Bekele BN, Zhou X, *et al*. Decision analysis for prophylactic cranial irradiation for patients with small-cell lung cancer. J Clin Oncol, 2006, 24: 3597–3603.
31. Xie SS, Li M, Zhou CC, *et al*. Prophylactic cranial irradiation may impose a detrimental effect on overall survival of patients with nonsmall cell lung cancer: a systematic review and meta-analysis. PLoS One, 2014, 9: e103431.

DOI 10.1007/s10330-016-0153-9
Cite this article as: Xu SN, Zhu JF, Dou YW, *et al*. Analysis of long-term outcomes and application of the tumor regression grading system in the therapeutic assessment of resectable limited-disease small cell lung cancer. Oncol Transl Med, 2016, 2: 227–233.

Oncology and Translational Medicine
DOI 10.1007/s10330-016-0139-7

October 2016, Vol. 2, No. 5, P234–P238

ORIGINAL ARTICLE

Evaluation of photon beam dose calculation accuracy of treatment planning systems using in vivo dosimetry

Mohamed Ibrahim[1], Wahib M. Attia[2], Khaled M. Elshahat[1] (✉)

[1] Radiation Oncology Department, El Hussein Hospital, Al Azahr University
[2] Physics Department, Faculty of Sciences, Suez Canal University

Abstract

Objective The treatment planning system currently represents one of the basics of radiation therapy, because it is the only method to estimate patient dose delivery fast forward and accurately represent estimated tumor location of the tumor with the possibility of estimating densities in the tissue surrounding the tumor to overcome dose calculation defects but radial estimated the patient. Despite the flaws associated with the systems and calculates the dose of your programs in all programs currently existing in the world. Than necessary, to the existence of a review of the accuracy of accounts and how to confirm the radiation dose to the patient programs.

Methods A total of 35 cancer patients were considered for this study, with 245 field measurements made with low- and high-energy diode detectors for brain and prostate cases. The treatments for all patients were planned using Eclipse Treatment Planning System version 13.6.

Results Of the 105 field measurements made for the prostate cancer patients, 16 included discrepancies outside the ±5% action level. Of the 145 measurements taken of the brain cases, there were four outside the ±5% action level. The results indicated a higher degree of accuracy. The study revealed that, for the prostate measurements, the higher discrepancy in the doses for the particular fields (exceeding the action level) may have been due to the isocenter being very close to the jaws and multi-leaf collimator of the linear accelerator machine. As a result, scatter from the jaws and the multi-leaf collimator could have contributed to the high dose delivered to the diode; hence, a probable higher discrepancy of the dose in more brain cases due highest quality of VMAT technique and fixation system.

Conclusion A greater percentage of the observed discrepancies were well within the set tolerance level. However, it is recommended that the positioning of the diode on the patient's skin and the angular sensitivity of the diodes be reconsidered. It is also recommended that a more accurate calculation of expected diode values be performed, especially for fields that pass through the table. These efforts would achieve action levels of ±5%.

Received: 29 January 2016
Revised: 8 April 2016
Accepted: 25 September 2016

Key words: diodes; *in vivo* dosimetry; radiotherapy; dose verification

The treatment planning system (TPS) currently represents one of the basics of radiation therapy because it is the only method that estimates patient dose delivery fast forward and accurately estimates tumor location with the possibility of determining estimate densities teams in the tissue surrounding the tumor to overcome dose calculation defects, but radial estimated the patient. Although the errors associated with the systems and calculates the dose of all programs currently existing in the world. For that necessary, to the existence of a review of the accuracy of accounts and how to confirm the radiation dose to the patient programs.

The rapid development of advanced treatment techniques and planning has placed higher demands on the verification of the dose delivered to the patient. *In vivo* dosimetry is an essential element in the quality assurance program used in today's radiotherapy departments. Furthermore, *in vivo* dosimetry is used to control the total

✉ Correspondence to: Khaled M. Elshahat. Email: khelshahat@yahoo.com
© 2016 Huazhong University of Science and Technology

accumulated dose in cases in which the TPS is less accurate, such as in total body irradiation (TBI), the build-up region, and at-risk organs in the head and neck region [1–2].

There is a simultaneous need to safely implement new treatment techniques in a radiotherapy department, which increases the workload and creates the potential for serious errors in radiotherapy planning and delivery. Therefore, an effective net of quality assurance procedures is highly recommended. *In vivo* dosimetry, recommended by various national and international organizations including the IAEA publication in 2013, can be performed at several levels. Two different goals can be identified: measuring doses to at-risk organs that are difficult to calculate (such as the eyes and gonads) and verifying the delivered dose to improve treatment accuracy and minimize the risk of dose misadministration. These measurements are compared to the planned doses specified by the oncologist and calculated by the TPS for the target and critical organs.

In this way, set-up calculations, motions, or transcription errors that may have gone unnoticed during pretreatment checks can be recovered prior to dose delivery. In the absence of errors, routine *in vivo* dose measurements indicate that the treatment was delivered correctly. The diodes are basically small detectors attached to a long wire that are used to measure the dose being received in real time while a patient is undergoing radiotherapy treatment. They are normally attached to the patient's body with adhesive tape at specific points where the treatment beam enters the body. Many professionals acknowledge their importance because they have the potential to detect any errors that may have slipped through the quality safety net [3]. While errors in the delivery of radiation therapy are rare and usually result in little or no patient injury, the real danger is an administration error going undetected. This may result in healthy tissues being exposed to unnecessary radiation levels or the tumor site not receiving the full therapeutic effect. According to previous studies, a severe misadministration may result in radiation necrosis to vital organs or structures and can be fatal. In recent publications, several radiotherapy reports have described erroneous patient exposure to radiation [4].

The errors in predicting the dose rate resulted in its underestimation by 10%–45%, which translates to the patients receiving corresponding overdoses of 10%–55%. It was eventually revealed that 426 patients received significant overdoses as a result. The IAEA also reported on an erroneous use of a TPS. In that report, the distance correction factor was erroneously applied twice for all patients treated isocentrically or at non-standard SSD. This error caused patients to receive doses lower than those prescribed [5–6]. This deficiency was 5%–35%, and in the end, it was revealed that, of 1045 patients whose calculations were affected by the incorrect procedures, 492 developed local recurrences that could be attributed to the error. The International Commission on Radiation Units and Measurements has recommended that radiation be delivered to within 5% of the prescribed dose [7–8].

Moreover, in a recent publication by the IAEA (2013), an appropriate goal is to be able to use a tolerance level of 5% for simple treatments, with a level of 7% for situations such as breast treatments and other treatments where measurement complications exist. However, it is recommended that, although in the initial stages of the introduction of in vivo dosimetry the tolerance levels may need to be higher, every effort should be made to achieve tolerance levels of about 5% by a process of progressive elimination of identified causes of dose differences [5]. This paper seeks to compare the entrance doses derived from the signal of the diode detectors placed on the skin with the theoretical values as calculated by the TPS under set tolerance values [9–11].

Materials and methods

The OmniPro-InViDos is a dosimetry management system that handles all tasks related to in vivo dosimetry. It simplifies the use of *in vivo* dosimetry by giving the user an overview of the calibration as well as the tools needed to perform the calibration efficiently by automatically selecting correction factors for each field. The OmniPro-InViDos provides instruments that improve treatment accuracy while reducing the time requirement. It may be linked to the verification and therapy system either locally on the same PC as the verification system or via the internal network. It is well known that some characteristic can be affected when the detector is exposed to high-energy radiation.

(1) The sensitivity will decrease over time; (2) For some detector types, the signal will not be proportional to the dose rate. In some cases, this non-linearity will change the cumulative dose, leading to an incorrect reading if the dose rate in the measuring position will differ from the calibration situation; (3) Sensitivity will vary with temperature; (4) Detector leakage current, which is correlated to the detector impedance. This parameter can be important if the measured dose rate is very low, and an effect voltage of the input amplifier will increase; (5) Directional and field size dependencies exist; (6) Increasing the number of parameters to handle will increase the workload for the physicist ensuring quality control of the vivo system.

When the test for several characteristics for diodes has been used in high-energy (15 MV) and low-energy (6 MV) situations for linear accelerator Varian model DMX:

(1) Diode sensitivity is one parameter that will be af-

fected (sometimes after a certain amount of use); (2) Dose linearity; (3)Dose rate linearity; (4) Temperature affects the signal per unit dose from the detector; (5) Directional and field size dependencies exist.

Dosimetry, mechanical, and safety checks are performed. These measurements ensure that the system is working as intended. The entrance dose D is defined as the maximum dose (Dmax) for the corresponding energy. The diode reading that is expected for each treatment field is given by the TPS at Dmax. The TPS uses the PBC and AAA algorithms to calculate doses and equivalent path length for homogeneity corrections. The Dmax for a 6-MV photon is 1.5 cm, while that for a 15-MV photon is 3 cm. The diodes were placed in the field based on the radiation type as well as its energy (low or high) being used to treat the patient at the time. For 6-MV photon energy, the P10 diode was used. For 15-MV photon energy, the P20 diode was used.

All measurements were performed in photon radiation beams generated by an accelerator. The *in vivo* dose measurements were taken immediately after patient set-up and before treatment was started for all radiation treatment fields. The diode should be stacked over the patient's skin for prostate tumors and over a mask for brain tumors (mask should be very stick on same patient should be measure) at the treatment site symmetrically or asymmetrically. For symmetrical fields, after set-up, the diodes were placed on the crosswire at the central beam and secured with adhesive tape. For asymmetrical fields, after set-up, the diodes were placed 2 cm from the field edge along one of the cross wires. If these were closer to the edge than 2 cm, the diodes were placed centrally into the field. However, care was taken to calculate the dose for the correct position by consideration of the inverse square correction factor when the field goes through the couch, and the diode was placed on the surface of the couch. For prostate cases, the uncertainties resulting from the angular dependence of the beam were analyzed. In these cases, a measurement point was found that could be uniquely defined and at which the expected dose could be calculated. If for some reason the diode could not be placed on the beam axis and a wedge was used, the diode was moved away from the beam axis.

Results

The external beam irradiation technique intensity-modulated radiation technique (IMRT) for tumor regions like the prostate and brain had a number of treatment fields (Fig. 1). The AAA algorithm was used to calculate dosage, with a dose grid size spacing of 0.5 × 0.5 mm. All of the patients included in this study were treated in a supine position. Computed tomography scans were acquired using a Siemens Emotion CT scanner.

Table 1 Ten IMRT brain patients for dose as total for all fields measured and calculated

Patient	Calculated dose cGY TPS	Measured dose cGY Diode	Variation %
1	212	210.5	0.75
2	214	211.0	1.5
3	203	201.0	1.0
4	200	198.2	0.9
5	211	210.1	0.45
6	200	197.5	1.25
7	215	214	0.5
8	207	201.0	3.3
9	219	216.6	1.5
10	214	209.5	2.25

Patient treatment was delivered using the linear accelerator equipped with a multi-leaf collimator (MLC) to execute the IMRT. Fig. 2 shows the data for 15 patients with prostate cancer. The standard deviation for each patient for prostate cancer by the Eclipse planning was approximately 3.5% between the calculated and measured values. In Fig. 3, data of 20 patients with brain cancer are shown. The standard deviation between the measurements and calculated values by Eclipse planning was approximately 1.2%.

As shown in Table 1, the variation between patients calculated used eclipse treatment planning and data measurement as QA for IMRT patient with max value in patient selected in this study was approximately 3.3%. (In some cases, the variation will increase due to diode displacement and not stick well in a good measurement position) (Fig. 4 and table 2).

Discussion

The *in vivo* dosimetry results for patients with brain cancer were better than those for patients with prostate cancer. Of the 105 field measurements made for the patients with prostate cancer, 16 fields had discrepancies outside the ±5% action level. Of the 145 field measurements made for the patients with brain cancer, only four field discrepancies outside the ±5% action level were recorded for each case. The results indicated a higher degree of accuracy for the brain cancer cases. In the case of the prostate measurements, the higher discrepancy in the doses for the particular fields (exceeding the action level) may have been due to the isocenter being very close to the jaws and the MLC of the linear accelerator machine and fixation system for prostate cancer and in some like example large patient dimensions. As a result, scatter from the jaws and the MLC may have contributed to the high dose delivered to the diode, hence a probable good result of the brain case due highest quality of IMRT technique and fixation system and separation of brain in comparison

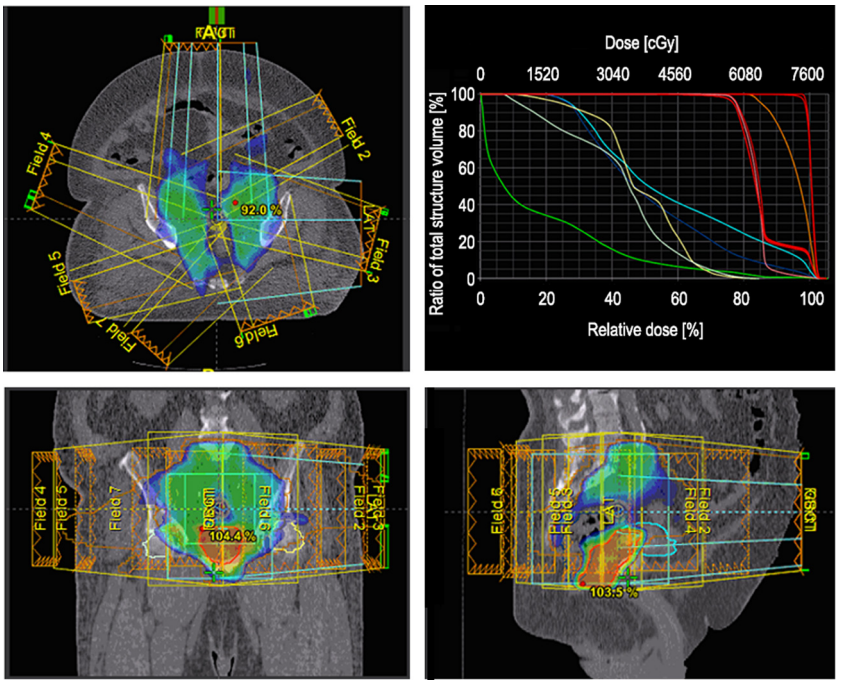

Fig. 1 Screen shot of the IMRT plan for a patient with prostate cancer difficultly plan for prostate IMRT for very large patient separation and check for dose plan. IMRT, intensity-modulated radiation technique

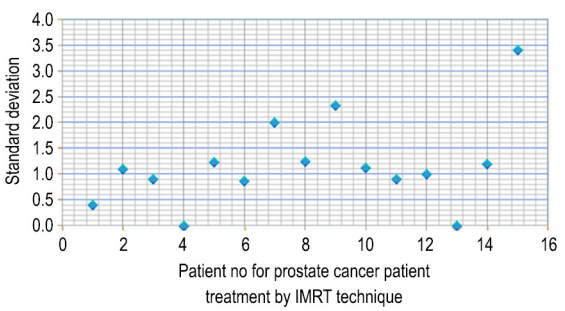

Fig. 2 Discrepancy for ten patients with prostate cancer

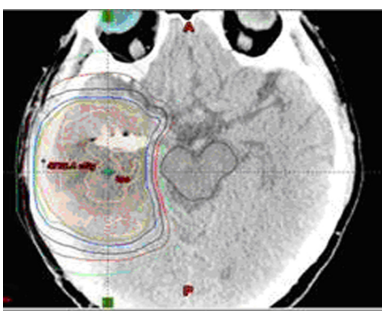

Fig. 3 Example for axilla view for IMRT for brain tumor patient

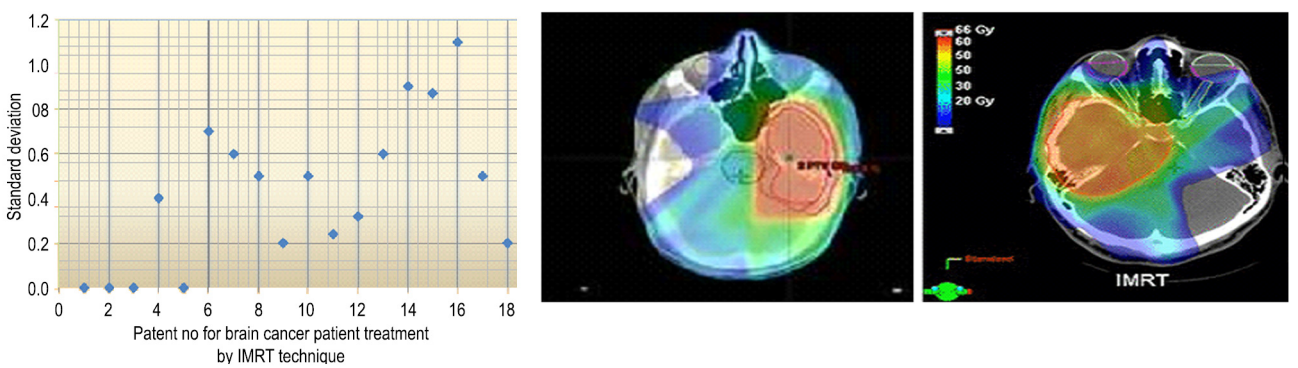

Fig. 4 Axial dose wash for intensity-modulated radiation technique for two brain cancer patients and variation between dose measured and calculated

with prostate patients.

During some of the treatment sessions, the diodes were slightly displaced as a result of adhesive tape loosening. Therefore, these diodes had recorded doses outside the isocenter, leading to some of the observed discrepancies.

Table 2 Ten IMRT prostate patients for dose as total for all fields measured and calculated

Patient	Calculated dose cGY TPS	Measured dose cGY Diode	Variation %
1	223	220.6	1.1
2	205	203.2	0.9
3	220	217.6	1.1
4	203	198.3	2.35
5	205	204.9	0.5
6	224	218	3.0
7	215	211	2
8	203	202	0.5
9	208	205.2	1.4
10	206	205.3	0.4

Illustrates the very small variation between data measurement and calculations for patients with brain cancer due to the good fixation system and lack of diode position displacement

Conclusion

In summary, *in vivo* dosimetry is an effective method for detecting radiotherapy errors, assessing clinically relevant differences between the prescribed and delivered doses, reducing potential patient harm, and fulfilling requirements set forth by national and international regulations. In this study, a much greater percentage of the observed discrepancies was well within the set tolerance level, while a greater percentage of the observed discrepancies were well within the set tolerance level. However, we recommend that the diode positioning on a patient's skin, and the angular diode sensitivity be reconsidered. We also recommended that a more accurate calculation of expected diode values be performed, especially for fields that pass through the table. These efforts would enable the achievement of action levels of ±5%.

Conflicts of interest

The authors indicated no potential conflicts of interest.

References

1. American Association of Physicists in Medicine Report No. 87, Diode *in vivo* dosimetry for patients receiving external beam radiation therapy. Madison: Medical Physics Publishing, 2005, 76.
2. Beauvais H, Goubard O. Guide of daily practice of *in vivo* dosimetry in external radiotherapy. Paris: French Medical Physics Society, 2008, 43.
3. National Commission for Nuclear Activity Control, Norms of radiological security in Radiotherapy Practice-NRS-12. Bucharest: Romanian Official Publishing, 2004, 61.
4. Huyskens DP, Bogaerts R, Verstraete J, *et al*. Thwaites, Practical guidelines for the implementation of *in vivo* dosimetry with diodes in external radiotherapy with photon beams (entrance dose). Brussels: ESTRO Publishing, 2001, 180
5. Georg D, De Ost B, Hoornaert MT, *et al*. Build-up modification of commercial diodes for entrance dose measurements in 'higher energy' photon beams. Radiother Oncol, 1999, 51: 249–256.
6. Jomet N, Ribas M, Eudaldo T. Calibration of semiconductor detectors for dose assessment in total body irradiation. Radiother Oncol, 1996, 38: 247–251.
7. Lanson JH, Essers M, Meijer GJ, *et al*. *In vivo* dosimetry during conformal radiotherapy: requirements for and findings of a routine procedure. Radiother Oncol, 1999, 52: 51–59.
8. Fiorino C, Corletto D, Mangili P, *et al*. Quality assurance by systematic *in vivo* dosimetry: results on a large cohort of patients. Radiother Oncol, 2000, 56: 85–95.
9. Cozzi L, Fogliata-Cozzi A. Quality assurance in radiation oncology. A study of feasibility and impact on action levels of an *in vivo* dosimetry program during breast cancer irradiation. Radiother Oncol, 1998, 47: 29–36.
10. Broggi S, Fiorino C, Calandrino R. A simple and robust method for *in vivo* midline dose map estimations using diodes and portal detectors. Radiother Oncol, 2001, 58: 169–178.
11. Development of procedures for *in vivo* dosimetry in radiotherapy, IAEA, 20131.

DOI 10.1007/s10330-016-0139-7
Cite this article as: Ibrahim M, Attia WM, Elshahat KM. Evaluation of photon beam dose calculation accuracy of treatment planning systems using *in vivo* dosimetry. Oncol Transl Med, 2016, 2: 234–238.

Oncology and Translational Medicine
DOI 10.1007/s10330-016-0159-3

October 2016, Vol. 2, No. 5, P239–P241

CASE REPORT

Epinephrine use during chemotherapy to treat severe tracheal stenosis secondary to advanced esophageal cancer: A case report and review of the literature

Qiang Yao, Yan Zhou, Chunni Xu, Ke Min (✉), Jun Jin

Department of Oncology, The Affiliated Hospital of Jiangsu University, Yixing People's Hospital, Wuxi 214200, China

Abstract

Dyspnea from tracheal stenosis due to compression by a tumor is an emergency that complicates therapy in oncology. We report a case of advanced esophageal cancer in a 56-year-old male who developed severe dyspnea due to airway compression by mediastinal lymph node enlargement. We used epinephrine by subcutaneous injection and aerosol inhalation to temporarily relieve dyspnea while the patient received bevacizumab and chemotherapy. The dyspnea had subsided considerably after 5 days, and the mediastinal lymph nodes were significantly reduced after 2 cycles of chemotherapy. However, the patient died of massive tracheal hemorrhage 2 months later.

Received: 18 May 2016
Revised: 15 August 2016
Accepted: 25 August 2016

Key words: tracheal stenosis; dyspnea; esophageal cancer; epinephrine

Dyspnea occurs mainly in patients with tracheal obstruction or external compression by either a foreign object or neoplasm, and can be difficult to treat. Stenting is widely used for palliation of airway stenosis in patients with metastatic disease [1–5]. However, tracheal hemorrhage and other complications are more common in patients who have not received radiation therapy before, because tissues are very fragile after radiotherapy.

Case report

A 56-year-old male with a history of esophageal cancer was admitted to our hospital (The Affiliated Hospital of Jiangsu University, Yixing People's Hospital, Wuxi, China) on November 23, 2013. He was diagnosed with esophageal cancer and underwent radical surgery on February 26, 2010 in our hospital. The postoperative pathology report found moderately differentiated esophageal squamous cell carcinoma, with invasion of the submucosa; some squamous cells with atypical hyperplasia in the upper margin; no carcinoma in the lower margin; 1 of 6 lymph nodes was found to have cancer cells. The patient was treated with 4 cycles of postoperative adjuvant chemotherapy, using TP (paclitaxel 120 mg on day 1 and 90 mg on day 8, and nedaplatin 50 mg on days 1 and 8), from March 27, 2010 to July 3, 2010. Computed tomography (CT) revealed mediastinal lymph node enlargement on January 3, 2013 (Fig. 1). The patient subsequently received 2 cycles of GP (gemcitabine 1.4 g on day 1 and 1.2 g on day 8, and cisplatin 20 mg on days 1 to 4) on January 14, 2013 and February 16, 2013. CT on March 20, 2013 showed no obvious changes in the mediastinal lymph node enlargement after 2 cycles of chemotherapy (Fig. 2). Following palliative chemotherapy, gamma-knife treatment was administered to the patient's enlarged mediastinal lymph nodes in April, 2013, followed by rest at home. The patient had no awareness of hoarseness as of June, 2013, but developed dyspnea as the disease gradually progressed.

He came to our hospital on November 23, 2013, when the symptoms were severe, and a three-concave sign was observed. CT showed that the mediastinal lymph nodes had enlarged significantly between March 20, 2013 and November 25, 2013 (Fig. 3). Anti-inflammatory drugs and asthma treatment had no apparent effect. By November 30, 2013, the patient could not lie down because of dyspnea, even with large doses of aerosol inhalation, and other conventional treatment methods. The dyspnea worsened on December 2, 2013; electrocardiography monitoring showed a heart rate up to 120 beats per minute and blood oxygen saturation decreased to 80%, but

✉ Correspondence to: Ke Min. Email: staff1055@yxph.com
© 2016 Huazhong University of Science and Technology

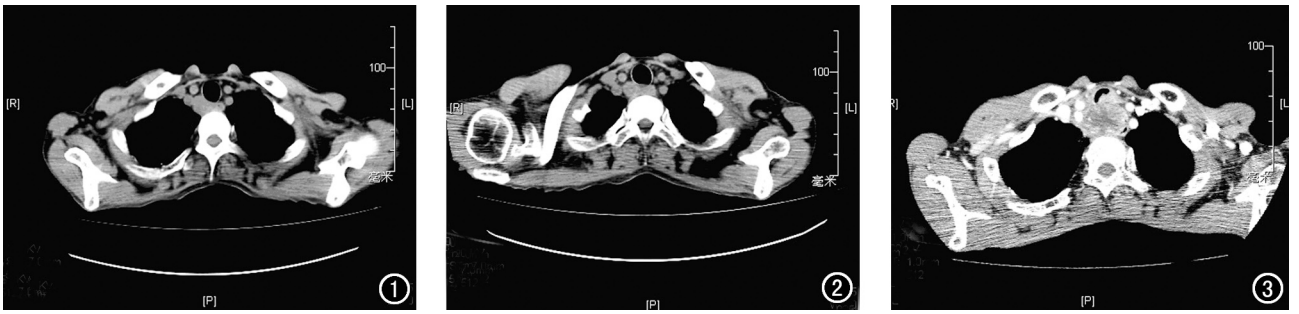

Fig. 1 CT showed mediastinal lymph node enlargement on January 03, 2013
Fig. 2 CT on March 20, 2013, showed no obvious change in mediastinal lymph node enlargement after 2 cycles of chemotherapy
Fig. 3 CT showed a significant increase in mediastinal lymph nodes between March 20, 2013 and November 25, 2013, and the primary bronchi were severely compromised by the enlarged lymph nodes

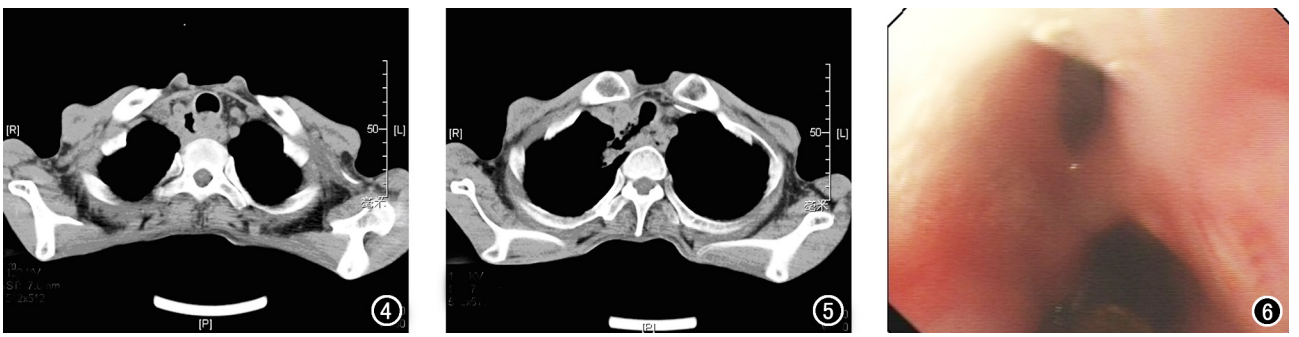

Fig. 4–5 CT showed a significant decrease in the mediastinal lymph nodes between November 25, 2013 and January 12, 2014, but a tracheoesophageal fistula appeared to have developed
Fig. 6 Gastroscopy showed a fistula in the esophagus, 20 cm distance from the incisors

the blood pressure was normal. We administered large doses of methylprednisolone immediately, with no apparent effect. As the patient was critical, we administered 0.5 mg of epinephrine by subcutaneous injection. To our surprise, the patient's dyspnea eased slightly after about 5 minutes; the heart rate decreased to 100 beats per minute, the blood oxygen saturation increased to 95%, and the blood pressure increased slightly. Subsequently, aerosol inhalation of budesonide, ambroxol, and epinephrine was administered every 4 to 6 hours. The patient's dyspnea eased slightly after each inhalation or epinephrine subcutaneous injection, but he still could not lie down. Bevacizumab combined with TP chemotherapy was administered on December 3, 2013 (bevacizumab 200 mg on day 1 and paclitaxel 120 mg on day 1, and cisplatin 20 mg on days 1 to 3). The patient's dyspnea had subsided by December 5, 2013. He was obviously in much better health by December 7, 2013, and could again lie down. Therefore, we discontinued aerosol inhalation of epinephrine on December 7, 2013. Third-degree bone marrow suppression subsequently developed. We again gave bevacizumab combined with TP chemotherapy on December 30, 2013 (bevacizumab 200 mg on day 1 and paclitaxel 120 mg on day 1, and cisplatin 20 mg on days 1 to 4). The patient's condition was stable, and he was hospitalized for additional treatment. Respiratory difficulty occurred after eating on January 12, 2014, but CT revealed a significant decrease in the mediastinal lymph nodes between November 25, 2013 and January 12, 2014 (Fig. 4). However, there was evidence of a tracheoesophageal fistula (Fig. 5), which was confirmed by gastroscopy (Fig. 6). Nasal feeding and peripheral parenteral nutrition were started. The patient died of a massive tracheal hemorrhage on February 16, 2014.

Discussion

Dyspnea caused by a neoplasm is not common in oncology, but is an emergency when it occurs. The consequences can be catastrophic, and the majority of patients die of hypoxia in a few days if tracheal stenosis is not corrected. Surgical resection is an option [6–7], but is not suitable in a critically ill patient. Airway stenting has been considered the "gold standard" for the treatment of benign and malignant airway stenosis in the past 20 years [4, 8]. Two patients with esophageal cancer received

chemoradiotherapy after airway stenting and survived for 24 months and 54 months, respectively. One patient with esophageal cancer died of airway bleeding 2 months after stent placement [9]. Some studies used airway stenting as a temporary measure, with removal after relief of tracheal stenosis [3, 5]. In this case, the patient's general status was very poor, and surgical resection would be difficult to implement; airway stenting was also ruled out because radiation therapy had been used for the enlarged mediastinal lymph nodes; moreover, the patient's family refused surgery. Chemotherapy seemed to be our only option, and the patient's family consented. With the family's full understanding, bevacizumab combined with chemotherapy was administered, but the dose was small because of the patient's poor condition. However, when he became critical, relief of dyspnea was essential, or death from hypoxia would occur within hours.

Epinephrine acts on α and β receptors, and is usually used to rescue patients with anaphylactic shock, sudden cardiac arrest, and severe dyspnea caused by bronchial spasm in emergencies, but it is seldom used to treat dyspnea caused by tumor compression. The side effects of epinephrine include elevation of blood pressure, palpitations, headache, and arrhythmia. We did not observe these side effects in this case, but some symptoms may have been concealed by severe dyspnea. In this case, epinephrine may have acted by alleviating edema in the compromised trachea and relaxing bronchial smooth muscles; the duration of effect was only 4–6 hours after each dose of epinephrine, which was consistent with the metabolism and pharmacokinetics of epinephrine.

We gave this patient a total of 24 mg of epinephrine, with 2 doses of 0.5 mg subcutaneously, and 23 mg by aerosol inhalation of 1 mg per dose. After each dose of epinephrine, the patient's dyspnea eased for about 4 to 6 hours. We simultaneously gave bevacizumab combined with TP chemotherapy. The general status of this patient was very poor, necessitating a relatively low chemotherapy dose. With these measures, the patient's dyspnea was relieved after 3 days, and he could lie down again after 5 days. Bevacizumab is a vascular endothelial growth factor-specific angiogenesis inhibitor indicated for the treatment of metastatic colorectal cancer, non-squamous non-small cell lung cancer, and metastatic breast cancer. It is not clear whether bevacizumab or chemotherapy, or possibly both, played a greater role in this case. We did not consider this in detail.

Airway stenting has only been performed in large medical centers. Most smaller hospitals do not have this technology. Our experience may be of use in the treatment of patients with dyspnea caused by tracheal stenosis in smaller hospitals, and possibly buy time until airway stenting can be performed at a large medical center. Airway stenting also has many complications, including cough, and massive tracheal hemorrhage due to stent irritation. One study showed that despite improvement in symptoms, the actual survival benefit was limited due to severe potential complications. Two patients with advanced lung cancer who underwent bronchial stenting for intractable dyspnea had dramatic improvement in symptoms and quality of life, but both died shortly after [10]. We prolonged the life of this patient more than 2 months, but he finally died of a massive tracheal hemorrhage on February 16, 2014. The patient's quality of life was clearly improved, however briefly. The experience from this case can also be of value for patients who do not want or cannot afford airway stenting. Moreover, radiotherapy may also be effective on a compressing neoplasm.

In conclusion, we present a case of using epinephrine combined with chemotherapy to relieve dyspnea caused by a neoplasm.

Conflicts of interest

The authors indicated no potential conflicts of interest.

References

1. Shin JH, Kim SW, Shim TS, *et al.* Malignant tracheobronchial strictures: palliation with covered retrievable expandable nitinol stent, J Vasc Interv Radiol, 2003, 14: 1525–1534.
2. Chen C, Jiang S. A novel anatomy-conforming metallic stent for tracheobronchial stenosis. Ann Thorac Surg, 2008, 85: 2100–2103.
3. Saueressig MG, Sanches PR, Macedo Neto AV, *et al.* Novel silicone stent to treat tracheobronchial lesions: results of 35 patients. Asian Cardiovasc Thorac Ann, 2010, 18: 521–528.
4. Tanigawa N, Kariya S, Komemushi A, *et al*. Metallic stent placement for malignant airway stenosis. Minim Invasive Ther Allied Technol, 2012, 21: 108–112.
5. Oki M, Saka H. Temporary use of silicone stents for severe airway stenosis in untreated malignant lymphoma. J Bronchology Interv Pulmonol, 2013, 20: 21–27.
6. Morikawa N, Honna T, Kuroda T, *et al.* Life-threatening airway obstruction caused by mediastinal germinoma in a 9-year-old girl. J Pediatr Surg, 2005, 40: 588–590.
7. Shimoyama T. Mediastinal bronchogenic cyst causing severe tracheal stenosis. Kyobu Geka (Japanese), 2013, 66: 814–817.
8. Dutau H, Musani AI, Plojoux J, *et al*. The use of self-expandable metallic stents in the airways in the adult population. Expert Rev Respir Med, 2014, 8: 179–190.
9. Nagahama T, Ami K, Nakamura M, *et al*. Four cases of airway obstruction successfully treated by airway stenting. Gan To Kagaku Ryoho (Japanese), 2012, 39: 1852–1854.
10. Bandyopadhyay D, Induru RR. Role of palliative tracheobronchial stenting in hospice patients: boon or bane? Am J Hosp Palliat Care, 2011, 28: 445–448.

DOI 10.1007/s10330-016-0159-3
Cite this article as: Yao Q, Zhou Y, Xu CN, *et al*. Epinephrine use during chemotherapy to treat severe tracheal stenosis secondary to advanced esophageal cancer: A case report and review of the literature. Oncol Transl Med, 2016, 2: 239–241.

Oncology and Translational Medicine
DOI 10.1007/s10330-016-0167-3

October 2016, Vol. 2, No. 5, P242–P245

CASE REPORT

Primary malignant melanoma of the liver: One case report and literature review

Dongfang Huang, Jinsheng Wu, Guofeng Chen, Jianhuai Zhang (✉)

Department of Hepatopancreatobiliary Surgery, Huai'an No. 1 Hospital, The Nanjing Medical University, Huai'an 223300, China

Abstract

Objective Primary malignant melanomas of the liver are exceedingly rare. Only 19 cases have been reported in the literature worldwide. In this report, we describe our pathological findings and review the literature in order to improve our understanding of the disease and prevent misdiagnosis, as well as provide evidence for its treatment and prognosis.

Methods We present a case of an isolated malignant melanoma of the liver in a 61-year-old male Chinese patient.

Results Comprehensive dermatological and ophthalmological examinations did not reveal any evidence of a primary cutaneous or ocular lesion. Similarly, serial physical examinations, auxiliary examinations, and bone scans did not demonstrate any other lesions in the brain, respiratory tract, and gastrointestinal tract. Microscopic examination of the resected specimen revealed malignant melanoma, which was confirmed by immunohistochemical staining for S-100 protein (+), ki67 (30%+), EMA (+), CD10 (+), and HMB-45 (++).

Conclusion Primary malignant melanoma may occur in the liver, and should be considered when the histopathological appearance is atypical of other hepatic neoplasms. The diagnostic criteria for hepatic malignant melanoma depend mainly on the clinical, radiographic, and histopathological findings. Pathomorphology and immumohistochemical staining can be utilized to confirm the diagnosis.

Received: 16 June 2016
Revised: 6 August 2016
Accepted: 25 August 2016

Key words: malignant melanoma; liver; pathomorphology; immunohistochemistry

Malignant melanoma occurs most frequently in the skin, but may also manifest in many other organs and tissues. However, primary hepatic malignant melanoma is exceedingly rare. Only 19 cases have been reported thus far, comprising 8 cases from PubMed and 11 cases from the Chinese literature. Only 4 cases of definite primary melanoma have been reported in PubMed (mean patient age 42.2 years, range 27–60 years). Microscopically, it may be easily misdiagnosed because of the morphological heterogeneity and hypomelanotic appearance. We report the only case of primary hepatic malignant melanoma encountered in our department.

Case report

A 61-year-old man was admitted to the Department of Hepatopancreatobiliary Surgery, Huai'an No. 1 Hospital, the Nanjing Medical University (Huai'an, Jiangsu Province, China) with a 3-month history of right upper abdominal pain that had been worsening over the past 2 days. His past medical history included a 1-year history of neck year, a 20-year history of hepatitis A, a 10-month history of hypertension, and a 10-day history of diabetes, all of which were under treatment. His family history was not significant. His vital signs were normal apart from a slightly elevated blood pressure (145/75 mmHg, normal range 90–140/60–90 mmHg). His skin and sclera were not yellow, no superficial nodular lesions were observed on his body, and no palmar erythema and spider nevi were present. On auscultation, his breath sounds were rough bilaterally, and bronchial wheezing was occasionally heard. The liver was not palpable below the costal margin, and the spleen was not palpable as well. Light percussion elicited pain in the hepatic region. Routine clinical biochemistry tests showed normal levels of serum aspartate aminotransferase (AST), alanine aminotransferase (ALT), lactate dehydrogenase (LDH), γ-glutamyltransferase (γ-GTP), total bilirubin (TB)，direct bilirubin

✉ Correspondence to: Jianhuai Zhang. Email: jh_z02@hotmail.com
© 2016 Huazhong University of Science and Technology

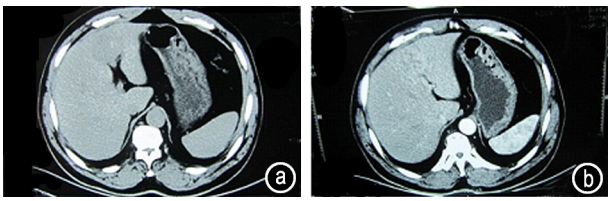

Fig. 1 (a) Computed tomography (CT) scan showing a 3.7 cm × 3.4 cm mass in the left lobe of the liver that appeared round in shape and uneven in density. (b) Contrast-enhanced CT scan displaying a 3.7 cm × 3.5 cm well-defined hepatic mass in the left internal lobe of the liver, which showed low-density enhancement

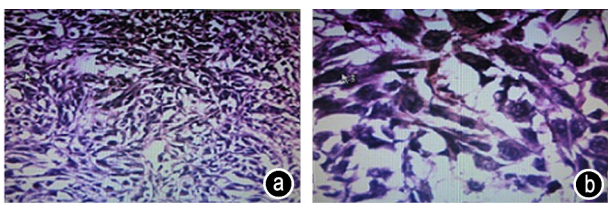

Fig. 2 Pathological findings. (a) The tumor cells were arranged diffusely or in nests, and mesenchymal fibrous tissue hyperplasia was observed. On deep dyeing with hematoxylin and eosin, spindle-shaped nuclei were observed in the tumor cells (original magnification, ×100). (b) Tumor cells were pleomorphic and eosinophilic, and had large volumes, abundant cytoplasm, large nucleus, and abundant nucleoli (original magnification, × 400)

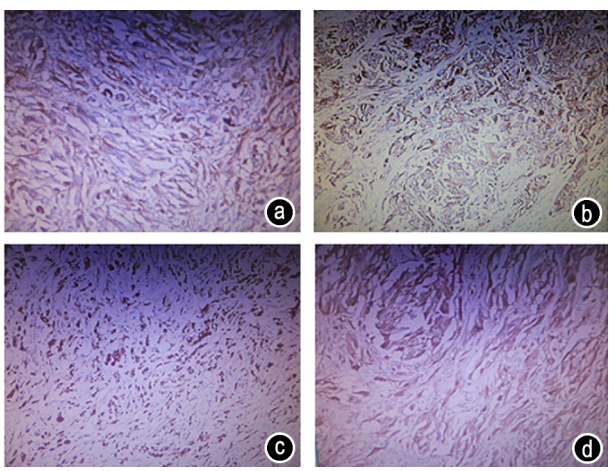

Fig. 3 Immunohistochemistry: revealing tumor cells positive for CD10 (× 100) (a); HMB-45 (× 100) (b); Ki67 (× 100) (c); and S-100 protein (× 100) (d)

(DB), indirect bilirubin (IB), and pre-albumin; however, his blood glucose level (GLU) was elevated (7.89 mmol/L, normal range 3.60–6.20 mmol/L). Levels of serum tumor markers including alpha-fetoprotein (AFP), carcinoembryonic antigen (CEA), and cancer antigen 50 (CA50) were within the normal range. Laboratory tests demonstrated negative hepatitis B surface antigen (HBsAg). An abdominal computed tomography (CT) scan showed a 3.7 cm × 3.4 cm mass in the left lobe of the liver, which appeared round in shape and uneven in density (Fig. 1a). A contrast-enhanced CT scan displayed a 3.7 cm × 3.5 cm well-defined hepatic mass in the left internal lobe of the liver, and revealed low-density enhancement without evidence of spread to the neighboring lymph nodes (Fig. 1b). A chest radiograph confirmed chronic bronchitis in both lungs. The working diagnosis was liver cancer on a background of chronic bronchopneumonia, hypertension, and diabetes.

Macroscopically, the resected mass had an intact capsule, and measured 4 cm × 4 cm × 3.5 cm at the junction of the left lateral lobe and left internal lobe. The mass was clearly differentiated from the normal surrounding tissue, and its cut surface was ash-black in color. Microscopically, the tumor cells showed diffuse infiltration, and fibrous tissue was observed between the lesion and the normal hepatocytes. Microscopically, the tumor cells were arranged diffusely or in nests, and mesenchymal fibrous tissue hyperplasia was observed. On deep dyeing with hematoxylin and eosin (HE × 100), spindle-shaped nuclei were observed in the tumor cells (Fig. 2a). The tumor cells were pleomorphic and eosinophilic, with large volumes, abundant cytoplasm, large nucleus, and abundant nucleoli (HE × 400) (Fig. 2b).

Immunohistochemically, the tumor cells were positive for S-100 protein (+), ki67 (30% +), EMA (+), CD10 (+), HMB-45 (++) (HE × 100) (Fig. 3). The complete absence of any cutaneous, ocular, or mucosal lesions in all organs on serial physical examinations, auxiliary examinations, and bone scans supported the final diagnosis of primary hepatic malignant melanoma. After local surgical resection, the patient was started on a comprehensive treatment regime of cisplatin, fluorouracil, interferon, epirubicin, and thymosin. He showed good recovery. However, recurrent foci were found 5 months postoperatively. The patient underwent 8 months of regular follow-ups in total, and no disease recurrence was observed.

Discussion

Melanomas were first described by Pilliet in 1887 [1]. They originate from epidermal melanocytes or neural cells, both of which derive from neural crest precursors. Chamaejasme extract is thought to inhibit proliferation and induce apoptosis of malignant melanoma B16 cells by down-regulating the expression of Akt and up-regulating the expression of PTEN [2]. Only 10%–30% of malignant melanomas are radio- or chemo-sensitive [3]. Malignant melanomas may present as single or multiple lesions, and are characterized by a coated appearance, easy hemorrhage, necrosis, cystic degeneration, tumor cells rich in melanin granules, a high degree of malignancy, rapid metastasis, and a poor prognosis. In particular, liver metas-

tasis portends a grave prognosis, with a median survival time of approximately 4 months. Malignant melanomas are most prevalent in Caucasian patients over the age of 30 years [4]. They mainly manifest in the skin (accounting for 79% of cases) [5], and usually originate from border hemorrhoids. Hepatic metastases occur in 20% of patients with malignant melanoma. In the early stages of the disease, metastasis occurs via the lymphatic route. However, in the advanced stages, the tumor cells spread to the lungs, liver (14%–20% of cases), bone, and brain via blood flow. Therefore, primary malignant melanoma of the liver is extremely rare and very few cases have been reported. Hepatic metastasis is more common in intraocular melanomas, which makes up 50% of such cases [6]. Melanomas of unknown primary sites (MUP) are estimated to account for 3.7% to 6% of all incident melanomas [7]. Previous studies have reported that hepatic malignant melanomas tend to present as single or multiple lesions, grow expansively, may have false capsules (mean diameter 8.8 cm, range 1.8–16 cm), and usually develop in the right lobe of the liver. Their origin and pathogenesis remain unclear, but interleukin (IL)-8 is thought to play a crucial role in disease progression. A relationship between Hepatitis B virus (HBV) and malignant melanoma has not been established. The HbsAg test result was negative for our patient. Genetic analyses have shown that abnormalities in chromosomes 1, 6, 7, 9, and 10 may be present.

The diagnosis of hepatic malignant melanoma depends mainly on the clinical, radiographic, and histopathological findings, and may be confirmed by pathomorphology and immumohistochemical staining. The clinical manifestations of hepatic malignant melanoma are non-specific, comprising symptoms such as epigastric discomfort, paroxysmal abdominal pain, and abnormal liver function. Indeed, our patient conformed to this pattern of presentation. Abdominal CT scans generally display single or multiple slightly high-density nodules with calcification. Contrast-enhanced CT scans may enhance the foci slightly. The garland manifestations of metastatic malignant melanoma can usually be identified on CT images [8]. Discoidin domain receptor (DDR)-2 promotes A375 melanoma metastasis to the liver [9]. As compared to CT scans, magnetic resonance imaging (MRI) scans can provide more detailed information for hepatic malignant melanomas. Wang *et al* has suggested that the most characteristic finding on imaging is a T2-weighted low-signal lesion with abundant hemosiderin from remote hemorrhages [10]. In our case, the CT scan showed a mass in the left internal lobe of the liver, which appeared round in shape and uneven in density. The focus showed mild strengthening on contrast-enhanced CT. Due to insufficient experience in diagnosing and treating hepatic malignant melanoma at that time, we did not request an MRI scan to be performed.

Pathologically, the tumor cells were pleomorphic, with a large nucleolus, and with or without melanin pigment deposition. Immunohistochemically, the tumor cells tended to express HMB-45, S-100 protein, vimentin, and Melan-A strongly [11]. Gong *et al* suggested that once the pathologic diagnosis is established, it is important to consider whether the tumor is a primary or secondary lesion. If an extensive investigation of potential primary sites demonstrates no evidence of primary melanomas, the hepatic tumor is likely to be a primary melanoma of the liver [12]. Our experience was in complete accord with this report.

A standard treatment approach for hepatic primary malignant melanoma and single metastatic malignant melanoma has yet to be established. While partial liver resection may be effective, the prognosis is poorer for cases with multiple or metastatic lesions. Surgical treatment is always palliative. Adjuvant measures such as chemotherapy, immunotherapy, and radiotherapy are extremely important in prolonging survival and improving quality of life postoperatively. Molecular targeting therapies have been used to manage Stage III melanomas effectively. Previous studies have reported that ipilimumab can prolong the median and 5-year survival rates [13], and that IL-18 can effectively prevent the inflammation associated with malignant melanoma [14].

Long-term follow-up is necessary for melanomas with a diameter of 2 cm or larger. Imaging examinations such as X-rays, positron emission tomography (PET)-CT, and MRI are commonly used to monitor patients. Serum LDH may also be used to monitor disease progression – higher LDH levels tend to indicate more aggressive tumors and poorer prognoses. Serum LDH may also be used to assess treatment effect [15].

No large randomized controlled studies have been conducted thus far. As such, we need to constantly summarize our experiences of diagnosing and treating malignant melanomas of the liver.

Acknowledgments

The authors thank all the patients and their families for participating in this research.

Conflicts of interest

The authors indicated no potential conflicts of interest.

References

1. Hu XR. A case of primary malignant melanoma of the liver. Chin J Radiol (Chinese), 2006, 40: 1115.
2. Zhang YZ, Liu HC, Li MW, *et al*. The effect and significance on Akt and PTEN expression in melanoma B16 cells with chamaejasme extract. Chinese-German J Clin Oncol, 2014, 13: 600–602.
3. Pawlik TM, Zorzi D, Abdalla EK, *et al*. Hepatic resection for metastatic melanoma: distinct patterns of recurrence and prognosis for ocular

versus cutaneous disease. Ann Surg Oncol, 2006, 13: 712–720.
4. Chen JS, Li HC. Primary malignant melanoma of the liver: one case report. J Fourth Mil Med Univ (Chinese), 2002, 23: 895.
5. Zhang C, An DJ, Yang XW, *et al*. A case of malignant melanoma of the liver. J Hepatopancreatobil Surg (Chinese), 2005, 17: 19.
6. Cheng XJ. A case of hepatic resection for metastatic melanoma. Chin J Hepatobiliary Surg (Chinese), 2007, 13: 83.
7. Shan GD, Xu GQ, Chen LH, *et al*. Diffuse liver infiltration by melanoma of unknown primary origin: one case report and literature review. Inter Med, 2009, 48: 2093–2096.
8. Wen Y, Lu FJ, Luo TY, *et al*. Malignant melanoma metastasis to mediastinum and liver: one case report. China JMIT (Chinese), 2002, 18: 962.
9. Badiola I, Villacé P, Basaldua I, *et al*. Downregulation of discoidin domain receptor 2 in A375 human melanoma cells reduces its experimental liver metastasis ability. Oncol Rep, 2011, 26: 971–978.
10. Wang J, Han XN, Hao NX, *et al*. CT and MRI manifestations of hepatic malignant melanoma. Chin J Radiol (Chinese), 1998, 32: 67.
11. Li HC, Xu HB, Wang HM. A case of malignant melanoma of the liver showing a enormous cystic occupy. Chin J Oncol (Chinese), 2003, 25: 110.
12. Gong L, Li YH, Zhao JY, *et al*. Primary malignant melanoma of the liver: a case report. World J Gastroenterol, 2008, 14: 4968–4971.
13. Karlen AI, Clark JJ, Wong LL. Two cases of partial hepatectomy for malignant melanoma. Hawaii J Med Public Health, 2012, 71: 92–96.
14. Salado C, Olaso E, Gallot N, *et al*. Resveratrol prevents inflammation-dependent hepatic melanoma metastasis by inhibiting the secretion and effects of interleukin-18. J Transl Med, 2011, 9: 59.
15. Huang HJ, Yu YH, Zheng ZY. Primary malignant melanoma of the liver: one case report and literature review. Chin J Clin Exp Pathol (Chinese), 2011, 27: 193–195.

DOI 10.1007/s10330-016-0167-3
Cite this article as: Huang DF, Wu JS, Chen GF, *et al*. Primary malignant melanoma of the liver: One case report and literature review. Oncol Transl Med, 2016, 2: 242–245.

Oncology and Translational Medicine

Aims & Scope

Oncology and Translational Medicine is an international professional academic periodical. The Journal is designed to report progress in research and the latest findings in domestic and international oncology and translational medicine, to facilitate international academic exchanges, and to promote research in oncology and translational medicine as well as levels of service in clinical practice. The entire journal is published in English for a domestic and international readership.

Copyright

Submission of a manuscript implies: that the work described has not been published before (except in form of an abstract or as part of a published lecture, review or thesis); that it is not under consideration for publication elsewhere; that its publication has been approved by all co-authors, if any, as well as – tacitly or explicitly – by the responsible authorities at the institution where the work was carried out.

The author warrants that his/her contribution is original and that he/she has full power to make this grant. The author signs for and accepts responsibility for releasing this material on behalf of any and all co-authors. Transfer of copyright to Huazhong University of Science and Technology becomes effective if and when the article is accepted for publication. After submission of the Copyright Transfer Statement signed by the corresponding author, changes of authorship or in the order of the authors listed will not be accepted by Huazhong University of Science and Technology. The copyright covers the exclusive right and license (for U.S. government employees: to the extent transferable) to reproduce, publish, distribute and archive the article in all forms and media of expression now known or developed in the future, including reprints, translations, photographic reproductions, microform, electronic form (offline, online) or any other reproductions of similar nature.

Supervised by

Ministry of Education of the People's Republic of China.

Administered by

Tongji Medical College, Huazhong University of Science and Technology.

Submission information

Manuscripts should be submitted to:
http://otm.tjh.com.cn
dmedizin@sina.com

Subscription information

ISSN edition: 2095-9621
CN: 42-1865/R

■ Subscription rates
Subscription may begin at any time. Remittances made by check, draft or express money order should be made payable to this journal. The price for 2015 is as follows: US $ 30 per issue; RMB ￥28.00 per issue.

Database

Oncology and Translational Medicine is abstracted and indexed in EMBASE, Index Copernicus, Chinese Science and Technology Paper Citation Database (CSTPCD), Chinese Core Journals Database, Chinese Journal Full-text Database (CJFD), Wanfang Data; Weipu Data; Chinese Academic Journal Comprehensive Evaluation Database.

Business correspondence

All matters relating to orders, subscriptions, back issues, offprints, advertisement booking and general enquiries should be addressed to the editorial office.

Mailing address
Editorial office of
Oncology and Translational Medicine
Tongji Hospital
Tongji Medical College
Huazhong University of Science and Technology
Jie Fang Da Dao 1095
430030 Wuhan, China
Tel.: +86-27-83662630
Fax: +86-27-83662645
Email: dmedizin@tjh.tjmu.edu.cn

Printer
Changjiang Spatial Information Technology Engineering Co., Ltd. (Wuhan)
Hangce Information Cartorgraphy Printing Filial, Wuhan, China
Printed in People's Republic of China

Managing director

Jun Xia

Executive editors

Yening Wang
Jun Xia
Jing Chen
Qiang Wu

Typesetting editor

Wenge Wang